LA-10003-MS

Los Alamos National Laboratory is operated by the University of California for the United States Department of Energy under contract W-7405-ENG-36.

Petrography and Mineral Chemistry of Units of the Topopah Spring, Calico Hills and Crater Flat Tuffs, and Older Volcanic Units, with Emphasis on Samples from Drill Hole USW G-1, Yucca Mountain, Nevada Test Site

Los Alamos
Los Alamos National Laboratory
Los Alamos, New Mexico 87545

This report was prepared by the Los Alamos National Laboratory as part of the Nevada Nuclear Waste Storage Investigations managed by the Nevada Operations Office of the US Department of Energy. Based upon their applicability to the investigations, some results from the Radionuclide Migration Project, managed by the Nevada Operations Office of the US Department of Energy, are included in this report.

Edited by Glenda Ponder, ESS Division

LA-10003-MS

UC-70
Issued: June 1984

Petrography and Mineral Chemistry of Units of the Topopah Spring, Calico Hills and Crater Flat Tuffs, and Older Volcanic Units, with Emphasis on Samples from Drill Hole USW G-1, Yucca Mountain, Nevada Test Site

Richard G. Warren
Frank M. Byers, Jr.
Florie A. Caporuscio*

*Department of Geology, University of California, Davis, Davis, CA 95616.

Los Alamos
Los Alamos National Laboratory
Los Alamos, New Mexico 87545

PETROGRAPHY AND MINERAL CHEMISTRY OF UNITS OF THE TOPOPAH SPRING, CALICO HILLS AND CRATER FLAT TUFFS, AND OLDER VOLCANIC UNITS, WITH EMPHASIS ON SAMPLES FROM DRILL HOLE USW G-1, YUCCA MOUNTAIN, NEVADA TEST SITE

by

Richard G. Warren, Frank M. Byers, Jr., and Florie A. Caporuscio

ABSTRACT

This report contains a comprehensive set of petrographic and mineral chemical data for phenocrysts in volcanic units of Yucca Mountain drill hole USW G-1. This study provides a basis for petrographic comparison of units within Yucca Mountain and the Nevada Test Site (NTS), investigates several new petrographic techniques, and evaluates the usefulness of mineral chemical data obtained by electron microprobe analysis in correlating units. Correlation of these data with similar data for other drill holes of Yucca Mountain provides a primary means to evaluate the subsurface environment of the Waste Repository Site. The findings are applicable to programs that require an accurate knowledge of the subsurface geologic environment, particularly the Nevada Nuclear Waste Storage Investigations and Containment Programs at Los Alamos.

Phenocryst modes provide a most effective means for subsurface correlation of volcanic units, but use of these data alone sometimes results in miscorrelations because substantial petrographic variations occur within some units. Phenocryst compositions, however, show little or no variation within each unit and they provide the most reliable data for correlation of volcanic units, particularly when combined with modal data. The modes and mineral compositions reflect the processes that were associated with eruption of the units, and so also greatly aid in the understanding of the subsurface geologic environment at USW G-1. Neither the phenocryst contents nor mineral compositions have been substantially affected by the wide range in alteration conditions that occur within USW G-1. Therefore, these findings are generally applicable to volcanic sequences of the NTS and elsewhere.

I. INTRODUCTION

Both the Containment and Waste Isolations Programs of Los Alamos rely on the subsurface geologic environment of the Nevada Test Site (NTS) to prohibit release of radioactive material into the surface or near-surface environment. Undesirable geologic features may occur in subsurface that are not evident or do not occur at the surface. These can result in escape of radioactive material: an example is the important contribution of a buried fault in the large atmospheric release of radioactive gases as a result of the Baneberry test (Glenn et al. 1981; Carr 1974). Buried faults might also affect containment of hazardous waste components within a repository by channeling groundwater flow rapidly away from the protective environment of the repository. The subsurface geologic environment is determined by correlation of volcanic units of the NTS (Byers et al. 1976) among drill holes. Clearly, the understanding of the subsurface environment of a waste repository or weapons test depends greatly on the recognition and correlation of volcanic units.

Each volcanic unit on the NTS occupies a definite stratigraphic position and is defined by a set of petrographic characteristics. These characteristics are often recognized by hand-sample inspection, but require microscope examination of thin sections for confident identification of many units. Quantitative determination of phenocryst mineral contents in thin section, such as quartz, feldspar, biotite, pyroxene, etc., provides a primary basis for recognition of NTS volcanic units (Byers et al. 1976). Although such petrographic data provide a primary basis for characterization and correlation of NTS volcanic units, few of these data are published. Furthermore, petrographic variations are known to occur within many units. These variations are highly evident within units that consist predominantly of rhyolitic tuff with a quartz-latite "caprock" such as the Topopah Spring Member of the Paintbrush Tuff (Lipman et al. 1966). Because of subtle petrographic variations within a unit, volcanic unis are sometimes misidentified even following petrographic examination. Preliminary electron microprobe results for samples of the petrographically similar members of the Crater Flat Tuff indicate that mineral compositions were less subject to variation throughout a volcanic unit than phenocryst contents (Bish et al. 1981). Consequently, mineral compositional data might allow correlations of NTS volcanic units to be made with greater confidence and accuracy than from petrographic data alone.

Yucca Mountain drill hole USW G-1 provides an ideal set of samples to study petrographic and mineral compositional characteristics of NTS volcanic units. Detailed lithologic descriptions, based on continuous core, are available to the total depth of 6000 feet (Spengler et al. 1981; Bish et al. 1981). Petrographic and some mineral compositional data are also available from nearby cored holes of Yucca Mountain and vicinity (Byers and Warren 1983; Sykes et al. 1979; Heiken et al. 1979). Additional outcrop samples collected from Yucca Mountain and vicinity were also included, resulting in a total of 175 thin sections examined. These samples were studied for the following purposes:

1. To provide a comprehensive set of petrographic data from subsurface units of Yucca Mountain for correlation purposes. The most important of these data are contents of felsic phenocrysts (quartz, plagioclase, sanidine), mafic minerals such as biotite, hornblende, and pyroxene, and accessory minerals such as sphene, allanite, apatite, and zircon.

2. To characterize the mineral chemistry of these units. Minerals include plagioclase, sanidine, biotite, hornblende, and pyroxene.

3. To determine the variation in phenocryst content and composition within each volcanic unit, both among widely separated locations, and within each unit at USW G-1.

4. To determine the possible effects of secondary alteration on mineral chemistry. Phenocryst compositions might be of little use for correlation if they are controlled by alteration that commonly occurs in volcanic rocks, such as zeolitization.

5. To provide guidelines for the use of petrographic and mineral compositional data in correlating volcanic units of the NTS, and to explore the use of these data to understand volcanic processes.

II. LOCATION AND DESCRIPTION OF SAMPLES

Petrographic results are based on 175 thin sections including 163 of core samples from drill holes on or near Yucca Mountain (Fig. 1): 140 from USW G-1; 12 from UE-25a#1, and 11 from J-13. Detailed descriptions are available in Caporuscio et al. (in prep.) and x-ray diffraction results in Bish et al. (1981) for individual samples of USW G-1. The remaining 12 are outcrop samples, whose locations are separated by as much as 35 miles (Fig. 1).

The study emphasizes units of the Crater Flat Tuff and older tuffs. About half of the samples are divided among the Prow Pass, Bullfrog, and Tram Members of the Crater Flat Tuff and most of the remaining samples are of older units including the Flow Breccia of USW G-1, the Lithic Ridge Tuff, and older

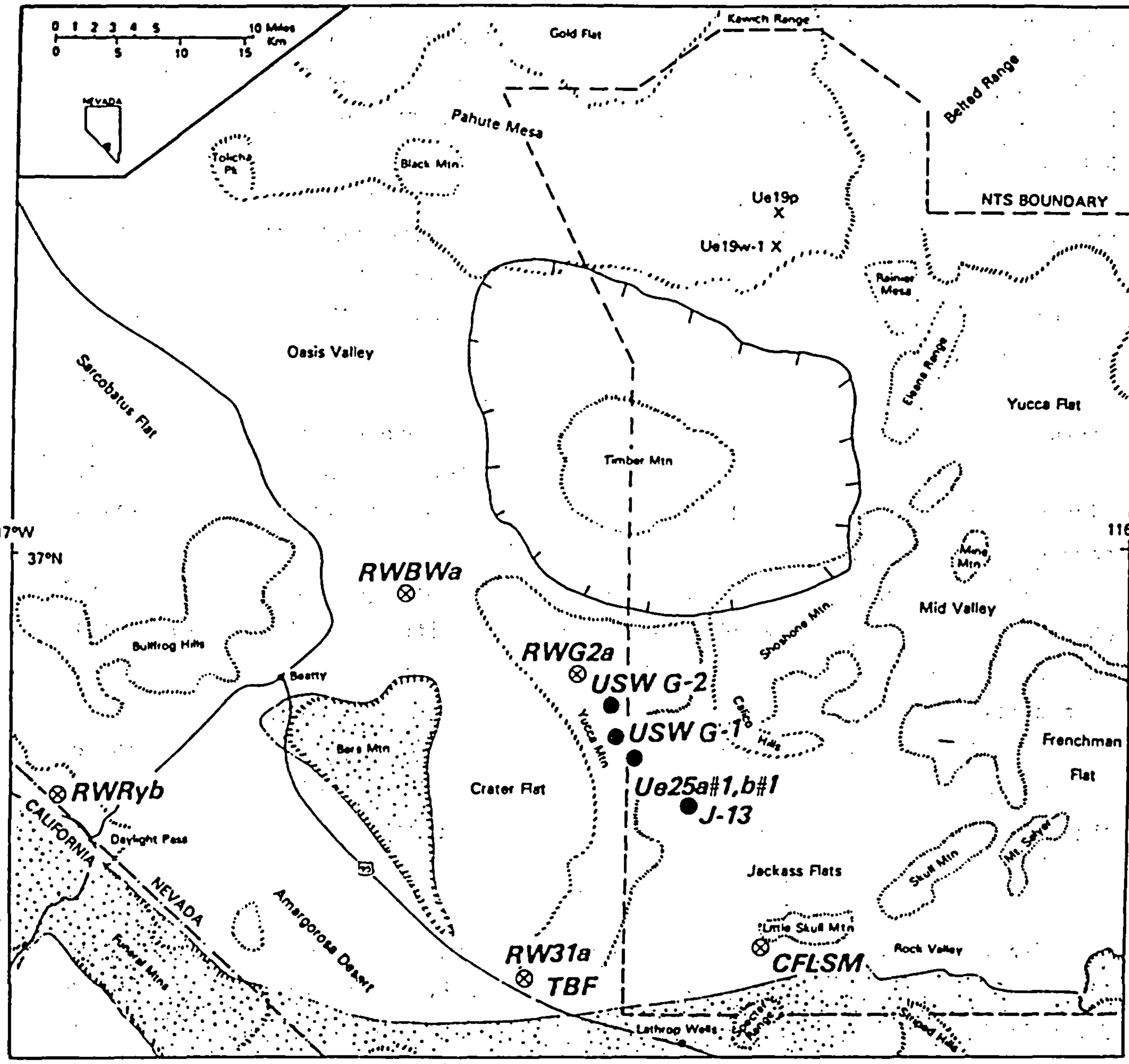

Fig. 1.
Map of NTS region showing sample locations. (○ = drill hole location, ⊗ = outcrop sample location, x = UE-19p and UE-19w#1, shown for reference only.)

tuffs of USW G-1 (divided into units A, B, and C). A few samples of the lower, mafic-poor portion of the Topopah Spring Member of the Paintbrush Tuff and the tuffs of Calico Hills, all from USW G-1, are also included. Symbols for each unit or subunit are defined in Table II; these are similar to symbols currently utilized by the USGS for these units. Stratigraphic positions for each sample within each unit are given in Table I for outcrop samples and in Table III for samples from drill core.

III. PETROGRAPHIC TECHNIQUES

Quantitative (modal) petrographic results are reported herein for two independently studied sample sets:

(1) Results for standard (glass-covered) thin sections are given in Table IV. Most results in Table IV are based on modal counts of 3500-4000 total points, and therefore provide modal estimates with relatively low counting statistical errors.

(2) Results for uncovered, polished thin (probe) sections are given in Table V. Estimates for major components are based on counts of about 500 total points at 100-200X, utilizing both reflected and transmitted light. Major components include macroscopic voids, pumice, lithic fragments, and total felsic phenocrysts (quartz, alkali feldspar, and plagioclase). Individual felsic phenocryst contents were also determined from the point count in some samples, but relative proportions were determined only for the largest felsic phenocrysts in most samples. Concentrations of mafic phenocrysts such as biotite, hornblende, and pyroxene, Fe-Ti oxide phenocrysts, and accessory minerals such as sphene and allanite were determined by scans at 100X. Areas were determined in reflected light for each such mineral located during the scan by using an ocular with a well-calibrated grid. Areas are summed and compared with the total area of the thin section, determined from the point count, to estimate volume contents for each mineral. The identity, area, and location of each primary mineral identified during the point count or scan was recorded on a standard form; the location was also marked on an 11 x 14 in. black and white photograph of the probe section for later microprobe analysis.

TABLE I

SAMPLE LOCATION AND STRATIGRAPHIC POSITION WITHIN UNIT
(All distances in feet. Accuracy for elevations ±20 ft for 7.5 min quadrangles and ±50 ft for 15 min quadrangles)

Sample	Nevada State Coordinates N	Nevada State Coordinates E	USGS quad[a]	Unit symbol[b]	Elevations: Sample location	Elevations: Unit top	Elevations: Unit base	Unit thickness	Sample distance from top of unit
USW G-1	770500	561000	TSSW			4349[c]			
UE-25a#1	764900	566350	TSSW			3933[c]			
J-13	749209	579651	TSSW			3218[c]			
RWG2a-3	788510	550250	TSNW	TCP	5320	>5400	5300	>100	80
RW31a-6	706350	538740	BD	TCP	3020	3060	2950	110	40
RWG2a-4	788730	550240	TSNW	TCB	5210	5220	<5080	>140	10
RWG2a-5	788860	549970	TSNW	TCB	5100	5220	<5080	>140	120
CFLSM-1	715350	598880	SH	TCB	3350	3350	<3000	>350	0
-5	715500	598540	SH	TCB	3230	3350	<3000	>350	120
TBF-4	705480	538610	BD	TCB	2860	2950	2700	250	90
-1	704950	538520	BD	TCB	2740	2950	2700	250	210
RWRyb-3	753610	414350	BF	TCB	4900	4960	4700	260	60
RWBWa-5	807680	507740	BM	TCT	3880		3850		
RWRyb-1	752980	415190	BF	TCT	4580	4620	4540	80	40
RWBWa-4	807680	505810	BM	TLR	3800	3830	<3780	>50	30

[a] BD = Big Dune 15' (topographic)
BF = Bullfrog 15' (topographic)
BM = Bare Mountain 15' (geologic: Cornwall and Kleinhampl 1961)
SH = Striped Hills 7.5' (geologic: Sargent et al. 1970)
TSNW = Topopah Spring NW (geologic: Christiansen and Lipman 1965)
TSSW = Topopah Spring SW (geologic: Lipman and McKay 1965)

[b] See Table II.

[c] Elevations are for surface levels of drill holes USW G-1, UE-25a#1, and J-13. Unit elevations and thicknesses are given in Table III.

TABLE II

SYMBOLS USED FOR PETROLOGIC UNITS, ROCK TYPES, ALTERATION, AND MINERALS

Unit	Unit Symbol
Paintbrush Tuff	TP
Topopah Spring Member - upper, mafic-rich portion	TPTu
Topopah Spring Member - lower, mafic-poor portion	TPTl
Tuffaceous beds of Calico Hills - upper, mafic-poor portion	TH1
Tuffaceous beds of Calico Hills - lower, mafic-rich portion	TH2
Crater Flat Tuff	TC
Prow Pass Member	TCP
bedded tuff	TCBa
Bullfrog Member	TCB
upper portion, 2152-2317.4 ft depth, USW G-1	TCBu
middle portion, 2317.4-~2425 ft depth, USW G-1	TCBm
lower portion, ~2425-2601.6 ft depth, USW G-1	TCBl
bedded tuff	TCTa
Tram Member	TCT
upper portion, 2601.6-3083.0 ft depth, USW G-1	TCTu
lower portion, 3083.0-3522.0 ft depth, USW G-1	TCTl
Flow Breccia of USW G-1	TFB
Rhyodacite Lava of USW G-2	TRD
bedded tuff between Flow Breccia of USW G-1 and Lithic Ridge Tuff	TLRa
Lithic Ridge Tuff	TLR
upper portion, 3920.0-~4365 ft depth, USW G-1	TLRu
lower portion, ~4365-4940.2 ft depth USW G-1	TLRl
Older Tuffs of USW G-1	TT
Unit A	TTA
Unit B	TTB
Unit C	TTC

Rock Type

tf = tuff

b = bedded tuff

t = ash-flow tuff (nw = nonwelded, pw = partially welded, mw = moderately welded, dw = densely welded, v = vitrophyric)

l = lava

intl= intermediate-composition lava (groundmass plagioclase present)

fb = lava flow breccia

tb = tuff breccia

ar = argillite

gr = granitoid

Table II (cont)

Alteration

Modifiers to terms below: m = minor, μ = micro-

Type	Symbol
None	Gl = vitric
Low T (secondary)	O = opaline Ar = argillic Z = zeolitic Zc = clinoptilolite Za = analcime cc = calcite py = pyritic Q = silicic (chalcedony)
High T (secondary)	Ab = albitic
High T (primary)	VP = vapor phase Gr = granophyric Sp = spherulitic Ax = axiolitic

Minerals

All concentrations in most samples are for unaltered or partly altered phenocrysts. In some samples, phenocrysts are partly or completely altered. In these samples, the symbol "A" indicates that the accompanying concentration is for partly altered grains only, and the symbol "ps" indicates that the accompanying concentration is based entirely on completely altered (pseudomorphic) forms.

Felsic Phenocrysts	Q = quartz K = sanidine (+anorthoclase, if present) P = plagioclase
Mafic Phenocrysts	B = biotite Hbld = hornblende Cpx = clinopyroxene Opx = orthopyroxene
Accessory Minerals	Sph = sphene All = allanite Per = perrierite/chevkinite Ap = apatite Zr = zircon

TABLE III

ELEVATIONS AND THICKNESSES FOR PETROLOGIC UNITS EXAMINED IN DRILL HOLES USW G-1, UE-25a#1, and J-13
(All distances in feet.)

Unit Symbol	Top of unit: Elevation	Top of unit: Depth	Number of Samples	Depths for samples examined
				USW G-1 [Contacts from Spengler et al. (1981); except those marked with footnote.]
TPT1	3892.1	456.6	5	1191, 1240, 1286, 1292, 1392
TH1	2923.1	1425.5	5	1436, 1561, 1561.8, 1639, 1689.5
TH2	2612.2	1736.4	1	1774
TCP	2547.1	1801.5	9	1811.7, 1829, 1854, 1884, 1943.4, 1983, 2009.8, 2083, 2124.7
TCB	2165.6	2152.0[a]	23	2166[a], 2231.0, 2233, 2246.0, 2247, 2289, 2291, 2300.4, 2318, 2354.6, 2363, 2397, 2411, 2436, 2461.5, 2470.6, 2477, 2478.3, 2486, 2507, 2555, 2594.2, 2601
TCT	1747.0	2601.6[b]	22	2641.5, 2678.0, 2699, 2772.6, 2790, 2851.7, 2854, 2869, 2901, 2931.4, 2938, 3001, 3013.9, 3117, 3192.8, 3197, 3258, 3284.5, 3321, 3372, 3501, 3515.1
TFB	790.4	3558.2	6	3598, 3659, 3706, 3724.0, 3850, 3908.2
TLR	428.6	3920.0[c]	24	3941[c], 3956.9, 3969.9, 3992, 3997, 4095, 4150.4, 4208, 4222.1, 4296, 4342, 4401, 4408.4, 4471.0, 4504, 4578.2, 4612, 4700, 4758.4, 4805, 4849.0, 4877, 4913, 4917.0
TTA	-591.6	4940.2	19	4946.4, 4969.0, 4998, 5002.3, 5026, 5045.0, 5094, 5097.9, 5115.5, 5127, 5141.5, 5142.2, 5167, 5187.0, 5213, 5265.6, 5296, 5312, 5316.0
TTB	-971.4	5320.0	5	5349, 5373.7, 5400, 5413, 5416.6
TTC	-1085.4	5434.0	21	5438.2, 5454.1, 5496.1, 5498, 5517.3, 5540.0, 5558.7, 5600.0, 5637, 5642.0, 5680, 5728.0, 5747, 5841.0, 5848, 5894.3, 5929.8, 5944.9, 5948, 5980.0, 5984.7
T.D.	-1651.4	6000.0	140	
				UE-25a#1 [Contacts from Spengler et al. (1979). Sample number of Sykes et al. (1979) in parentheses.]
TCP	2097.1	1835.7	9	1852 (YM43), 1869 (YM44), 1930 (YM45), 2002 (YM46), 2088 (YM47), 2114 (YM48), 2220 (YM49), 2305 (YM50), 2332 (YM51)
TCB	1599.6	2333.2	3	2361 (YM52), 2419 (YM53), 2491 (YM54)
T.D.	1432.2	2500.6	12	
				J-13 [Contacts from Byers and Warren (1983). Sample number of Heiken and Bevier (1979) in parentheses.]
TCP	1578	1740	1	1882 (JA25), 1992 (JA26)
TCB	1303	2015[a]	3	2135 (JA29), 2175 (JA30)
TCT	998	2320[b]	5	2382 (JA31), 2535 (JA32), 2680 (JA33), 2980 (JA34), 2997 (JA35)
TLR	98	3220[d]	2	3253 (JA36), 3493 (JA37)
T.D.	-180	3498	11	

[a] Bedded tuff beneath TCP ash flow included with TCB unit.
[b] Bedded tuff beneath TCB ash flow included with TCT unit.
[c] Bedded tuff beneath TFB lava included with TLR unit.
[d] Bedded tuff beneath TCT ash flow (thickness 20 ft) included with TCT unit.

TABLE IV

SUMMARY OF PETROGRAPHY FOR CORE SAMPLES OF USW G-1, DETERMINED BY POINT COUNT OF GLASS-COVERED THIN SECTIONS

(See Table II for definition of symbols; ppmV = parts per million by volume.)

Sample depth (ft)	Unit	Rock type	Alteration	Points counted	Major components, vol%		Felsic phenocrysts, relative %			Mafic phenocrysts, ppmV				ppmV Fe-Ti Oxide	Accessory minerals, grains identified			
					Lithics	Felsics	Q	K	P	Biot	Hbld	Cpx	Opx		Sph	All	Ap	Zr
1561.8	TH1	nwt	Zc	3750	2.8	2.2	43	16	41	270	0	0	0	0	0	0	0	0
1689.5	TH1	nwt	Zc	8000	1.8	2.0	51	24	25	375	0	0	0	125	0	0	0	4
1811.7	TCP	pwt		3600	0.14	6.2	15	53	32	<280	0(ps)	0	1900(ps)	560	0	0	0	4
1943.4	TCP	mwt	VP	3300	0.45	14.4	13	39	48	<280	0	0	910(ps)	610	0	0	0	8
2009.8	TCP	pwt		3750	2.6	7.9	15	47	38	<280	<280	0	2100(ps)	530	0	1	rare	5
2124.7	TCP	nwt		3600	0.6	8.8	6	50	44	280	0(ps)	0	0	1100	0	2	rare	7
2231.0	TCBu	pwt		3700	0.03	12.2	22	36	42	2700	1300(ps)	0	0	810	0	0	rare	9
2246.0	TCBu	p-mwt		3000	0.00	11.8	19	45	36	4300	1000(ps?)	0	0	1700	0	0	gone	7
2300.4	TCBu	pwt		3750	0.00	13.6	24	31	45	1600	2400(ps)	0	0	1600	0	0	rare	13
2354.6	TCBm	mwt	Gr	3750	0.03	14.6	27	30	43	3500	2400(ps)	0	0	1900	0	0	rare	10
2397	TCBm	pwt'	VP	3750	0.2	13.0	23	32	45	5300	1300(ps)	0	0	530	0	0	rare	7
2461.5	TCBl	mwt	VP	3650	0.9	7.1	5	44	51	2200	1600(ps)	0	0	550	0	0	rare	8
2470.6	TCBl	pwt	VP	3700	1.6	8.3	18	29	53	4900	1100(ps)	0	0	1300	0	0	rare	10
2478.3	TCBl	pwt	VP	3750	0.5	10.0	14	39	47	4000	530(ps)	0	0	270	0	0	rare	5
2507	TCBl	mwt		3700	1.2	9.6	13	36	51	4100	3200(ps)	0	0	2400	0	0	rare-sparse	12
2555	TCBl	mwt	Zc	3520	0.8	9.9	9	40	51	2300	2300	280(ps?)		280	0	0	shot?	5
2594.2	TCBl	pwt		3750	2.2	7.1	17	32	51	4300	270(ps)	0	0	800	0	4	rare	10
2678.0	TCTu	pwt		3980	1.3	7.5	15	34	51	7300	0	0	0	1000	2	1	sparse	6
2772.6	TCTu	pwt		3800	2.1	10.2	29	34	37	5800	———	1600(ps?)	———	530	0	0	sparse	5
2851.7	TCTu	mwt		3900	4.5	13.6	41	37	22	4400	0	0	0	1800	0	0	rare	11
2869	TCTu	m-dwt		3360	3.8	12.1	41	35	24	6000	0	0	0	890	0	0		7
2931.4	TCTu	m-dwt		4000	3.3	12.8	37	32	31	7000	0	0	0	500	0	0		9
3013.9	TCTu	pwt		3500	12.3	12.9	27	44	29	4900	:(ps)	0	0	860	0	10		>2

Table IV (cont)

Sample depth (ft)	Unit	Rock type	Alteration	Points counted	Major components, vol%: Lithics	Felsics	Felsic phenocrysts, relative %: Q	K	P	Mafic phenocrysts, ppmV: Biot	Hbld	Cpx	Opx	ppmV Fe-Ti Oxide	Accessory minerals, grains identified: Sph	All	Ap	Zr
3192.8	TCT1	pwt		3600	23.8	9.4	33	30	37	4200	0	0	0	280	0	0	many	3
3197	TCT1	mwt		3460	22.3	7.4	38	29	33	3200	0	0	0	<280	0	0	?	3
3284.5	TCT1	pwt	Ar,(cc)	3600	9.0	8.6	35	31	34	3300	0(ps)	0	0	1700(py)	0	4	alt.	>8
3515.1	TCT1	pwt		3800	25.8	8.3	34	22	44	2900	260(ps)	0	0	1300(py)	0	1	pres.	pres.
3724.0	TFB	fb	Gl,0	3700	0.00	8.8	0.0	0.0	100	0	11100	15100(ps)		8100	0	0	large	0
3908.2	TFB	fb	Gl	3150	0.00	10.0	0.0	0.0	100	0	7900	2500	8200(ps)	5700	0	0	large	0
3956.9	TLR	pwt	Ar												2	2	pres.	pres.
3969.9	TLR	mwt	Ar	3300	9.0	17.5	2	34	64	5500	0(ps?)	0	0	2400	11	3	pres.	pres.
3992	TLR	pwt		3500	26.5	11.3	4	31	65	9700	0	0	0	2000	12	1	pres.	pres.
4150.4	TLR	pwt		3400	13.8	8.5	2	35	63	1200	0	0	0	600	6	1	rare	8
4222.1	TLR	pwt		3200	42.7	6.1	7	40	53	1600	0	0	0	1600	6	0	sparse	5
4408.4	TLR	pwt		1800	11.8	9.2	1	37	62	5000	0	0	0	1100	1	1	rare	7
4471.0	TLR	pwt		3600	26.4	5.1	7	36	57	3600	0	0	0	560	8(ps)	1	pres.	12
4578.2	TLR	pwt		3800	23.8	7.6	5	39	56	2600	0	0	0	530	2(ps)	2	sparse	9
4758.4	TLR	pwt		3900	19.0	9.2	9	38	53	2600	0	0	0	1500	6(5ps)	0	sparse	10
4849.0	TLR	pwt		3900	13.0	8.9	10	35	55	3300	0	0	0	1000	7(ps)	0	shot	10
4917.0	TLR	nwt		3800	5.9	5.6	14	51	35	3200	0	0	0	1800	11(ps)	3	present	12
4946.4	TTA	nwt		3450	4.4	9.8	20	58	22	3000	0	0	0	300	4(ps)	2		12
4969.0	TTA	pwt		3700	3.1	11.9	24	31	45	4900	0	0	0	2700	5(ps)	0	partly shot	10
5002.3	TTA	nwt		3700	2.5	17.0	32	31	37	5100	0	0	0	2400	3(ps)	3	rare	13
5045.0	TTA	mwt		3700	8.9	19.9	28	43	29	4100	0	0	0	1900	2(1ps)	0	1 μph	19
5097.9	TTA	mwt		3600	0.58	17.4	28	41	31	2200	0	0	0	2000	1(ps)	3	rare	10
5115.5	TTA	mwt		3750	3.1	18.3	24	42	34	4800	0	0	0	1900	2	11	sparse	20
5141.5	TTA	mwt		3700	9.2	14.1	27	33	40	2100	0	0	0	1200	4	4	sparse	15
5142.2	TTA	pwt		3750	2.2	19.4	28	36	36	3700	<270	0	0	1900	7	5	present	13
5187.0	TTA	nwt		3650	2.1	17.6	24	38	38	1600	270	0	0	2200	6	7	sparse	26
5265.6	TTA	pwt		3400	5.4	17.4	35	31	34	2400	590	0	0	1800	6	8	sparse	17
5316.0	TTA	b		3600	2.4	21.6	33	36	31	1400	0	0	0	2800	4	12	rare	13
5373.7	TTB	pwt		3650	0.69	11.3	13	26	61	9000	0	0	0	3300	15	1	sparse	20
5400.0	TTB	pwt		3800	2.3	13.6	12	30	58	4500	0	0	0	3200	8	1	sparse	24
5416.6	TTB	pwt		3700	12.8	11.2	11	27	62	2700	0(ps?)	0	0	3200	5	1	rare, shot	20

Table IV (cont)

Sample depth (ft)	Unit	Rock type	Alter-ation	Points counted	Major components, vol%: Lithics	Felsics	Felsic pheno-crysts, relative %: Q	K	P	Mafic phenocrysts, ppmV: Biot	Hbld	Cpx	Opx	ppmV Fe-Ti Oxide	Accessory minerals, grains identified: Sph	All	Ap	Zr
5438.2	TTC	pwt		3900	0.74	12.9	1	3	96	12000	0	0	0	4600	0	1	pres.	50
5454.1	TTC	b		3800	1.9	14.9	16	18	66	7100	0	0	0	5000	9	9	sparse	42
5496.1	TTC	pwt		3900	7.5	10.1	1	4	95	21000	0	0	0	4900	8	3	sparse	21
5517.3	TTC	pwt		3600	10.3	11.8	2	9	89	11400	0	0	0	4500	9	2	sparse	20
5540.0	TTC	pwt		3700	8.5	13.5	0.4	0.0	99.6	19200	810(ps)	0	0	4300	1	0	sparse-comm	29
5558.7	TTC	pwt		3600	0.64	19.1	4	4	92	16400	1100(ps)	0	0	5300	12	3	sparse(large)	20
5600.0	TTC	mwt		3750	8.4	14.8	5	7	88	10100	800(ps)	0	0	6400	16	4	sparse	24
5642.0	TTC	mwt		3300	5.8	15.4	2	4	94	21500	1500(ps)	0	0	5800	12	3	sparse	22
5728.0	TTC	mwt		1650	21.1	21.6	0.0	1	99	18200	0(ps)	0	0	7900	4	3	sparse(lrg)	24
5841.0	TTC	mwt		1650	10.8	18.0	0.0	4	96	12100	600(ps?)	0	0	8500	3	1	sparse-comm	26
5894.3	TTC	mwt		1650	7.2	15.5	0.0	4	96	6100	6100	0	0	3600	6	1	sparse	14
5929.8	TTC	mwt		1650	5.9	18.2	4	4	92	13300	5500(ps)	0	0	6100	7	8	sparse-comm	24
5944.9	TTC	m-dwt		1600	6.3	21.6	1	6	93	6900	7500(ps)	0(ps)	0	5000	8	5	sparse-comm	24
5980.0	TTC	m-dwt		1650	3.3	20.9	0.0	0.3	99.7	24200	7300(ps)	1800(ps)	0	7300	4	1	sparse-comm	24
5984.7	TTC	m-dwt		1650	2.3	25.3	0.0	0.0	100	27200	8500(ps)	1200(ps)	0	9700	1	3	sparse-comm	25

TABLE V

SUMMARY OF PETROGRAPHY FOR OUTCROP SAMPLES AND CORE SAMPLES OF USW G-1, UE25a#1, AND J-13, DETERMINED BY POINT COUNT OF POLISHED THIN (PROBE) SECTIONS.
(See footnotes for explanation of asterisks and Table II for definition of symbols; ppmV = parts per million.)

Sample no. depth (ft)	Unit	Rock type	Alteration	Probe section area (mm^2)	Points counted	Major components, vol%: Voids	Pumice	Lithics	Felsics	Felsic phenocrysts, relative%: Q	K	P	Mafic phenocrysts, ppmV: Biot	Hbld	Cpx	Opx	ppmV Fe-Ti Oxide	Accessory minerals, ppmV: Sph	All	Per	Ap	Zr	Other
USW G-1-1191	TPT1	dwt	mVp	775	500	0.0	32	1.2	1.8	1*	8*	91*	290	0	0	0	590	0	280	0	8	21	
-1240	TPT1	dwt	Ax,Gr,Sp	659	500	0.0	27	3.2	2.6	5*	13*	82*	280	0	0	0	460	0	0	0	8	17	
-1286	TPT1	dw-vt	Sp,Gr,Ar,Zc	746	500	0.4	13	10	1.7	16*	46*	38*	180	7	0	0	310	0	0	0	9	6	
-1292	TPT1	vt	Gl	769	539	0.0	22	4.5	0.9	10*	17*	73*	200	0	0	0	170	0	2	0	2	0.8	
-1392	TPT1	pwt	Gl	453	500	8.6	20	1.2	0.6	3*	7*	90*	280	0	0	0	160	0	0	0	6	13	
USW G-1-1436	TH1	nwt	Zc	727	500	11	29	3.2	4.8	56*	22*	22*	210	0	0	0	170	0	8	0	0.4	4	
-1561	TH1	nwt	Zc	651	500	5.0	47	2.8	2.4	52*	22*	26*	300	0	0	0	110	0	0	0	0.2	2	
-1639	TH1	nwt	Zc	516	500	2.4	40	1.4	3.6	58*	17*	25*	150	0	0	0	320	0	0	0	0.2	12	
USW G-1-1774	TH2	b	Zc	602	500	3.4	25	3.0	25	32*	14*	54*	3000*	0	0	0	1100*	0	0	0	17	53	a
USW G-1-1820	TCP	pwt	Zc	610	500	2.6	21	1.4	7.8	12*	43*	45*	210	0	0	UA	450	0	0	0	8	10	
-1854	TCP	pwt	Zc	712	486	3.1	25	1.0	11	15*	39*	46*	500	3	0	UA	660	0	0	0	7	28	
-1884	TCP	pwt	Ax/Sp	579	500	0.4	26	1.0	16	13*	46*	41*	580	0	0	UA	1200	0	0	0	0	26	
-1983	TCP	p-mwt	Ax/Sp	707	500	1.0	24	0.4	11	8*	49*	43*	1A	0	0	0	1300	0	0	0	0.7	9	
-2083	TCP	pwt	Zc	673	500	3.8	21	0.6	9.6	10*	42*	48*	ps	0	0	OA	630	0	62	0	0.7	13	
UE-25a#1-1852	TCP	wt	mVP		298	0.0	43	0.7	9.0[b]														
-1869	TCP	wt	mVP		300	0.0	36	0.0	9.6														
-1930	TCP	wt	mVP		505	9.3	9.9	0.6	13														
-2002	TCP	dwt	Sp		300	0.0	31	0.3	13														
-2088	TCP	nwt	Zc		300	0.0	18	5.0	13														
-2114	TCP	nwt	Zc		501	0.4	24	1.4	7.8														
-2220	TCP	nwt	Zc		461	0.0	11	1.7	8.3														
-2305	TCP	nwt	Zc		300	0.0	18	5.0	9.4														
-2332	TCP	b	Zc		300	0.0	2.7	2.0	6.0														
J-13-1882	TCP	pwt	Ax(cc)	675	300	0.0		1.0	19	17*	40*	43*	1200	0	0	OA	A	0	0	0	22	34	
-1992	TCP	b	Za		300	0.0		1.0	18														
RWG2a-3	TCP	dwt	Gl,Gr	530	516	0.0	23	0.8	16	14	45	41	860	310	0	4800	1400	0	350	0	56	46	
RW31a-6	TCP	nwt	VP	614	597	13		0.2	4.9	28	31	41	150	13	0	UA	1200*	0	9	0	12	23	

TABLE V (cont)

Sample no. depth (ft)	Unit	Rock type	Alteration	Probe section area (mm^2)	Points counted	Major components, vol% Voids	Pumice	Lithics	Felsics	Felsic phenocrysts, relative% Q	K	P	Mafic phenocrysts, ppmV Biot	Hbld	Cpx	Opx	ppmV Fe-Ti Oxide	Accessory minerals, ppmV Sph	All	Per	Ap	Zr	Other
USW G-1-2166	TCBa	b	Zc	649	527	0.4	41	2.6	9.1	0	52	48	880	0	0	0	950	0	0	0	0.5	13	
USW G-1-2233	TCBu	nwt	Zc	552	500	2.2	20	0.4	15	32*	26*	42*	2700	0.9A	0	0	660	0	0	0	0.9	14	
-2247	TCBu	nwt	Zc	419	500	3.4	16	0.4	12	32*	29*	39*	3200	0	0	0	1600	0	0	0	0.5	27	
-2289	TCBu	nwt	Zc	659	500	1.4	15	1.0	14	13*	29*	58*	2900*	ps	0	0	2200*	0	0	0	8	26	c
-2291	TCBu	nwt	Zc	490	500	3.0	20	0.6	13	33*	32*	35*	2000	ps	0	0	820	0	0	0	4	17	
USW G-1-2318	TCBm	nwt	Sp/Gr	544	500	4.8	28	0.0	25	31*	33*	36*	4200*	0	0	0	2100*	0	0	0	17	87	
-2363	TCBm	pwt	Sp/Gr	601	500	0.4	26	0.2	20	22*	40*	38*	2800*	ps	0	0	1700*	0	0	0	45	40	
-2411	TCBm	pwt	Sp/Gr	637	431	0.9	13	3.0	16	22*	34*	44*	2400*	ps	0	0	920	0	0	0	27	82	
USW G-1-2436	TCBl	mwt	Sp/Gr	640	500	0.0	39	0.6	10	12*	39*	49*	2900*	ps	0	0	1800*	0	0	0	54	43	
-2477	TCBl	p-mwt	Sp/Gr	676	459	0.0	20	0.9	8.3	13*	33*	54*	2800*	ps	0	0	1400*	0	0	0	41	66	
-2486	TCBl	p-mwt	Ax/Sp	655	500	0.0	17	5.2	9.6	6*	52*	42*	2200*	ps	0	0	1300*	0	0	0	28	12	
-2555	TCBl	p-mwt	Zc	755	2516	0.6	15	2.3	11	7	45	48	1700*	2300*	0	0	820	0	0	0	33	32	
-2601	TCBl	pwt	Zc	769	500	1.4	8.6	2.0	8.8	11*	39*	50*	1900*	ps	0	0	1100*	0	340	0	26	38	
UE-25a#1-2361	TCB	wt	Sp/Gr		326	1.5	17	0.0	12														
-2419	TCB	wt	Sp/Gr		304	0.7	8.4	0.0	17														
-2491	TCB	wt	Sp/Gr		488	0.0	45	0.0	16														
J-13-2135	TCB	pwt	Sp		301	0.3		0.3	20														
-2175	TCB	mwt	Gr	671	300	0.0		0.0	24	26*	39*	45*	3700*	0	0	0	1300*	0	0	0	54	34	
RWG2a-4	TCB	nwt	mVP	521	509	16		0.2	8.4	18	42	40	3400*	ps	0	0	1600*	0	0	0	80	28	
-5	TCB	mwt	mVP	569	462	3.7		0.0	15	22	39	39	4600*	ps	0	0	1800*	11A	0	0	79	67	
CF LSM-1	TCB	mwt	Sp,Gr	847	516	0.8	14	2.5	11	24	38	38	1700	0	0	0	1500	0	0	0	15	11	
-5	TCB	pwt	Zc,Ar	591	480	0.2	11	4.4	15	15	32	53	3600	290A	0	0	1100	0	0	0	24	15	
TBF-4	TCB	nwt	VP	688	558	0.5	15	1.1	9.0	20	31	49	2700*	2400*	0	0	1800*	0	440	0.3	130	71	
-1	TCB	vt	Gl,Ax	760	464	0.2	41	1.5	13	12	32	56	3700*	1300*	0	0	4500*	420	150	0	120	91	
RWRyb-3	TCB	p-mwt	Gr	629	614	2.3		0.5	10	30	36	34	1900*	0	0	0	540	0	0	0	18	26	
USW G-1-2641.5	TCTu	pwt	Zc	600	500	2.8	12	1.6	14	12*	32*	56*	5700*	0	0	0	2000*	0	0	0	43	25	
-2699	TCTu	pwt	Zc	644	500	5.2	31	1.0	10	48*	31*	21*	5200*	0	0	0	1700*	0	0	0	92	25	
-2790	TCTu	pwt	Sp/Gr	443	599	6.5	11	9.3	9.2	68*	17*	15*	3400*	0	0	0	630	0	0	0	32	20	
-2854	TCTu	p-mwt	Sp/Gr	538	441	3.4	31	2.0	12	65*	26*	9*	3400*	0	0	0	980*	0	0	0	46	39	
-2869	TCTu	mwt	Sp/Gr	641	2023	3.6	23	4.4	14	40	35	25	4500*	0	0	0	1000*	0	0	0	73	48	
-2901	TCTu	dwt	Sp/Gr	710	500	1.4	18	2.0	15	56*	25*	19*	3700*	0	0	0	1100*	0	0	0	70	9	
-2938	TCTu	m-dwt	Ax	608	425	0.5	35	1.9	11	43*	38*	19*	6300*	0	0	0	1400*	0	0	0	89	61	
-3001	TCTu	dwt	Ax	718	500	6.4	16	5.4	15	45*	30*	25*	3200*	0	0	0	1900*	0	0	0	63	68	

7

TABLE V (cont)

Sample no. depth (ft)	Unit	Rock type	Alteration	Probe section area (mm^2)	Points counted	Major components, vol%				Felsic phenocrysts, relative%			Mafic phenocrysts, ppmV				ppmV Fe-Ti Oxide	Accessory minerals, ppmV					
						Voids	Pumice	Lithics	Felsics	Q	K	P	Biot	Hbld	Cpx	Opx		Sph	All	Per	Ap	Zr	Other
USW G-1-3117	TCT1	pwt	Za	709	500	4.6	12	21	12	68*	13*	19*	1400*	0	0	0	A	0	90	0	36	13	
-3197	TCT1	nwt	Zc/py	689	2154	0.8	9.7	27	8.9	29	29	42	2500	0	0	0	22A	0	0	0	13	8	
-3258	TCT1	nwt	Zc/py	707	2157	0.0	9.1	20	10	34	33	33	2300*	0	0	0	16A	0	68	0	18	13	
-3321	TCT1	nwt	Za/py	718	500	2.2	4.4	23	12	68*	19*	13*	2100*	0	0	0	250A	0	180	0	22	5	d
-3372	TCT1	nwt	Za/py	611	500	0.0	1.6	37	6.4	43*	36*	21*	1900*	0	0	0	0A	0	30	0	3	2	
-3501	TCT1	pwt	Za/py	693	500	0.2	6.6	34	9.8	40*	19*	42*	1500	0	0	0	0A	0	120	0.3	28	8	
J-13-2382	TCT	nwt	Za	667	300	0.0		1.3	7.0	25*	34*	41*	4800*	0	0	0	2400*	33	0	0	130	48	
-2535	TCT	wt	Za		300	1.0		0.0	11														
-2680	TCT	wt	Sp		300	0.0		6.3	8.6														
-2980	TCT	mwt	Sp(cc)	559	300	0.0		5.3	13	40*	26*	34*	3500*	0	0	0	1900*	0	0	0	73	42	
-2997	TCT	wt	Sp(cc)		300	1.7		10	9.0														
RWBWa-5	TCT	mwt	Sp/Gr	479	467	0.4		0.0	12	24	40	36	3700*	0	0	0	1400*	0	310	0	120	66	
RWRyb-1	TCT	mwt	Zc,Ar	815	497	3.6		8.0[e]	12	34	31	35	4100*	0	0	0	520*	0	46	0	58	26	
USW G-1-3598	TFB	fb	Zc,Q,cc	770	500	0.0	0.0	0.0	11[f]	0*	0*	100*	0	2300*	1200*	ps	2100*	0	0	0	440	0.1	
-3659	TFB	fb	Ar	703	500	0.0	0.0	0.0	17[f]	0*	0*	100*	0	9500*	2700*	11300*	4500*	0	0	0	1300	0.4	
-3706	TFB	fb	Zc,Q	843	500	0.0	0.0	0.0	18[f]	0*	0*	100*	0	1500A	ps	ps	2300*	0	0	0	1700	0	
-3850	TFB	fb	Zc,Q,Ar	752	500	0.0	0.0	0.0	17[f]	0*	0*	100*	1	2400A	250A	ps	3200*	0	0	0	880	0	
USW G-1-3941	TLRa	b	Ar	830	599	0.3	17	6.8	15	0*	0*	100*	3200*	600*	0	0	A	9	0	1	29	3	
USW G-1-3997	TLR	nwt	Za	833	577	4.8	6.9	13	13	6*	58*	36*	5400*	0	0	0	2400*	230	0	3	110	68	
-4095	TLR	nwt	Za	798	597	1.7	9.5	26	10	2*	45*	53*	1100*	0	0	0	1200*	200	170	4	22	18	
-4208	TLR	nwt	Za	869	610	0.0	6.2	39	9.5	0*	71*	29*	1900*	0	0	0	1100*	200	180	0	54	28	
-4296	TLR	nwt	Za	910	675	0.9	8.6	19	12	8*	70*	22*	1600*	0	0	0	1500*	84	20	6	44	23	
-4342	TLR	nwt	Ab,Za	827	557	0.4	10	10	13	7*	35*	58*	1900*	6	0	0	1600*	190	66	3	65	64	
-4401	TLR	nwt	Za,Ab	826	560	7.1	9.3	17	10	1*	67*	32*	1800*	0	0	0	1800*	30	15	2	110	88	
-4504	TLR	nwt	Za	858	629	1.3	11	20	8.2	5*	68*	28*	2900*	0	0	0	1600*	0	0	0	76	31	
-4612	TLR	nwt	Za	884	650	0.0	6.6	30	9.0	3*	47*	49*	2000*	0	0	0	1100*	0	43	0	45	4	
-4700	TLR	pwt	Za	832	579	4.8	12	19	7.1	10*	35*	55*	1800*	0	0	0	880*	0	0	0.05	40	13	
-4805	TLR	pwt	Za	779	601	0.0	10	19	13	1*	44*	55*	3000*	0	0	0	1600*	0	59	0	83	45	
-4877	TLR	pwt	Za(cc)	907	656	0.3	11	11	8.6	6*	50*	44*	2700*	0	0	0	730*	0	18	0	13	26	
-4913	TLR	pwt	Za	808	553	0.0	13	9.6	6.9	12*	50*	38*	1200*	0	0	0	1000*	0	0	0	40	27	
J-13-3253	TLR	nwt	Ab		307	0.0		12	12														
-3493	TLR	mwt	Zc(cc)	636	300	1.7		11	12	4*	45*	48*	2200	0	0	0	1800	0	260	0	65	40	
RWBWa-4	TLR	mwt	Ar	575	467	8.3	4.3	19	6.6	3	39	58	1600	0	0	0	590	0	0	0	26	24	

TABLE V (cont)

Sample no. depth (ft)	Unit	Rock type	Alteration	Probe section area (mm²)	Points counted	Major components, vol%				Felsic phenocrysts, relative%			Mafic phenocrysts, ppmV				ppmV Fe-Ti Oxide	Accessory minerals, ppmV					
						Voids	Pumice	Lithics	Felsics	Q	K	P	Biot	Hbld	Cpx	Opx		Sph	All	Per	Ap	Zr	Other
USW G-1-4998	TTA	b	Ar,Ab,Za	784	457	4.4	18	4.2	20	37*	31*	32*	4000*	0	0	0	1500*	0	210	0	100	54	
-5026	TTA	pwt	Ab	866	650	0.0	22	1.8	16	34*	40*	26*	2200*	0	0	0	1600*	0	0	0	74	37	
-5094	TTA	pwt	Ab,Za	792	546	0.2	28	2.0	13	49*	19*	32*	1700*	0	0	0	1800*	0	46	0	88	84	
-5127	TTA	pwt	Za	858	632	0.0	19	3.5	23	29*	33*	38*	2300*	0	0	0	2300*	62	140	0	110	42	
-5167	TTA	nwt	Za,Ab,cc	840	688	0.9	14	15	18	22*	42*	36*	880*	730*	0	0	2000*	200	210	0	70	25	
-5213	TTA	pwt	Za	802	571	0.0	21	7.5	21	39*	36*	25*	2300*	160*	0	0	2400*	51	270	0	100	66	
-5296	TTA	pwt	Za,Ab	760	584	1.0	32	2.7	19	23*	55*	22*	2400*	830*	0	0	2400*	210	130	0	84	57	
-5312	TTA	b	Ab,Za	748	626	0.3	16	3.8	14	35*	46*	19*	940*	0	0	0	1800*	58	66	0	32	17	
USW G-1-5349	TTB	b	Ab(cc)	469	421	0.0	22	20	17	13*	16*	71*	1900*	0	0	0	3300*	65	46	0	100	20	
-5413	TTB	pwt	Za,Ab	763	610	0.2	18	11	17	44*	8*	48*	5600*	0	0	0	2200*	110	130	42	130	33	g
-5498	TTC	pwt	Za,Ab	749	622	0.3	25	6.8	14	0*	8*	92*	5400*	0	0	0	3100*	47	160	0	210	78	
-5637	TTC	mwt	Za,Ab,cc	783	659	0.1	4.6	5.9	16	0*	5*	95*	10500*	ps	0	0	4100*	110	45	0	260	56	
-5680	TTC	b	Za	758	660	0.3	23	5.9	20	0*	2*	98*	3800*	470A	0	0	3800*	200	410	0	200	66	
-5747	TTC	pwt	Za,Ab	747	583	1.4	16	6.3	27	0*	0*	100*	9900	0	0	0		55	65	0			
-5848	TTC	pwt	Ab	819	627	0.0	15	20	23	0*	10*	90*	6200*	0	0	0	4700*	10	15	0	210	98	
-5948	TTC	pwt	Za,Ab	795	636	0.0	13	4.2	23	0*	12*	88*	5200*	340A*	0	0	4700*	0	0	30	180	50	

[a] 6 ppmV monazite.
[b] Plagioclase phenocrysts completely altered and not included in total.
[c] 0.1 ppmV monazite.
[d] 8 ppmV anatase.
[e] 3.8% from a single lithic.
[f] Includes microphenocrysts.
[g] 2 ppmV tourmaline.

(Explanation of asterisks: a) Relative phenocryst proportions: such proportions are based on relative areas of the largest 30+ felsic phenocrysts.

b) Mafic and Fe-Ti oxide phenocrysts: such concentrations, given in parts per million by volume (ppmV), are obtained by extrapolating concentrations determined for the largest phenocrysts alone. The extrapolations are based on a comprehensive reference data set. For mafic minerals, the areas measured for the largest phenocrysts generally represents >75% of the total mafic phenocryst area, and for Fe-Ti oxides, 50-80%.

IV. ANALYTICAL TECHNIQUES

Analysis by electron microprobe consisted of two phases: first, qualitative (energy-dispersive) spectroscopy (EDS) and second, quantitative (wavelength-dispersive) analysis. All samples for which mineral compositions have been determined have also been analyzed by EDS.

EDS results in the simultaneous measurement and display of x-ray intensities vs x-ray energies for all elements that have atomic numbers $(Z)\geq 11$ (sodium). The display is highly distinctive for each primary mineral encountered in volcanic rocks of the NTS; representative spectra for some such minerals commonly found in NTS rocks are shown in Fig. 2. Grains as small as 0.00005 mm^2 were routinely analyzed by EDS for this study. Essentially 100% accuracy in mineral identification is assured by this procedure.

Following EDS, at least eight grains each of sanidine and plagioclase, and several grains of each type of mafic mineral present were analyzed by wavelength-dispersive analysis. Three grains each of sanidine and plagioclase were analyzed at spots near the center (core), edge (rim), and midway between center and edge (mid). The remaining feldspar phenocrysts were analyzed at a single spot near the center. It is important, particularly for biotite and secondary minerals or glass, to select the best spots available for analysis during petrographic study; guidelines are presented with the discussion of phenocryst alteration.

Although a wide range in compositions is obtained for plagioclase in most units, a distinct dominant composition prevails, characterized by a narrow compositional range. The dominant composition (equivalent to the statistical mode in a frequency diagram of plagioclase compositions) is most frequently found at plagioclase rims, and is considerably more useful for purposes of stratigraphic correlation than other compositions for plagioclase. Subsequent to this study, procedures have been modified to optimize the probability for analyzing plagioclase grains at spots where the dominant composition exists. Currently, those plagioclase grains analyzed at a single spot are analyzed within 5-20 microns from the rim, rather than at the core. All spots for plagioclase analyses are selected during petrographic analysis; core analyses are obtained where zoning originates, and rim analyses are obtained where zoning terminates at a euhedral edge. Because most plagioclase phenocrysts in tuffs have been broken during eruption, zoning may originate

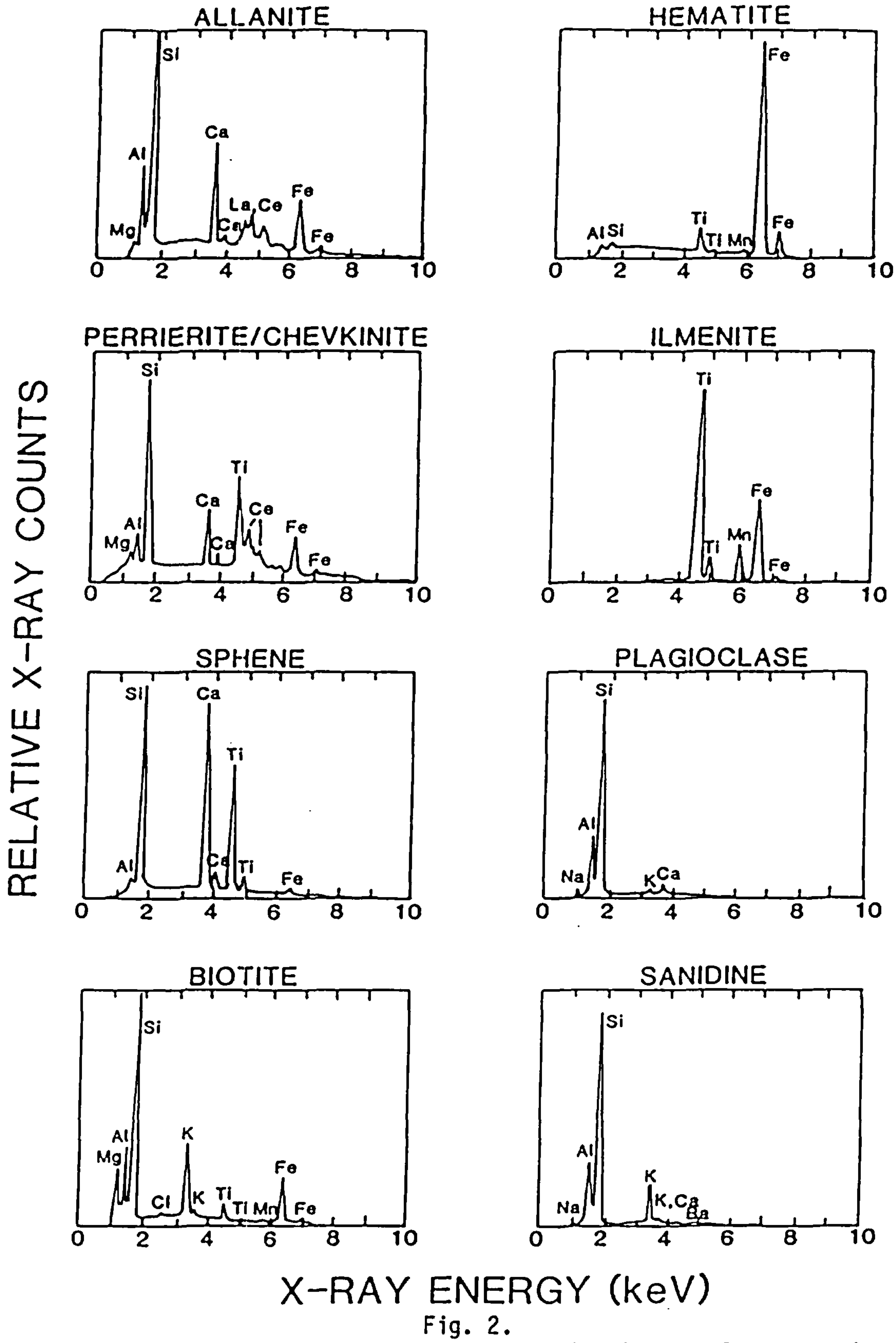

Fig. 2.

Representative energy-dispersive spectra produced by electron microprobe analysis for several minerals commonly found in NTS volcanic rocks.

from an edge, and failure to pre-select spots for analyses results in a less reliable determination of the nature of zoning in plagioclase.

All analyses for this report were determined by employing well-analyzed feldspar and pyroxene standards, and using standard correction procedures (Bence and Albee 1968). There is a small interference for Ti from Ba because of incomplete resolution of the Ti Kα and Ba Lα lines by the PET crystal used for analysis. All analyses reported herein have been corrected for this interference, which results in an apparent 0.10% TiO_2 per 1.19% BaO. The correction is about 2% for most biotite analyses reported herein, and is insignificant for other mafic minerals.

V. PETROGRAPHIC RESULTS

The combined petrographic results of Tables IV and V for USW G-1 are summarized in Table VI. Discussion emphasizes petrographic results for USW G-1 because of the excellent stratigraphic control available (Spengler et al. 1981).

A. Lithic Fragments

The volume contents of lithic fragments are quite similar within each unit or portion of each unit (Fig. 3); median lithic contents are given in Table VI. The median contents of the TCTl unit (23%) and TLRu and TLRl units (16 and 19%, respectively) in USW G-1 are notably higher than those for all other units (0-6.3%, excluding the value of 11% for the TTB unit), and indicate that the volcanic setting for these units differs from those of other units. The only other unit within the extensive volcanic pile on the NTS that has such a consistently high content of lithic fragments is the lithic-rich ash-flow tuff of the tuffs of Area 20 [TRA(lr) unit of Warren 1983]. Warren (1983) presents evidence that a major volcano-tectonic subsidence (VTS) occurred during or shortly after eruption of the TRA(lr) unit. Because of the similarity of lithic contents between the TRA(lr), TCT, and TLR units, the latter two are also considered to occur within a VTS structure. Rocks are intensely pyritized in the lower portion of drill hole UE-19w#1, which is located near the margin of the Silent Canyon VTS structure (Orkild et al. 1969). The extensive pyritic alteration that is confined to the TCTl unit is considered evidence that USW G-1 is sited quite close to a structure formed during eruption of the TCT unit. Additional evidence (based on phenocryst

TABLE VI

MEDIAN VALUES FOR VOLUME CONTENTS OF LITHIC FRAGMENTS AND PHENOCRYSTS IN UNITS OF USW G-1

Unit Symbol	Samples	% lithics	% felsics	Relative proportions, % Q	K	P	Biot ppmV	Biot % of total phenos.	Fe-Ti oxides ppmV	Fe-Ti oxides % of total phenos.	Accessory minerals, ppmV Sph	All	Ap	Zr
TPT1	5	3.2	1.7	5	13	82	280	1.6	310	1.8	0	0	8	13
TH1	5	2.8	2.4	52	22	26	270	1.1	125	0.5	0	0	0.2	4
TH2	1	3.0	25	32	14	54	3000	1.2	1100	0.5	0	0	17	53
TCP	9	0.6	9.6	11	46	43	210	0.2	630	0.7	0	0	0.7	13
TCB(u)	8	0.4	13	24	33	43	2700	2.0	1300	1.0	0	0	0.9	17
(m)	5	0.2	16	23	33	44	3500	2.1	1700	1.0	0	0	27	82
(l)	11	1.2	9.6	11	39	50	2400	2.4	900	0.9	0	0	33	38
TCT(u)	14	2.7	13	34[a]	35[a]	31[a]	5100	3.8	1000	0.7	0	0	67	32
(l)	10	23	8.7	34[a]	30[a]	36[a]	2400	2.7			0	80	20	8
TFB	6	0	14[b]	0	0	100	0[c]	13[c]	3900[b]	2.4	0	0	1100[b]	0
TLR(u)	10	16	12	3[a]	34[a]	63[a]	1900	1.5	1500	1.2	195	43	49	26
(l)	13	19	8.6	8[a]	37[a]	55[a]	2700	3.0	1100	1.2	0	15	45	27
TTA	19	3.5	18	28	39	33	2400	1.3	1900	1.0	55	130	86	48
TTB	5	11	14	13	26	61	4500	3.1	3200	2.2	90	90	120	27
TTC	21	6.3	18	0.5	4	95.5	12000	6.2	5000	2.6	50	55	210	66

[a] Proportions for largest felsic phenocrysts (Table V) clearly differ from those for all felsic phenocrysts (Table IV) and are excluded from median.

[b] Estimates include substantial areas of finely-autobrecciated lava (phenocrysts are not recognizable in these areas). Estimates of Table IV are for phenocrysts only, those of Table V also include groundmass plagioclase.

[c] Median concentrations from 3724.0, 3659, and 3908.2 ft depths of USW G-1 are: Hbld (0.95%), Opx (0.98%), and Cpx (0.26%); these mafics comprise 13% of the total phenocrysts.

compositions) that the TCT and TLR units represent units related to VTS at or near USW G-1 is presented in a following section of the report. Carr (1982), however, considers that the possible caldera for the TCT unit is located considerably west of USW G-1.

Lithic contents for the TCT, TLR, and TTC units decrease within the uppermost portions of each unit, although this occurs only within the uppermost 50 ft of the latter two units in USW G-1. A similar decrease was found for the TRA(lr) unit in Pahute Mesa drill holes UE-19p and U19ab (Warren, in prep.). Lithic contents decrease within the lowest 100 ft of the TLR and TTC units in USW G-1 (although the depth to the base of the TTC unit is unknown).

In many cases, the unit that a lithic fragment was derived from can be confidently identified due to particularly distinct petrographic characteristics or mineral chemistry for the fragment. Mineral analysis by electron microprobe indicates that most lithic fragments within a particular host unit were derived from a single petrologic unit. The angular nature of lithic fragments in these rocks indicates that they were incorporated during eruption, probably from the vent area.

Petrochemical results were obtained for the largest lithic fragments present in samples of the TPT1, TH, and TCB units (Table VII). Those in the TPT1 unit are petrographically similar to the host and also have a similar mineral chemistry (see discussion in a following section) and represent earlier, stratigraphically lower TPT1 or a petrochemically very similar unit. All lithic fragments examined in samples of the TH unit consist of welded tuff that most likely was derived from the underlying TCP unit; although mineral compositions were not obtained from any of these fragments, compositions for sanidine xenocrysts found in the TH unit match those of phenocrysts in the TCP unit (see a following section for discussion of the relationship of xenocrysts to lithic fragments). Two important rock types occur as lithic fragments in samples of the TCB unit; a hedenbergite-bearing rock related to peralkaline units of the Silent Canyon area, and a metamorphic rock (pyroxenite), both in sample TBF-1. The presence of peralkaline lithic fragments establishes that the TCB unit is younger than some peralkaline rocks of the Silent Canyon Area, an age relationship that cannot be otherwise established because of the absence of these peralkaline rocks in the Yucca Mountain area. The pyroxenite (see Appendix F-II for clinopyroxene analyses) is a high-grade metamorphic rock that might conceivably be derived from the magma chamber walls.

B. Felsic Phenocrysts (Quartz, Sanidine, Plagioclase)

Total felsic phenocryst contents are generally quite consistent within each unit of USW G-1 (Fig. 4). Members of the TC and TLR units have median felsic phenocryst contents between 9-16%; median contents for the TT unit are 14-18% (Table VI). Samples of the TPT1 and TH1 units are phenocryst poor, with felsic phenocryst contents from 0.6-4.8% (Fig. 4), but the single sample of TH2 unit contains 25% felsic phenocrysts and is phenocryst rich. Felsic phenocryst contents are slightly, but consistently higher within the upper half of several units, including the TLR unit and all members of the TC unit (see Fig. 4, Table VI). However, samples within the uppermost 50 ft of each unit tend to have slightly lower phenocryst contents than samples beneath (see Fig. 4 for TCP, TCB, and TTA units).

The relative proportions of felsic phenocrysts are also generally consistent within each unit of USW G-1 (see Fig. 5 for quartz and Fig. 6 for

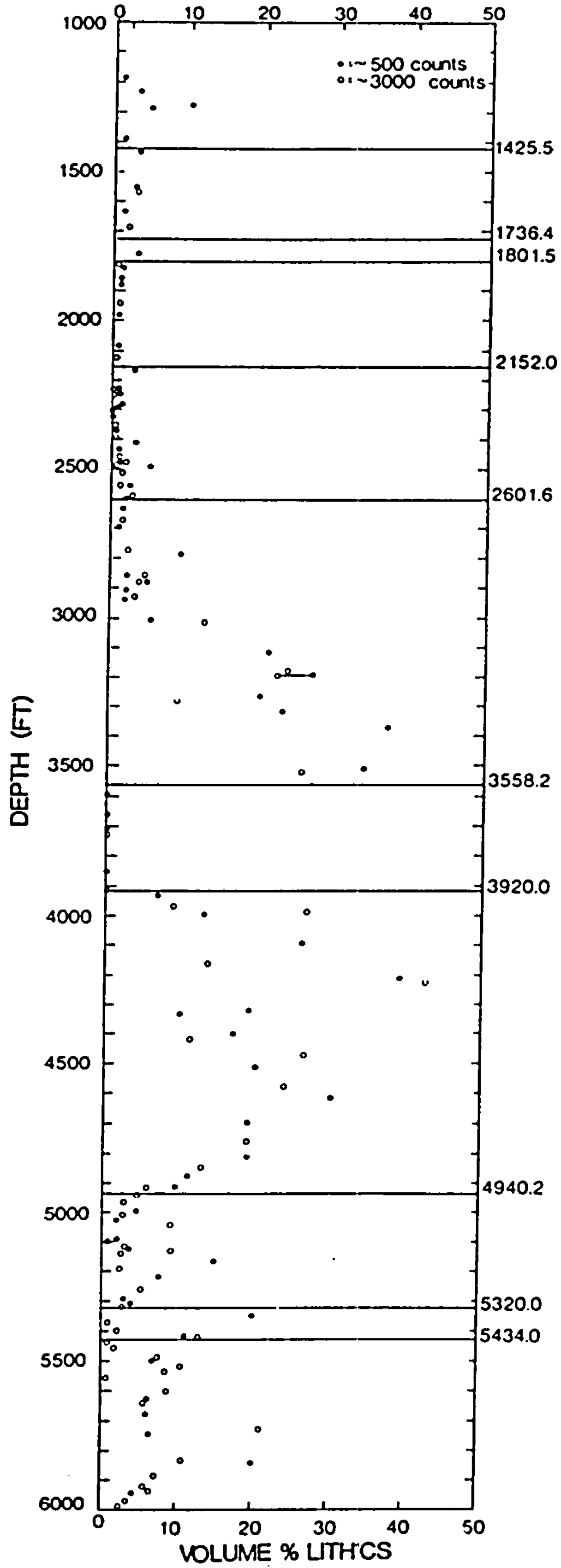

Fig. 3.
Plot of volume content of lithic fragments versus depth for samples from drill hole USW G-1.

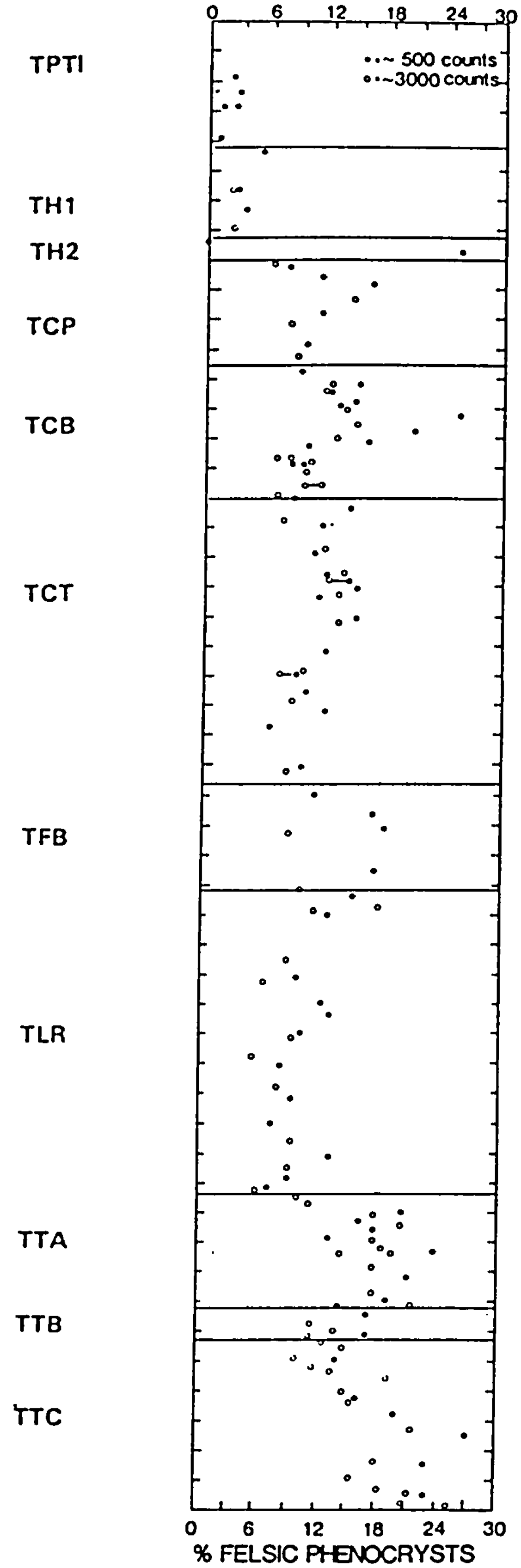

Fig. 4.
Plot of volume content of felsic phenocrysts versus depth for samples from drill hole USW G-1.

TABLE VII

SUMMARY OF PETROGRAPHY FOR LITHIC FRAGMENTS IN SELECTED SAMPLES OF THE TPTl, TH, AND TCB UNITS

Sample number	Host unit: Unit symbol	Host unit: % lithics	n[a]	Lithic Fragments: Total area (mm^2)	Unit symbol[b]	Lithic rock type	Alteration	% felsic phenos.	Relative %: Q	Relative %: K	Relative %: P	ppmV: Biot	ppmV: Hbld	Accessories (size in 0.0001 mm^2)	Analyses[c]
USW G-1-1240	TPTl	3.2	1	14.3	TPTl(?)	pwt	Ax	0						Zr	
-1286	TPTl	10.4	2	89	TPTl(?)	pwt	Ax	3	0	77	23	960		Zr(40)	x
-1292	TPTl	4.5	4	22.4	TPTl(?)	mwt	Sp/Gr	7	2	18	80	1900		Ap(2,1)	x
-1436	TH1	3.2	5	17.2	TCP	p-mwt	Ax/Sp	6	8	69	23	400			
-1561	TH1	2.8	8	6.5	TCP	pwt	Sp/μGr	5	19	44	37	0			
-1639	TH1	1.4	6	4.3	TCP	n-pwt	μGr/Sp	6	16	70	14	1400			
-1774	TH2	3.0	5	5.1	TCP	p-mwt	μGr/Sp/Gr	11	73	10	17	0			
-2166	TCB	2.6	3	3.0		l(?)	Ax/Sp/Vp	15	0	100	0	0		Zr(49)	
CFLSM-1	TCB	2.5	1	10.8		intl	μGr	4	0	0	100	11000	A		x
			1	4.6	TSCP(?)	l(?)	Gr	0							
CFLSM-5	TCB	4.4	2	16.7	TSCP(?)	mwt	Gr/Ab	18	38	62	0				
TBF-4	TCB	1.1	1	5.0	TSCP(?)	l(?)	μSp	3	33	67	0				
TBF-1	TCB	1.5	1	6.3	TSCP	l(?)	Gr	0						Cpx(15,2,2,), Sph (3)	x
			2	0.3		Px[d]			(10% Q, 90% Cpx)						

[a] Total number of fragments examined that probably were derived from the same unit. Results are combined for all such fragments.
[b] TSCP = peralkaline rocks of the Silent Canyon Center.
[c] An "x" indicates that quantitative analyses are available for phenocrysts in Appendices A-II through D-II.
[d] Px = pyroxenite (metamorphic texture).

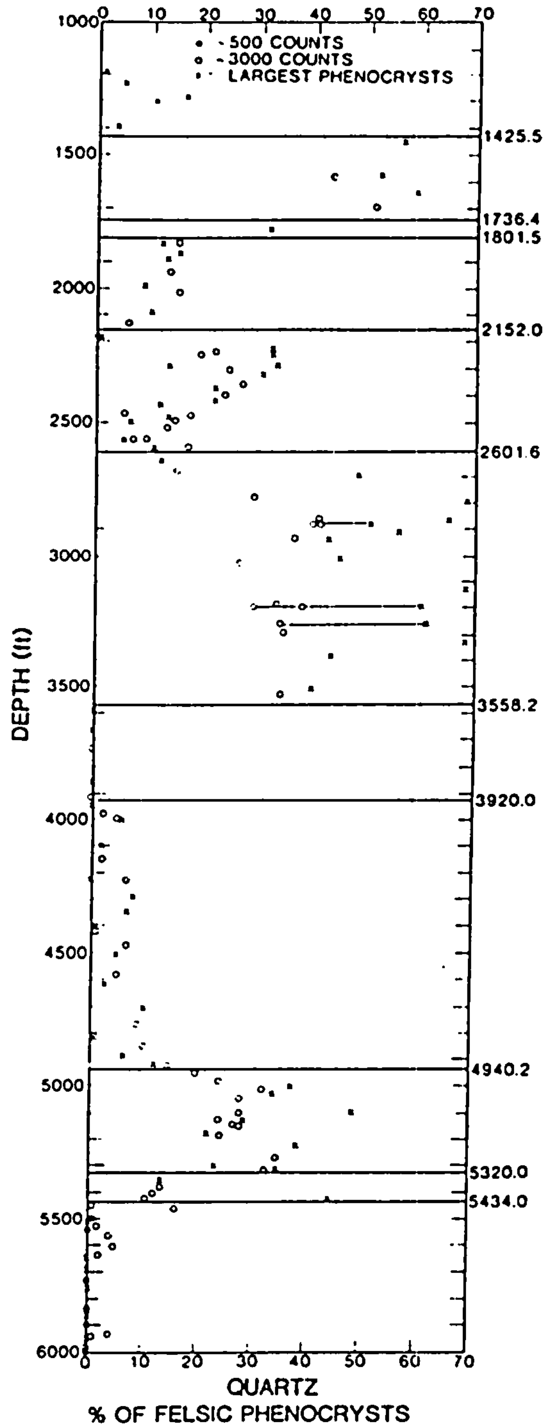

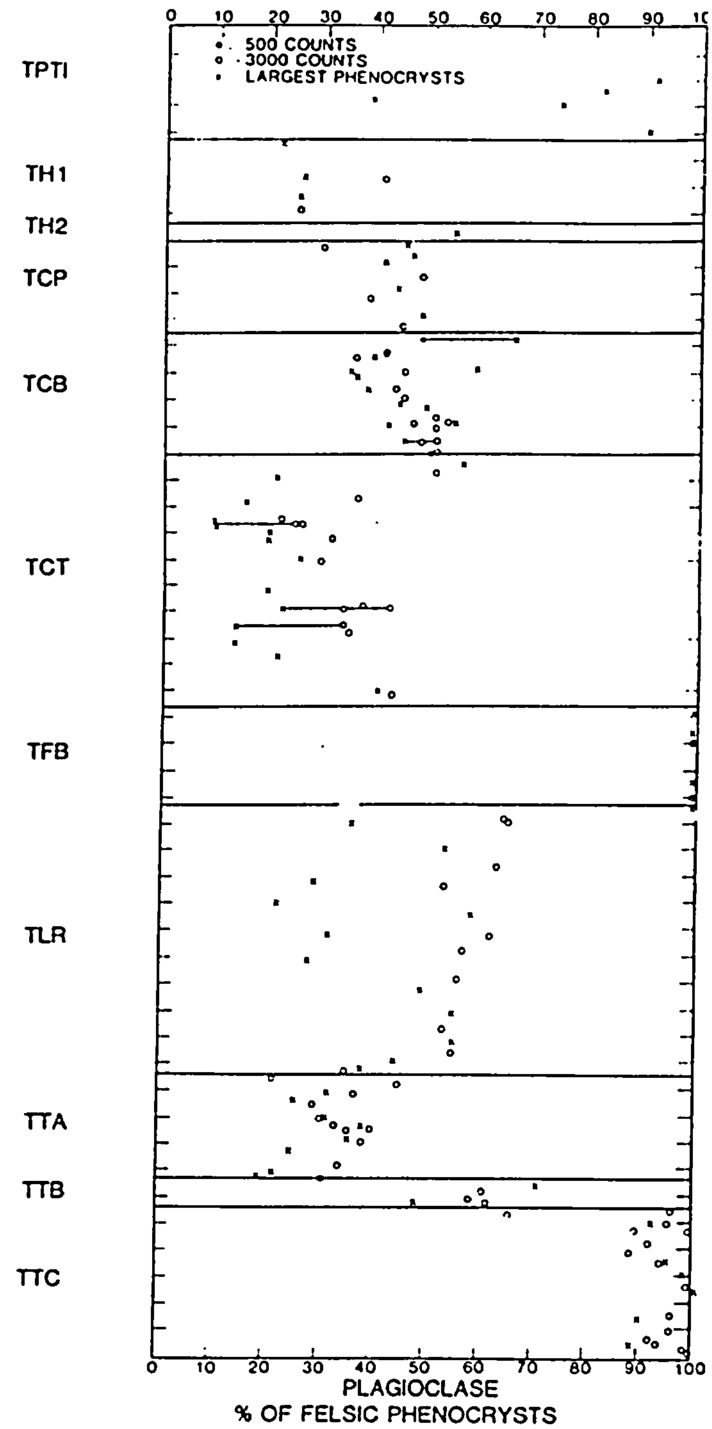

Fig. 5.
Plot of the content of quartz as the percent of felsic phenocrysts versus depth for samples from drill hole USW G-1. (Tie lines connect values obtained by different methods in the same sample.)

Fig. 6.
Plot of the content of plagioclase as the percent of felsic phenocrysts versus depth for samples from drill hole USW G-1. (Tie lines connect values obtained by different methods in the same sample.)

plagioclase). Median values are given in Table VI. Often, these proportions differ distinctively between units and serve as a very important basis for unit recognition (Byers et al. 1976).

All samples of the TFB unit lack quartz, and most samples of the TPTl, TLR, and TTC units are quartz poor (felsic phenocrysts <10% quartz). All samples of the THl unit are quartz rich (>40% quartz), and most samples of the TCT unit contain substantially more quartz than samples of the TCP and TCB units of the Crater Flat Tuff. For the TCT unit, the relative proportions of quartz estimated from phenocrysts of the largest sizes (symbol x in Fig. 5) is noticeably higher than the proportions estimated from phenocrysts of all sizes (symbols •,o in Fig. 5). Tie lines connect proportions determined in each manner for the same sample. This difference is due to a considerably larger median size for quartz phenocrysts compared to sanidine and plagioclase phenocrysts present in the TCT unit (see Fig. 10 in Bish et al. 1981). Relative quartz contents estimated by the two methods are not significantly different for any other unit of USW G-1. Only the TCB unit shows a consistently different quartz content related to stratigraphic position in USW G-1 (see Fig. 5, Table VI); the upper and middle portions (TCBu, TCBm) contain consistently higher quartz (median, 24% of felsic phenocrysts) than the lower portion (TCBl, median 11% of felsic phenocrysts).

All samples of the TFB unit contain plagioclase as the sole felsic phenocryst (Fig. 6). Except for a single sample, plagioclase comprises >88% of the felsic phenocrysts for the TTC unit. Although samples of the TPTl unit are phenocryst poor, plagioclase is the dominant felsic phenocryst present in most samples. Excluding proportions determined from the largest phenocrysts, plagioclase comprises >20% of the felsic phenocrysts for all samples of USW G-1 examined (Fig. 5). There is a noticeably lower value for the relative proportion of plagioclase estimated from phenocrysts of the largest sizes (symbol x in Fig. 5) than from phenocrysts of all sizes (symbols •,o in Fig. 5) for the TCT and TLR units. Tie lines connect proportions determined in each manner for the same sample. For the TCT unit, this difference is due to a considerably smaller median size for plagioclase phenocrysts compared to sanidine and quartz phenocrysts (see Fig. 10 in Bish et al. 1981). Relative plagioclase contents estimated by the two methods are not significantly different for any other unit of USW G-1.

There are five samples within the stratigraphic column of USW G-1 that exhibit strikingly different felsic phenocryst proportions than samples from the remainder of the unit. Four of these are in the uppermost 50 ft of a unit; all are depleted in quartz and enriched in plagioclase compared to samples from the remainder of the unit. Samples at 2166- and 3941-ft depths, which are bedded tuff at the top of the TCB and TLR units, completely lack quartz and the latter contains only plagioclase phenocrysts (see Figs. 4 and 5). Samples from 2641.5- and 2678.0-ft depths, near the top of the TCT unit, are strongly depleted in quartz and enriched in plagioclase compared to samples from the remainder of the unit. A fifth sample, from 5454.1-ft depth, matches felsic phenocryst proportions for the TTB unit, rather than for the TTC unit, with which it is included (see Figs. 5 and 6), but this sample is from an ash-fall tuff, in contrast to other subunits sampled in the TTC unit.

C. Mafic and Fe-Ti Oxide Phenocrysts

Biotite is the dominant mafic phenocryst present in most samples, and titanomagnetite or its alteration products (mixtures of hematite, pleonaste, pseudobrookite, secondary ilmenite, and rutile) is the dominant Fe-Ti oxide present. Concentrations of primary ilmenite (also generally altered) are considerably lower than those of titanomagnetite in most samples. The TFB unit provides a striking exception; biotite is absent from most samples and abundant orthopyroxene, clinopyroxene, and hornblende are present. Also, primary ilmenite constitutes nearly 50% of the Fe-Ti oxides present in samples of the TFB unit.

Biotite (see Fig. 7) and Fe-Ti oxide contents are exceptionally low in the TPT1, TH1, and TCP units; median biotite contents are <300 parts per million by volume (ppmV) and Fe-Ti oxides <700 ppmV for these units. The highest biotite contents are found in the TCTu, TTB, and TTC units (Fig. 6), but biotite contents for the latter two units are extremely variable. Median Fe-Ti oxide contents for the TFB, TTB, and TTC are considerably higher than those of all other units (see Table VI). When median biotite concentrations are expressed as the percentage of total phenocrysts, units with the lowest values (Table VI) are those that contain appreciable amounts of other mafic mineral phases; examples are the orthopyroxene-bearing TCP unit (biotite = 0.2% of total phenocrysts) and the hornblende-bearing TCB and TTA units. The concentrations of these mafic minerals other than biotite could not be

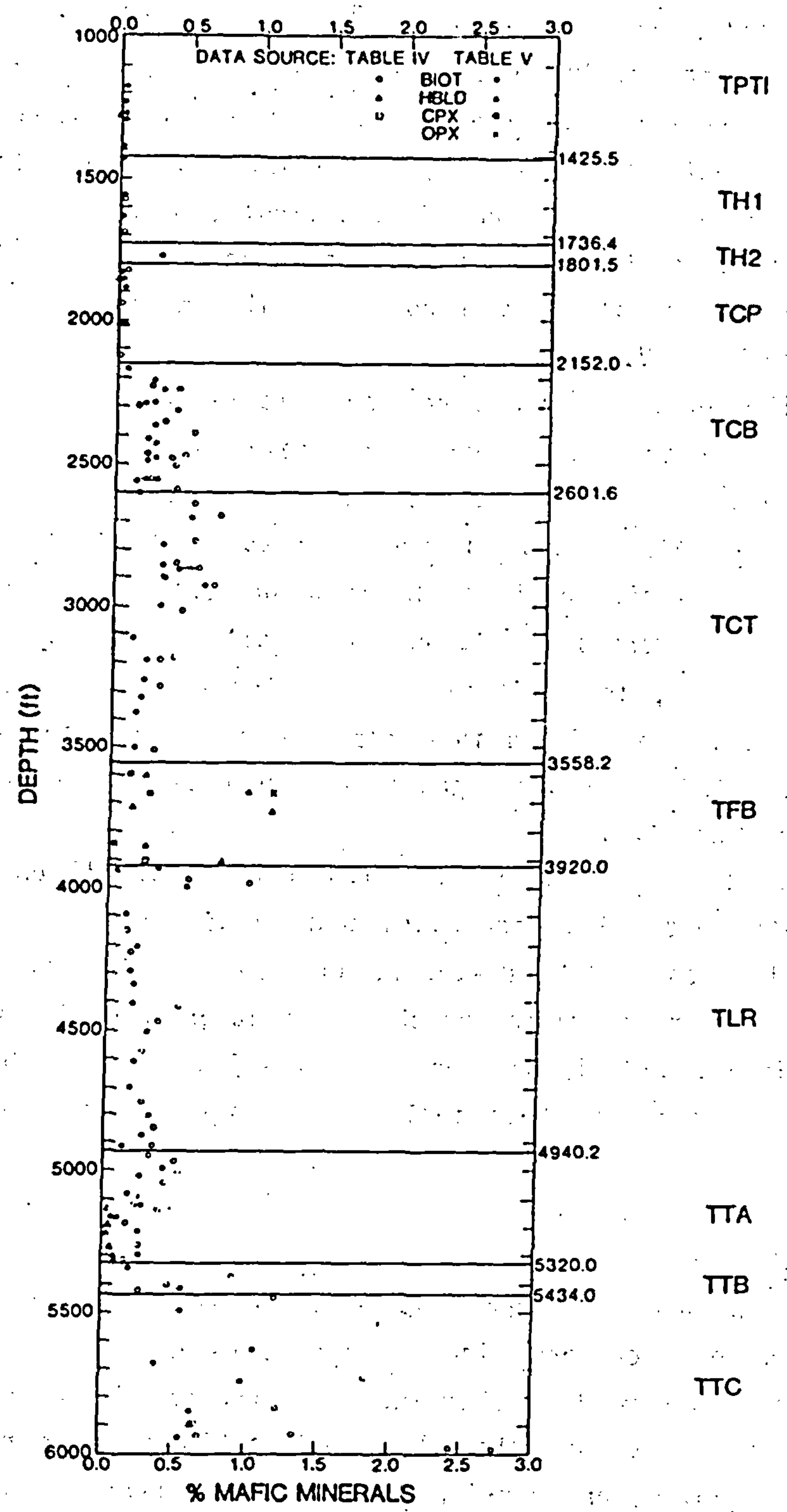

Fig. 7.
Plot of the volume contents of mafic minerals versus depth for samples from drill hole USW G-1.

accurately determined, as a result of alteration. If they could, it is believed that all units of USW G-1 except the TFB and TTC units would show similar mafic mineral concentrations (expressed as the percentage of total phenocrysts). The TTC unit, however, is clearly mafic-rich (see Table VI) compared to other units of USW G-1. Interestingly, although the biotite and Fe-Ti oxide volume contents differ greatly between the TH1 and TH2 units but the fraction of total phenocrysts for both minerals is virtually identical for the two units (see Table VI).

Substantial amounts of unaltered hornblende are present in several samples of the TCB unit, but large, completely altered hornblende relicts (pseudomorphs) are more commonly present (see Tables IV and V). Hornblende or its pseudomorphs are also found in many samples of the TTA and TTC units. Small amounts or traces of hornblende are also present in some samples of the TPT1, TCP, TCT (pseudomorphs only), and TLR units. Orthopyroxene, usually destroyed by alteration, is found in most samples of the TCP and TFB units. Fresh clinopyroxene was not found in any sample other than those from the TFB unit of USW G-1, although pseudomorphs were recognized in several samples of the TTC unit (see Table IV).

Mafic-rich zones are absent in the upper portion of all units of USW G-1 except for the TLR unit. This contrasts sharply with the petrologic sequence reported in drill holes UE-19p, UE-19p#1, and U19ab at Pahute Mesa, in which many units show substantial mafic enrichment stratigraphically upward (Warren, in prep.). It is recognized, however, that the TPT1 unit of USW G-1 is the lower portion of a sequence that includes the strongly mafic-enriched TPTu unit above.

D. Accessory Minerals

In contrast to major components described above, the accuracy with which the concentrations of accessory minerals can be estimated in thin section is limited either by their small size or the small number of such grains present. The five most common accessory minerals found in NTS volcanic rocks (apatite, zircon, sphene, allanite, and perrierite/chevkinite) have the distribution of sizes shown in Table VIII, combining results for all samples listed in Table V. Clearly, sphene and allanite grains are considerably larger, on the average, than perrierite/chevkinite, zircon, and apatite; median sizes are shown in Table IX. Accessory mineral grains smaller than about 0.0005 mm^2 are

TABLE VIII

FREQUENCY DISTRIBUTION FOR AREAS OF ACCESSORY MINERALS IN 0.0001 mm^2, COMBINED FOR ALL PROBE SECTIONS
(Each value represents the number of grains within the class interval indicated.)

	n	0	1	2	3	4	5	6	7	8	9	10	11	12	13	14	15	16	17	18	19	20
All sphene	124	1	1	3	2	2	3	3	1	1	3		3			2	1		1	1		1
All allanite	155									1	1	1	2	1		2			1	3		
All perrierite	13	1	3							1			1				2					1
All zircon	2935	749	527	373	227	202	135	70	57	65	51	26	42	30	21	22	37	5	27	15	18	12
Apatite: TFB unit	1236	120	145	113	129	109	133	88	56	37	34	29	35	20	21	10	14	9	16	11	7	10
Apatite: All other units	9541	3539	2292	1287	671	449	304	189	127	94	85	54	84	39	32	38	41	2	29	17	9	11

	n	21	22	23	24	25	26	27	28	29	30	40	50	60	70	80	90	100	200	300	400	500	1000	2000
All sphene	124	2			1				1		7	7	5	8	3	4	7	19	9	3	6	10	3	
All allanite	155	1		1	1		1	1	1	1	9	11	7	3	6	6	6	30	17	17	8	12	4	
All perrierite	13										1		1					1	2					
All zircon	2935	22	3	15	12	9	12	10	4	7	42	29	18	9	6	2	2	11	1					
Apatite: TFB unit	1236	7	5	5	1	5	4	3	4	3	23	15	4	6		4		1						
Apatite: All other units	9541	12	6	10	16	2	7	5	2	9	37	15	10	6	2	3	3	3						

TABLE IX

MEDIAN SIZE AND EXPECTED STATISTICAL VARIABILITIES
FOR CONCENTRATIONS OF ACCESSORY MINERALS
(Median size was determined from complete set of samples in Table V.
Variability is the concentration calculated for four grains of the median size in a probe section with an area of 700 mm².)

		Median size (mm²)	Variability ppmV
Sphene		0.0085	50
Allanite		0.0150	85
Perrierite		0.0016	9
Zircon		0.00025	1.5
Apatite	TFB unit	0.00055	3
	All other units	0.0002	1

highly concentrated within mafic minerals and particularly within Fe-Ti oxides (for an example, see Fig. 8). Consequently, it is impossible to accurately estimate concentrations for apatite, zircon, and perrierite/chevkinite without using reflected light. Because large numbers of zircon and apatite are present in most samples, the expected statistical variation for their estimated concentrations is small, and comparisons among individual samples are meaningful. However, only a few sphene or allanite grains are present in most samples, and the expected statistical variation of their estimated concentrations is large. Expected statistical variations for estimated concentrations of each mineral (Table IX) are based on four grains of the median size and on a thin section size of 700 mm^2.

Allanite is found in at least one sample of each unit of USW G-1, except for the TFB unit (see Tables IV and V). By contrast, allanite was not found in any of several samples of Paintbrush Tuff and related lavas or Timber Mountain Tuff examined by Warren (in prep.); instead, perrierite/chevkinite is found in these units. Perrierite/chevkinite is consistently present only in samples of the TLRu unit in USW G-1. Allanite and perrierite/chevkinite are chemically similar light rare-earth bearing minerals except that the former is greatly enriched in Ca and Al and depleted in Ti compared to the latter (see Fig. 2). Perrierite and chevkinite have identical structural formulae and are

Fig. 8.
Reflected light photomicrograph of altered Fe-Ti oxide from USW G-1, 2869 ft depth, showing numerous inclusions of zircon and apatite. (Largest inclusion at edge of Fe-Ti oxide is zircon and most of smaller inclusions are apatite. Field of view 1.8 x 1.2 mm.)

difficult to distinguish (Izett and Wilcox 1968; Ito 1967); no attempt has been made to determine which of these minerals actually occurs in NTS rocks.

Sphene is absent from all units younger than the TLR unit in USW G-1, except for a single sample from the uppermost portion of the TCT unit at 2678.0 ft depth (see Tables IV, V). Sphene was found in a single sample of the TCT unit from drill hole J-13, also in the uppermost portion (Table V). By contrast, sphene is abundant in the TLR and older units; its absence in the TLR1 and upper part of the TTA units may be due to alteration (see Table IV). The highest concentration of sphene was determined for an outcrop sample of TCB unit (TBF-1, Table V), yet no sphene was found in any of the 23 samples of this unit examined from USW G-1. Two additional samples of TCB unit that have intermediate stratigraphic positions between TBF-1 and TBF-4 were examined, and both contain sphene (results are not reported in Table V). The observation of sphene only in the uppermost portion of the TCT unit and in three samples of the TCB unit at the TBF location compared to none at USW G-1 indicates that sphene concentrations may differ markedly both vertically and horizontally within a unit.

Apatite and zircon occur primarily as inclusions in host mafic minerals and Fe-Ti oxides (see Fig. 8), and consequently median concentrations of apatite and zircon for many units of USW G-1 closely parallel those of these hosts (see Table VI). This is particularly true for apatite; its concentration is extremely high in the highly mafic-rich TFB unit and also very high in the mafic- and Fe-Ti oxide-rich TTC unit, and low in the mafic- and Fe-Ti oxide-poor TRT1, TH1, and TCP units. The TCBu unit, however, has a consistently and conspicuously low apatite content (see Fig. 9), despite having a moderate biotite and Fe-Ti oxide content (Table VI). Median zircon concentrations show a greater independence from concentrations of mafic minerals and Fe-Ti oxides. This is apparent for the TTB and especially the TFB units, which have low zircon contents despite high concentrations of mafic minerals and Fe-Ti oxides, and the TCBm unit, which has a high zircon content and moderate contents for mafic minerals and Fe-Ti oxides.

Statistical uncertainties in the estimate of concentrations for zircon and apatite are very low (see Table IX), and unlike allanite and sphene, comparisons of concentrations among individual samples are meaningful. Apatite and zircon concentrations are both highest in the central portion of the TCB, TCT, TLR, and TFB (apatite only) units (Fig. 9). Apatite is also substantially higher in samples from the upper portion of the TCT and TLR units (Fig. 9).

VI. ANALYTICAL RESULTS

Analytical results are based on 3000 individual analyses of phenocryst phases. Clearly, it is a major concern to select a method of presentation that allows concise yet comprehensive comparison of these data. Classic representations of chemical data often suffer because they are unwieldy; for example, a comparison of feldspar compositions among individual samples using ternary diagrams would consume an enormous amount of space, and in so doing would become hopelessly ineffective. Histograms offer a more compact solution, although they, too, are unwieldy if more than a few comparisons are made. The presentation scheme adopted is similar to that of a histogram, except that the actual number of individual analyses within each class interval is given rather than plotting this value on a vertical axis. The horizontal axis is the same as for a histogram, and with a little imagination, the reader can visualize a histogram for each sample. Only a single compositional parameter

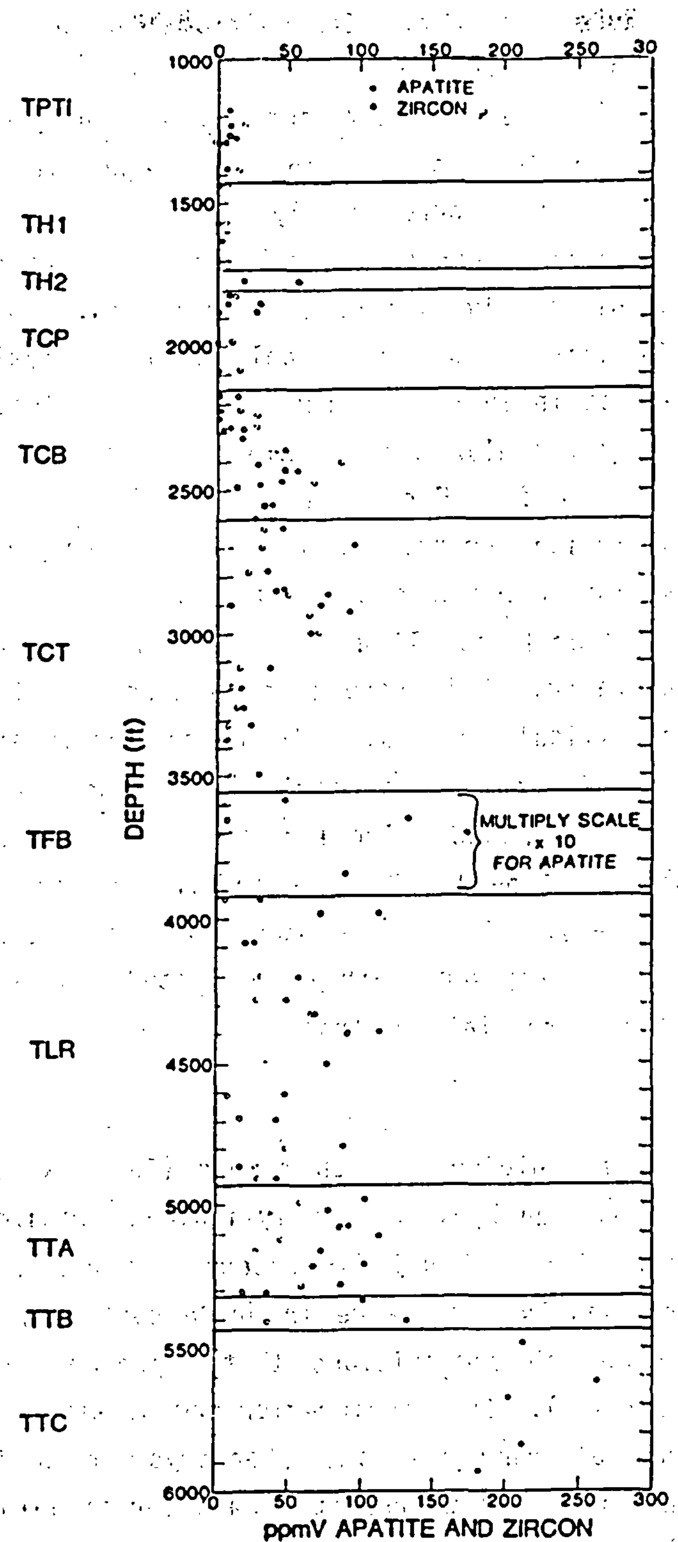

Fig. 9.
Plot of the volume contents of apatite and zircon versus depth for samples from drill hole USW G-1.

can be represented in such a manner. Compositional parameters utilized are the orthoclase + celsian (Or+Cn) end member and barium oxide contents for sandine, the anorthite (An) end member content for plagioclase, and the molecular Mg/(Mg+Fe) ratio for mafic minerals. The width of intervals selected for each parameter are approximately equal to ±3σ confidence limits for their analytical accuracy. Therefore, analyses that differ by more than a single interval have significantly different compositions. Conversely, within any given interval, all analyses are identical within analytical error. No sample-to-sample difference in analytical results for any element was apparent when all analyses for a particular unit within the same class interval of a given parameter were compared. For example, the Fe_2O_3 values are indistinguishable, within analytical error, for 11 sanidine analyses in samples of the TCT unit that have Or+Cn contents between 66.1-68.0 mol%, as are values for all other elements. Therefore, all analyses within a single interval of a given parameter were averaged. This results in a considerable simplification and condensation of analytical results. Microprobe analyses are averaged, unit-by-unit, based on Or+Cn contents of sanidine (Appendix A-I), An contents of plagioclase (Appendix B-I), and molecular Mg/(Mg+Fe) contents of biotite (Appendix C-I), hornblende (Appendix D-I), orthopyroxene (Appendix E-I), and clinopyroxene (Appendix F-I). There are many fewer analyses available for phenocrysts in lithic fragments; hence, they are listed individually following averaged analyses for the appropriate mineral.

A. Sanidine Phenocrysts

The Or+Cn contents of sanidine in each sample (Table X) show a compositional range approximately equal to the analytical uncertainty. Individual phenocrysts are unzoned. The TPT1 unit is exceptional and contains sanidine phenocrysts having a relatively wide range in Or+Cn contents, as well as some with exceptionally sodium-rich compositions that approach albite end member composition (see Appendix A-I). Such sodium-rich compositions, and the sodium-rich compositions found at many sanidine phenocryst rims (see underlined values in Table X) are considered to result from alteration and are discussed in a following section. Furthermore, compositions are identical for all samples of each unit in USW G-1. Sandine compositions from all other locations (Fig. 1) including USW G-2 and UE-25b#1 (Broxton et al. 1982) match those for the appropriate unit from USW G-1 (Table XI). Clearly, except for

TABLE X

FREQUENCY DISTRIBUTION OF Or+Cn AND BaO CONTENTS FOR SANIDINE PHENOCRYSTS IN CORE SAMPLES FROM USW G-1

(Each value represents the number of analyses that have orthoclase+celsian (Or+Cn) end member contents, and barium oxide weight percents within the interval indicated. Value underlined if all compositions within interval are for phenocryst rims.)

Or+Cn, mol%

Unit symbol	Sample depth (ft)	76–74	74–72	72–70	70–68	68–66	66–64	64–62	62–60	60–58	58–56	56–54	54–52	52–50	50–48	48–46	46–44	44–42	<42
TPTI	1191								2	2	1	3							
	1240							2	2	3		2	<u>1</u>			<u>1</u>			
	1286								1	3	2				1		1		2
	1292										1	1	1					2	7
	1392			1			2	3	1	2	1					<u>1</u>			
TH1	1436				7	5										1			
	1561				3	10								2		1			
	1639				11	2													
TH2	1774	1	12	1															
TCP	1820											6	9						
	1854											1	6	6	<u>1</u>				
	1884									1		3	7	2		1			
	1983												10	3				<u>1</u>	
	2083											2	7	3	1	1			
TCB	2166							3	3	4	1	<u>1</u>							
	2233								8	4	<u>1</u>	<u>1</u>							
	2247							8	6										
	2289							5	8				<u>1</u>						
	2291							1	12							<u>1</u>			<u>1</u>
	2318							5	7	<u>2</u>									
	2363							2	11	1									
	2411							4	10										
	2436							4	10										
	2477						<u>1</u>	1	6	5	1								
	2486							5	5	2	<u>1</u>							<u>1</u>	
	2555							<u>1</u>	14										
	2601							5	10	1									
TCT	2641.5			2	8	6													
	2699				5	7	1				<u>1</u>			<u>1</u>					
	2790		1		2	8	2	<u>1</u>											
	2854					6	6		<u>2</u>	<u>1</u>									
	2869				1	8	5												
	2901	1			2	10	2												
	2938					1	6	4	<u>3</u>										
	3001			1	4	10	1	1											
	3117				1	9	4												
	3197				1	11	3												
	3258				3	11													
	3321					10	5												
	3372					15													
	3501				2	8													
TLR	3997					1	8	3	<u>1</u>						<u>1</u>				
	4095					1	11	2											
	4208					5	7	2											
	4296					1	7	4	<u>1</u>	<u>1</u>									
	4342					5	7	2											
	4401		1			1	2	8	<u>1</u>	<u>1</u>									
	4504					2	10	<u>1</u>											
	4612					1	8	5											
	4700					4	10												
	4805					2	10	1											
	4877					1	12	<u>1</u>											
	4913			1		2	10	1											
TTA	4998					1	4	9											
	5026						10	4											
	5094					<u>1</u>	6	7	1										
	5127					1	9	4											
	5167					3	7	4											
	5213				1	1	14												
	5296					2	6	6											
	5312							11	<u>3</u>										
TTB	5349					7	6			1									
	5413				3	6													
TTC	5498		4	2															
	5637		6	4															
	5680			3															
	5848		6	8															
	5948		11																

BaO, wt%

Unit symbol	Sample depth (ft)	0–0.3	0.3–0.6	0.6–0.9	0.9–1.2	1.2–1.5	1.5–1.8	1.8–2.1	2.1–2.4	2.4–2.7	2.7–3.0	3.0–3.3	3.3–3.6	3.6–3.9	3.9–4.2	4.2–4.5	4.5–4.8	>4.8
TPTI	1191	7		1														
	1240	10	1															
	1286	10																
	1292	9			2	1												
	1392	10	1															
TH1	1436	12	1															
	1561	16																
	1639	7	6															
TH2	1774	1	2	2	4	4	1											
TCP	1820	13	2															
	1854	14																
	1884	12	2															
	1983	12	2															
	2083	12	2															
TCB	2166	5	4	2	1													
	2233	2	6	4	2													
	2247	3	8	3														
	2289		6	7	1													
	2291	6	7	1	1													
	2318	3	6	4	1													
	2363		5	7	2													
	2411	2	6	5	1													
	2436	1	8	5														
	2477	3	4	6	1													
	2486	1	8	3	2													
	2555	2	7	6														
	2601		7	8			1											
TCT	2641.5	10	1	3	1	1												
	2699	3	3	1	5	3												
	2790	7	4	1	1	1												
	2854	2	3	8	2													
	2869	5	4	4	1													
	2901	5	3	2	2	2	<u>1</u>											
	2938	5	3	2	4													
	3001		6	6	2	2			<u>1</u>									
	3117	3	5	5		1												
	3197	1	10	4														
	3258	1	3	3	7													
	3321	8	4	2	1													
	3372	4	5	6														
	3501		3	4	3													
TLR	3997		6	3	1	2					1						1	
	4095	2	3	2	2	3	1						1					
	4208	1	8	2		1	1						1					
	4296	2	5	4	1	2												
	4342	1	3	2	2	3	1	1		1								
	4401		3	7	1				1			1					1	
	4504	2	5	3	2			1										
	4612	2	6	2	3													1
	4700		4	4	2	2						2						
	4805		5	1	2	3			1	1								
	4877	2	6		2	2	1		1									
	4913	3	5	4	1						1							
TTA	4998	2	3	3	2	2	1	1										
	5026	11		1	2													
	5094	5	3	3	2		2											
	5127	4	2	4	1		3											
	5167	1	2	3	1	3	2	2										
	5213	6	3	6								1						
	5296	1	6	4	1				1		1							
	5312	12			1	1												
TTB	5349	1	3	6	1	3												
	5413			1	4	2		1	1									
TTC	5498									1		1	1		1	2		
	5637								1	1	1		5	2				
	5680					1	1			1								
	5848									3		1	5	4			1	
	5948										4	2	5					

TABLE XI

FREQUENCY DISTRIBUTION OF Or+Cn and BaO CONTENTS FOR SANIDINE PHENOCRYSTS IN SAMPLES FROM ALL LOCATIONS SHOWN IN FIG. 1

[Each value represents the number of analyses that have orthoclase+celsian (Or+Cn) end member contents and barium oxide weight percents within the interval indicated. Value underlined if all compositions within interval are for phenocryst rims. Individual values for USW G-1 shown in Table X. Values for USW G-2 and UE-25b#1 are from Broxton et al. (1982) and those for UE-25a#1 are from data summarized in Sykes et al. (1979).]

Unit Symbol	Sample Location	(n)	Or+Cn, Mol%																		BaO, wt%													
			76			70					60					50				42 <	0		0.6		1.2	1.8		2.4			3.0		3.6	3.9 >
TPT1	USW G-1	(5)			1			2	5	6	10	5	6	2		1	2	1	2	9	46	2	1	2	1									
TH1	USW G-1	(3)				21	17								2		2				35	7												
TH2	USW G-1	(1)	1	12	1																1	2	2	4	4	1								
TCP	USW G-1	(5)									1		12	39	14	2	2		1		63	8												
	USW G-2-2744													1	5						5	1												
	-2869													3	3						6													
	-2950												1	3							1	3												
	-3067													2	2						4													
	-3192													1	1						1	1												
	UE-25a#1-1852												3	1							3	1												
	-1869											1									1													
	-1930													1	1						2													
	-2088																			1			1											
	-2114														2	1	1				4													
	-2220													2							2													
	-2305												1								1													
	J13-1882													12	2						14													
	RWG2a-3												3	9	2			1			15													
	RWG31a-6												2	10	2						13	1												
	Total	(20)									1	1	22	84	34	3	3	1	1	1	135	15	1											
TCB	USW G-1	(13)						1	44	110	19	4	2	1			1		1	1	28	82	61	12		1								
	USW G-2-3492									2											1	1												
	UE-25a#1-2491								4													4												
	UE-25b#1-2402								1		1										1	1												
	-2832								1	3											1	2	1											
	-2855								1	1											2													
	J13-2175								3	8	3										2	9	3											
	RWG2a-4								1	10	2		1								5	8	1											
	-5								2	8	2	2									3	6	4	1										
	CFLSM-1								1	12	1										2	8	4											
	-5								3	6	1	1		1		1				1		2	5	5	2									
	TBF-4							1	1	11	1										2	1	9	2										
	-1									13	1											4	5	4	1									
	RWRyb-3									7	7	2									3	5	6	2										
	Total	(26)						2	62	191	38	9	3	2		1	1		1	2	50	133	99	26	3	1								
TCT	USW G-1	(14)	1	1	3	29	120	35	6	5	1	1			1						54	57	51	29	10	1		1						
	USW G-2-3541				1		3														2	1	1											
	-3671						4															2	1	1										
	-3933						1															1												
	UE-25b#1-3050						1	1														1	1											
	-3095						3														1	1	1											
	-3163					1																			1									
	-3326						1																	1										
	J13-2382					6	8														2	2	6	1	2			1						
	-2980					2	11	1													8	2	2	2										
	PWBWa-5					1	9	2	2												4	5	4	1										
	RWRyb-1						9	5													4	3	3		2	2								
	Total	(25)	1	1	4	39	170	44	8	5	1	1			1						75	75	71	35	15	3		2						
TLR	USW G-1	(12)		1	1		26	102	30	3	2					1					15	59	34	19	18	4	2	3	2	2	3	2		3
	USW G-2-4467						2	8	2					1							6	5	3											
	J13-3493						1	10	1		1					1					3	8	3											
	RWBWa-4						3	10	1													3	7	2		1			1					
	Total	(15)		1	1		32	130	34	3	3			1		2					24	75	47	21	18	5	2	3	3	2	3	2		3
TTA	USW G-1	(8)				1	9	56	45	4											42	19	24	10	6	8	3	1		1	1			
TTB	USW G-1	(2)				3	13	6			1										1	3	7	5	5		1	1						
	USW G-2-4805						2	3					1									1	2	2	1									
TTC	USW G-1	(5)		27	17																				1	1		1	6	5	4	16	6	4

the TPTl unit, sanidine compositions for all units of USW G-1 examined show no vertical or horizontal variations that exceed the rather small analytical uncertainties.

Median values for Or+Cn contents are distinctly different among members of the TC unit; they are 53 mol% for the TCP unit, 61% for the TCB unit, and 67% for the TCT unit (Table XII). Note that about 300 individual sanidine analyses have been obtained for 40 samples of the TCB and TCT units, many from widely separated locations. But not a single sanidine analysis was obtained with an Or+Cn value >66.0 mol% from a sample of TCB unit, and not a single analysis with an Or+Cn value <62.1 mol% was obtained for core or mid locations from a sample of TCT unit (a few analyses with such compositions were obtained at rims, see Table XI). Consequently, there is a high level of significance for the difference between sanidine compositions of the TCB and TCT units, and even a single sanidine analysis provides a highly reliable discrimination between these units. The four analyses of sanidine in a sample of bedded tuff from USW G-2 between the TCT and TCB units allow a confident reassignment of the bedded tuff to the TCT unit (see Table XI).

Sanidine compositions are essentially identical for the TLR and TTA units (see Table XII). Those for the TTC unit are remarkably Ba-rich, and differ distinctly from compositions of the TLR and TTA units. Sanidine compositions of the TTB unit are intermediate between those of the TTA and TTC units, although more closely similar to those of the TTA unit. This suggests that the TTB unit may have a geochemistry transitional between the TTA and TTC units; this is also suggested by the slight increase in Or+Cn and BaO contents from the sample at 5349-ft depth to those at 5413-ft depth in USW G-1 (see Table X), but such small changes cannot be considered significant.

All units examined in USW G-1 contain sanidine phenocrysts that have a unimodal distribution of barium contents (see Table XI). By contrast, bimodal distributions for Ba in sanidine are reported for units not present in USW G-1, such as the Rainier Mesa Member of the Timber Mountain Tuff (Warren, in prep.). Such units are characterized by distinct zonation into mafic-poor and mafic-rich zones, and such zonation is lacking, or not pronounced, for units of USW G-1.

TABLE XII
DOMINANT VALUES FOR COMPOSITIONAL PARAMETERS
OF PHENOCYRSTS FOR UNITS OF USW G-1

(The dominant value is equivalent to the statistical mode. The median value very closely approximates the statistical mode for compositional parameters of sanidine and mafic minerals and is the value given for these minerals. Values for all locations [Fig. 1] were used to determine dominant values.)

Unit symbol	Samples	Sanidine mol% Or+Cn	Sanidine wt% BaO	Plagioclase mol% An rim	Plagioclase mol% An core	Mafic Minerals molecular Mg/(Mg+Fe) Biot	Hbld	Opx	Cpx
TPT1	5	59	0.00	15	17	0.43			
TH1	3	68	0.18	19	21	0.37			
TH2	1	73	1.0		37	0.45			
TCP	14	53	0.14	11	11	0.42		0.29	
TCB	22	61	0.56	15	16	0.40	0.44		
TCT	18	67	0.55	21	21	0.42			
TFB	4			61	61		0.66	0.70	0.73
TLR	15	65	0.67	18	19	0.59			
TTA	8	64	0.55	17	19	0.55			
TTB	2	66	0.96	23	29	0.59			
TTC	6	72	3.4	29	32	0.62			

B. Plagioclase Phenocrysts

In contrast to sanidine and mafic phenocrysts, most plagioclase phenocrysts are strongly zoned. The wide compositional range for analyses from core and mid locations (Table XIII) reflect this zonation. Nonetheless, compositions for plagioclase are similar throughout each unit and for all units there is a characteristic dominant value (equivalent to the statistical mode) that occurs, within analytical error, at the most An-poor compositions measured. Most rim analyses match the dominant value for core and mid analyses (Table XIV). Plagioclase compositions from all other locations (Fig. 1), including USW G-2 and UE-25b#1 (Broxton et al. 1982), match those for the appropriate unit from USW G-1 (Tables XV, XVI). Except as discussed below, plagioclase compositions show no vertical or horizontal variations for all units of USW G-1 examined.

The dominant An values for plagioclase rim compositions differ as distinctly among members of the TC unit as do the sanidine Or+Cn values (see Tables XII, XV, XVI); they are 11 mol% for the TCP unit, 15 mol% for the TCB

TABLE XIII

FREQUENCY DISTRIBUTION OF An CONTENTS FOR CORE AND MID ANALYSES OF PLAGIOCLASE PHENOCRYSTS IN CORE SAMPLES FROM USW G-1

(Each value represents the number of analyses that have anorthite (An) end member contents within the interval indicated.)

An, Mol%

Unit symbol	Sample depth (ft)	8–10	10–12	12–14	14–16	16–18	18–20	20–22	22–24	24–26	26–28	28–30	30–32	32–34	34–36	36–38	38–40	40–42	42–44	44–46	46–48	48–50	50–52	52–54	54–56	56–58	58–60	60–62	62–64	64–66	66–68	68–70	70–72	72–74	74–76	76–78	78–80
TPTI	1191					5	1				2			1			1						1														
	1240				3	2			1	2				1					1			1	1														
	1286				2	4	1						1	1																							
	1292				2	1	2					1		2	1		1							1													
	1392				1	3	1	1							2	1	1			1		1															
TH1	1436					2	2	6																													
	1561				4	1	3	2			1																										
	1639						4	6	2																												
TH2	1774									1	1	1		1	2	3	1	1																			
TCP	1820	3	9	1																																	
	1854		4	3										2	1					1																	
	1884		9													1					1																
	1983	2	2						1		1	1	1	1		2																					
	2083		4	2								1	1										1	2													
TCB	2166				2	3	1	1	1		1	1	1		1						1				1												
	2233			2	5	2											1				1																
	2247				4	5		1										1																			
	2289				5	3	1	1												1																	
	2291			2	4	3	1													1																	
	2318				1	6				1						1	1				1																
	2363				3	5	2	1																													
	2411				6	3			1		1	1																									
	2436			1	1	4	1	1			1			1																							
	2477			1	3	2		2		1				2		1																					
	2486			2	4	2		1		1		1	2																								
	2555				6	1					1						1	1			1																
	2601			6	24	7	1					2	1							2	1	1															
TCT	2641.5						1	9	4	2	2	4	5	6	6	3			1	1	1	1		1	2				2		1						
	2699						1	2	2			2		1	1							2															
	2790						1	2	1	2		1	1				1		1																		
	2854					1	1	2		3	3			1																							
	2869						4	3	2	1	1																										
	2901						2	2	2	1	1		1	1																							
	2938					1	2	2		2	1	1				1		1																			
	3001								1		1	1		1	1	1																					
	3117							5	1		1	1				1	1	1																			
	3197					1	3	1	2					1	1			1	1																		
	3258						1	1	2			2	1		2		1			1																	
	3321				1		2								1		3					2						1		1							
	3372											1	1			2	3	1	1				2	1													
	3501															2								1		1	1	1									
TFB	3598																									1	2		2	1	2				1		3
	3659																								1	1		4		1			1		1	1	
	3706																									2		5	1	1				1		1	
	3850																									2		1	1	1	2			2			
TLR	3941										1						2	2	3		1	2		1													
	3997					1	3	1	1	2		1		1	1		1	1																			
	4095				1	2	1		3		1	1	2																								
	4208						1	2		3	1		1			1	1				1																
	4296					1	3	1	1					1	1		1					1																	
	4342				1	1	3	2	1			1															1										
	4401					1	1	2								2	1		1								1										
	4504					2	1	1	1	4	1																										
	4612					2	2		2	1	1				1			1			1																
	4700					1	2	1		1	1	1	1		1		1			1	1																
	4805				1		1		2	1		4		1			1																				
	4877					2	1		1	1	1	1		2		1		1																			
	4913				1		1	3	2		1			2	1																						
TTA	4998						1	2	1	1	2		1	1						1						1											
	5026						2	2	1		2	2			2																						
	5094					1	1		1		2	2	1	1				1	2																		
	5127						2		2	1	3		3																								
	5167					2	3	1		1	1	1	1							1																	
	5213						3	2		1	1	2				1		1																			
	5296					2	2	1	1	1		1	1									1	1														
	5312					2	1	2				2		1	2	1																					
TTB	5349				1		1			1		2	1	1	1				1		1																
	5413							1	1	1	1	4	2	1	1																						
TTC	5498											1		5	2	1			2																		
	5637											2	3	1	3		1	1																			
	5680											4	5	2	2																						
	5747											1	3	2	4					2																	
	5848										4	3	1	2																							
	5948												2	1	2	1	3	1	1	1																	

TABLE XIV

FREQUENCY DISTRIBUTION OF An CONTENTS FOR RIM ANALYSES OF PLAGIOCLASE PHENOCRYSTS IN CORE SAMPLES FROM USW G-1

(Each value represents the number of analyses that have anorthite (An) end member contents within the interval indicated. Value for TFB unit underlined if all compositions within interval are for tiny, groundmass laths. Value marked with asterisk is for one groundmass and one rim analysis.)

Unit Symbol	Sample depth (ft)	An, Mol%: <10	10-12	12-14	14-16	16-18	18-20	20-22	22-24	24-26	26-28	28-30	30-32	32-34	34-36	36-38	38-40	40-42	42-44	44-46	46-48	48-50	50-52	52-54	54-56	56-58	58-60	60-62	62-64	64-66	66-68
TPT1	1191				2	1																									
	1240				2	1																									
	1286				2																										
	1292				1	1	1		1																						
	1392				1								1		1																
TH1	1436						2	1																							
	1561				1	1	1																								
	1639						1	1	1																						
TH2	1774								1			1				1															
TCP	1820	2	1																												
	1854		1	1						1																					
	1884	1	2																												
	1983	1									1		1																		
	2083		3																												
TCB	2166					2	1																								
	2233			1	2																										
	2247				2	1																									
	2289				3																										
	2291			2	1																										
	2318				2	1																									
	2363				1	2																									
	2411				3																										
	2436				1	1	1																								
	2477			1	2																										
	2486		1			1			1																						
	2555				3																										
	2601																														
TCT	2641.5																														
	2699								2		1																				
	2790					1			1			1																			
	2854						2	1																							
	2869							2	1																						
	2901							2	1																						
	2938							3																							
	3001								1	1	1																				
	3117							2									1														
	3197						2											1													
	3258							2							1																
	3321						1									1												1			
	3372															1	2														
	3501																	2						1					1		
TFB	3598																				1̲	1̲	1̲			1̲	2	1̲	1		
	3659																				3̲	1̲	1̲				1	1		1	
	3706																				3̲	2̲	1̲		1			1	1	1	1
	3850																			1̲	2̲		1̲		2*	1		1	1	1̲	
TLR	3941																														
	3997						1	1	1																						
	4095						2																								
	4208						3																								
	4296					2	1																								
	4342					1	2																								
	4401					1	1																								
	4504						2	1																							
	4612					1	2																								
	4700					2		1																							
	4805					1		1				1																			
	4877					1					1			1																	
	4913					1		1									1														
TTA	4998					2	1																								
	5026					1	1		1																						
	5094						1				1		1																		
	5127					1	1				1																				
	5167					3																									
	5213				1	1	1																								
	5296				2	1																									
	5312				1	1	1																								
TTB	5349						1		1				1																		
	5413							1	2																						
TTC	5498											3																			
	5637											1			1		1														
	5680										1	3																			
	5747												2	1																	
	5848											1	1	1																	
	5948											1		1																	

TABLE XV

FREQUENCY DISTRIBUTION OF An CONTENTS FOR CORE AND MID ANALYSES OF PLAGIOCLASE PHENOCRYSTS IN SAMPLES FROM ALL LOCATIONS SHOWN IN FIG. 1

[Each value represents the number of analyses that have anorthite (An) end member contents within the interval indicated. Individual analyses for USW G-1 shown in Table XIII. Values for USW G-2 and UE-25b#1 units are from Broxton et al. (1982) and those for UE-25a#1 from analyses summarized in Sykes et al. (1979).]

An, mol%

Unit Symbol	Sample location	(n)	<10	10–12	12–14	14–16	16–18	18–20	20–22	22–24	24–26	26–28	28–30	30–32	32–34	34–36	36–38	38–40	40–42	42–44	44–46	46–48	48–50	50–52	52–54	54–56	56–58	58–60	60–62	62–64	64–66	66–68	68–70	70–72	72–74	74–76	76–78	78–80	>80
TPTI	USW G-1	(5)				8	15	5	1	1	2	2	1	1	5	3	1	3		1	1		2	2	1														
TH1	USW G-1	(3)				4	3	9	14	2		1																											
TH2	USW G-1	(1)									1	1	1		1	2	3	1	1																				
TCP	USW G-1	(5)	5	28	6					1		1	2	2	3	1	3				1	1		1	2														
	USW G-2-2950		1	3					1						1																								
	-3067		2	3																																			
	-3192															1																							1
	UE-25a#1-1869			2																																			
	-2002		3	1													1																						
	-2114		2	1				1			1																												
	-2220				2																																		
	-2305			4																																			
	J13-1882		4	4	1						1							1																					
	RWG2a-3			2	5	1							1							1			1																
	RW31a-6			3	2											1		1	1			2							1										
	Total	(16)	18	51	16	1		1	1	1	2	1	3	2	4	2	4	2	1	1	2	3	1	1	2				1										
TCB	USW G-1	(13)			14	68	46	7	8	2	3	4	5	4	3	1	2	3	2		4	5	1			1													
	USW G-2-3250						1				1					1				1																			
	-3308						1																																
	-3492					3								1							1																		
	UE-25a#1-2361					2																																	
	-2419				3	1																																	
	UE-25b#1-2402				1	3		1																															
	-2832				1	1																																	
	-2855						1			2						1																							
	J13-2175				1	5	3	2																															
	RWG2a-4				1	1	3		1					1	2	1	1																						
	-5				1	1	3	2	1		1					1		1																					
	CFLSM-1					6	2									1	1		1																				
	-5					5	3		1			1				1																							
	TBF-4				1	3			1					1	1			1	2	1	1																		
	-1			1	1	1	2	2	2			1	1					1																					
	RWRyb-3				2	5	4									1																							
	Total	(29)		1	26	105	69	14	14	4	5	6	6	7	6	8	4	6	5	2	6	5	1			1													
TCT	USW G-1	(14)				1	3	18	29	17	11	10	12	9	11	12	10	10	4	4	2	1	5	2	3	2	1	1	2	2	1	1							
	USW G-2-3541								2																														
	-3671						1		2	1					2	1	3																						
	-4005																1			2																			
	UE-25b#1-2953							1																															
	-3095									1																													
	-3163													1																									
	-3185								2																														
	-3326												1					1																					
	J13-2382							1	3	1	1	2	1		1						1																		
	-2980					1			3	2	1		1	1	1	1																							
	RWBWa-5						1	2	2		1	1	2		1		1		1																				
	RWRyb-1							2	4		2								1		1			1		1													
	Total	(26)				2	5	24	47	22	16	13	17	11	16	14	15	11	6	6	4	1	5	3	3	3	1	1	2	2	1	1							
TFB	USW G-1	(4)																								1	6	2	10	4	4	4		1	3	2	2	3	
TRD	USW G-2-4090																			6	6	4	3	2	1	1	2												
TLR	USW G-1	(13)				4	13	20	13	14	13	8	9	4	7	5	4	8	5	4	1	4	3		1			2											
	USW G-2-4199													1	2	4	6	6	5	3	3	2	1		1														
	-4467						5	2	2			1	2	1		1																							
	J13-3493					1		2	1	1	1		1	1	1				1	1																			
	RWBWa-4						1	2	1	2	1	2	1						1																				
	Total	(17)				5	19	26	17	17	15	11	13	7	10	10	10	14	12	8	4	6	4		2			2											
TTA	USW G-1	(8)					7	15	10	6	5	11	10	7	3	4	2		2	2	2		1	1			1												
TTB	USW G-1	(2)				1		1	1	1	2	1	6	3	2	2				1		1																	
	USW G-2-4838																						1																
TTC	USW G-1	(6)										4	11	14	13	13	2	4	2	3	3																		
	USW G-2-5017												3	6	3	1	1																						
	-5493												1	7	7	4	1	3	2																				
	Total	(8)										4	15	27	23	18	4	7	4	3	3																		

TABLE XVI

FREQUENCY DISTRIBUTION OF An CONTENTS FOR RIM ANALYSIS OF PLAGIOCLASE PHENOCRYSTS IN SAMPLES FROM ALL LOCATIONS SHOWN IN FIG. 1

[Each value represents the number of analyses that have anorthite (An) end member contents within the interval indicated. Individual analyses for USW G-1 shown in Table XIV. Value for TFB unit underlined if all compositions within interval are for tiny, groundmass laths. Each value marked with asterisk represents a single groundmass analysis and additional rim analyses to total the value given.]

An, Mol% (10–40)

Unit Symbol	Sample Location	(n)	<10	10-12	12-14	14-16	16-18	18-20	20-22	22-24	24-26	26-28	28-30	30-32	32-34	34-36	36-38	38-40
TPT1	USW G-1	(5)				8	3	1		1				1		1		
TH1	USW G-1	(3)				1	1	4	2	1								
TH2	USW G-1	(1)								1			1				1	
TCP	USW G-1	(5)	4	7	1						1	1		1				
	J13-1882			3														
	RWG2a-3		1	2														
	RW31a-6			2							1							
	Total	(9)	5	14	1						2	1		1				
TCB	USW G-1	(12)		1	4	20	8	2		1								
	J13-2175			1		2												
	RWG2a-4				1	2												
	-5				1		1	1										
	CFLSM-1				1	1	1											
	-5				2	1												
	TBF-4				1	1	1											
	-1				1		1		1									
	RWRyb-3					2	1											
	Total	(20)		2	11	29	13	3	1	1								
TCT	USW G-1	(13)					1	5	12	6	1	2	1			1	2	3
	J13-2382								1	2								
	-2980							1	2									
	RWBWa-5								2				1					
	RWRyb-1							3										
	Total	(17)					1	9	17	8	1	2	2			1	2	3
TFB	USW G-1	(4)																
TLR	USW G-1	(12)					10	14	5	1		1	1		1			1
	J13-3493					1	2											
	RWBWa-4						1	2										
	Total	(14)				1	13	16	5	1		1	1		1			1
TTA	USW G-1	(8)				4	10	6		1		2		1				
TTB	USW G-1	(2)						1	1	3				1				
TTC	USW G-1	(6)										1	9	3	3	1		1

An, Mol% (40–80)

Unit Symbol	Sample Location	(n)	40-42	42-44	44-46	46-48	48-50	50-52	52-54	54-56	56-58	58-60	60-62	62-64	64-66	66-68	68-70
TCT	USW G-1	(13)	3						1				1	1			
	Total	(17)	3						1				1	1			
TFB	USW G-1	(4)			1	9	4	4	3*	2*	3		4*	3	3*	1	

TABLE XVII

FREQUENCY DISTRIBUTION OF An CONTENTS FOR ALL RIM ANALYSES OF PLAGIOCLASE PHENOCRYSTS THAT HAVE CORE OR MID An CONTENTS OF >28.0 mol% An.

(Each value represents the number of rim analyses that have anorthite (An) end member contents within the interval indicated. Analyses for all locations in Fig. 1 used. Analyses for locations other than USW G-1 combined with the upper members of the TCT and TLR units. Results for TTB and TTC units not included.)

Host Unit Symbol	An, mol% 10–12	12–14	14–16	16–18	18–20	20–22	22–24	24–26	26–28	28–30	30–32	32–34	34–36	36–38	38–40	40–42	42–44	44–46	46–48	48–50	50–52	52–54	54–56	56–58	58–60	60–62	62–64	64–66	66–68	68–70
TPTl			3	1	1						1		1																	
TCP	5							2	1		1																			
TCB			4	6	5																									
TCTu					2	6	5		2	1																				
TCTl						1							1	2	3	3						1				1	1			
TLRu			1	4	3		1																							
TLRl				5	1	1			1	1		1																		
TTA			2	7	4		1		1																					

unit, and 21 mol% for the TCT unit. Dominant An values for plagioclase rims are virtually identical for the TLR and TTA units, but those of the TTC unit are considerably more An-rich. Dominant An values for the TTB unit are intermediate between those of the TLR/TTA units and the TTC unit. These relationships for plagioclase compositions exactly parallel those for sanidine among the four stratigraphically lowest units of USW G-1. Plagioclase of the TFB unit is remarkably An-rich; many cores have An contents between 70-80 mol% (see Table XV) and even rim compositions (54-68 mol% An, Table XVI) and groundmass compositions (44-66 mol% An, Table XVI) are exceptionally An-rich. Such compositions are characteristic of andesites rather than dacites (see, for example, Carmichael et al. 1974).

Although most units of USW G-1 show a wide range in plagioclase compositions, three units show particularly small ranges: the TH1, TH2, and TTC units (Table XV). The compositional range for the TCP unit shows a very low frequency of analyses between 14-24 mol% An. This gap also occurs within single plagioclase phenocrysts analyzed at core, mid, and rim (see Table XVII) that have Ca-rich cores, and indicates mantling by plagioclase of the dominant composition in the TCP unit (see Table XII). In all units, except the TCTl unit, plagioclase with An-rich cores zone to the dominant composition. Few plagioclase with An-rich cores in the TCTl unit are zoned to the dominant composition of the TCTl unit (see Table XII), indicating that most plagioclase phenocrysts with An-rich cores have had virtually no contact with the magma and are probably xenocrysts incorporated during eruption.

C. Mafic Minerals

Biotite compositions, as represented by the molecular Mg/(Mg+Fe) ratio, are generally consistent within each unit of USW G-1 (Table XVIII). Individual phenocrysts are unzoned but their Mg/(Mg+Fe) contents span a range of about 0.1 for most samples. All units of USW G-1 younger than the TFB unit have Mg-poor biotites (Table XIX) with very similar dominant molecular Mg/(Mg+Fe) values (see Table XII). All units of USW G-1 older than the TFB unit have relatively Mg-rich biotites; dominant molecular Mg/(Mg+Fe) values are also similar among these units (Table XII).

Biotites within the uppermost portion of the TCB, TCT, and TLR units are Mg-rich compared to those in the remainder of the unit (see Table XVIII for USW G-1, Table XVIX for TCT unit in J-13, and for TCB and TLR units in USW G-2). Note that the upper plagioclase-rich portion of the TLR unit that includes Mg-rich biotite lies within the ash-flow cooling unit in USW G-2, but in USW G-1 it is a bedded tuff included with the TFB unit (Spengler et al. 1981). Several biotites of the TCTl unit in USW G-1 also are notably Mg-enriched compared to dominant compositions for biotite throughout the TCT unit (Table XVIII). These match compositions of biotite in the abundant lithics within the TCTl unit (see following section) and in one case such biotite has the same peculiar alteration commonly observed for biotite in the lithics (see discussion of alteration of mafic minerals). Many samples of the TCB unit from locations other than USW G-1 also contain Mg-rich biotite, particularly the sphene-rich sample TBF-1 (see Table XIX). There is a distinctly low frequency of biotite compositions between the Fe-rich dominant composition and Mg-rich compositions for both the TCB and TCT units (see Table XIX).

Molecular Mg/(Mg+Fe) contents for hornblende (Table XX) are similar to those for biotite of the same unit: Note the particularly large compositional range of hornblende for the TCP unit, the occurrence of a dominant, Mg-poor composition as well as an Mg-rich composition for hornblende of the TCB unit, and the occurrence of Mg-rich hornblende in the uppermost portion of the TLR unit of USW G-1. The molecular Mg/(Mg+Fe) ratio follows the order

TABLE XVIII

FREQUENCY DISTRIBUTION OF MOLECULAR Mg/(Mg+Fe) CONTENTS FOR BIOTITE PHENOCRYSTS IN CORE SAMPLES FROM USW G-1

[Each value represents the number of analyses that have molecular Mg/(Mg+Fe) contents within the interval indicated.]

Unit Symbol	Sample Depth (ft)	molecular Mg/(Mg+Fe) 0.34–0.36	0.36–0.38	0.38–0.40	0.40–0.42	0.42–0.44	0.44–0.46	0.46–0.48	0.48–0.50	0.50–0.52	0.52–0.54	0.54–0.56	0.56–0.58	0.58–0.60	0.60–0.62	0.62–0.64	0.64–0.66	0.66–0.68	0.68–0.70	0.70–0.72	0.72–0.74	0.74–0.76	0.76–0.78	0.78–0.80
TPT1	1240			1													1							
	1286			1				1																
	1292			1	1	1				1														
	1392				1	1	1	1																
TH1	1436	1	1	1																				
	1561		3	1		1																		
	1639		2			1																		
TH2	1774					1	2	2																
TCP	1820				1	1	1																	
	1854			2	1	1	1																	
	1884	1			2																			
TCB	2166				2		1				1													
	2247			2																				
	2289			2	2																			
	2291			2																				
	2363		1	1																				
	2486			1	1																			
	2555			2	2																			
	2601		1		1																			
TCT	2641.5				1								2	3		1								
	2699				1	1			2	1														
	2790				2	2																		
	2854	1		3	2																			
	2869		1		2	2																		
	2901			1	2	1																		
	2938			1	1	1	1																	
	3001				2	1			1															
	3197				1	2	1																	
	3258					1											1		1					
	3321					4																		
	3372						2									1								
	3501					2	1																	
TFB	3850																							1
TLR	3941																1	1						
	4095														4									
	4208											2	1		1	1								
	4342												1	2										
	4504												1	2		1								
	4612											2	3											
	4805												1	1										
	4877											1		2		1								
TTA	5026										2	2												
	5127											4	2											
	5213											2												
TTB	5413													3	1									
TTC	5680														1	2								
	5848														1	1		1						

TABLE XIX

FREQUENCY DISTRIBUTION OF MOLECULAR Mg/(Mg+Fe) CONTENTS FOR BIOTITE PHENOCRYSTS IN SAMPLES FROM ALL LOCATIONS SHOWN IN FIG. 1

[Each value represents the number of analyses that have molecular Mg/(Mg+Fe) contents within the interval indicated. Individual analyses for USW G-1 shown in Table XVIII. Values for USW G-2 and UE-25b#1 for TCP and older units are from Broxton et al. (1982).]

Unit Symbol	Sample Location	(n)	0.30–0.32	0.32–0.34	0.34–0.36	0.36–0.38	0.38–0.40	0.40–0.42	0.42–0.44	0.44–0.46	0.46–0.48	0.48–0.50	0.50–0.52	0.52–0.54	0.54–0.56	0.56–0.58	0.58–0.60	0.60–0.62	0.62–0.64	0.64–0.66	0.66–0.68	0.68–0.70	0.70–0.72	0.72–0.74	0.74–0.76	0.76–0.78	0.78–0.80
TPT1	USW G-1	(5)					3	2	2	1	2		1							1							
TH1	USW G-1	(3)			1	6	2		2																		
TH2	USW G-1	(1)							1	2	2																
TCP	USW G-1	(3)			1		2	4	2	2																	
	J13-1882								1	2			1	2				1									
	RWG2a-3							2					1														
	RW31a-6									1																	
	Total	(6)			1		2	6	3	5			2	2				1									
TCB	USW G-1	(8)				2	10	8		1				1													
	USW G-2-3250													3		3											
	-3308						7	3	4																		
	-3336					1		1																			
	UE-25b#1-2832						2		1																		
	J13-2175				1	2	5	5	1																		
	RWG2a-4							8	2																		
	-5						3	3											1	1							
	CFLSM-1						2	2										1									
	-5						3	5										1									
	TBF-4				1	1	1	1																			
	-1							1								1	4										
	RWRyb-3		1		1			1	1								1										
	Total	(20)	1		3	6	33	38	9	1				4		4	5	2	1	1							
TCT	USW G-1	(13)			1	1	5	14	17	5		3	1			2	3		2	1		1					
	USW G-2-3671																							1			
	J13-2382							1	1		4	3															
	-2980					3	2	5	5																		
	RWBWa-5			1	3	1	1	2	1	2																	
	RWRyb-1								3	6																	
	Total	(18)		1	4	5	8	22	27	13	4	6	1			2	3		2	1		1		1			
TFB	USW G-1	(1)																								1	
TRD	USW G-2-4090																			6							
TLR	USW G-1	(8)													5	7	7	5	3	1	1						
	USW G-2-4199																				1	4					
	-4467																1										
	J13-3493															2	3	3									
	RWBWa-4														1	1	2	1	1								
	Total	(12)													6	10	13	9	4	1	2	4					
TTA	USW G-1	(3)												2	8	2											
TTB	USW G-1	(1)															3	1									
TTC	USW G-1	(2)																2	3		1						
	USW G-2-5206																	1		1					1		
	-5493																		3								
	Total	(4)																3	6	1	1				1		

TABLE XX

FREQUENCY AND DISTRIBUTION OF MOLECULAR Mg/(Mg+Fe) CONTENTS FOR HORNBLENDE, ORTHOPYROXENE, AND CLINOPYROXENE PHENOCRYSTS IN SAMPLES FROM ALL LOCATIONS SHOWN IN FIG. 1

[Each value represents the number of analyses that have molecular Mg/(Mg+Fe) contents within the interval indicated.]

A. Hornblende

Molecular Mg(Mg+Fe)

Unit Symbol	Sample	0.30–0.32	0.32–0.34	0.34–0.36	0.36–0.38	0.38–0.40	0.40–0.42	0.42–0.44	0.44–0.46	0.46–0.48	0.48–0.50	0.50–0.52	0.52–0.54	0.54–0.56	0.56–0.58	0.58–0.60	0.60–0.62	0.62–0.64	0.64–0.66	0.66–0.68	0.68–0.70	0.70–0.72	0.72–0.74	0.74–0.76	0.76–0.78	0.78–0.80
TCP	RWG2a-3		1		1												1									
	RW31a-6											1														
	Total		1		1							1					1									
TCB	USW G-1-2555							1	1																	
	CFLSM-5								1																	
	TBF-4				1			3	2																	
	-1							3	1									2								
	Total				1			7	5									2								
TFB	USW G-1-3598																		4	3						
	-3659																		2	2						
	-3706																		1	5						
	-3850																	1	2	2						
	Total																	1	9	12						
TLR	USW G-1-3941																				2					

B. Orthopyroxene

Molecular Mg(Mg+Fe)

Unit Symbol	Sample	<0.30	0.30–0.32	0.32–0.34	0.34–0.36	0.36–0.38	0.38–0.40	0.40–0.42	0.42–0.44	0.44–0.46	0.46–0.48	0.48–0.50	0.50–0.52	0.52–0.54	0.54–0.56	0.56–0.58	0.58–0.60	0.60–0.62	0.62–0.64	0.64–0.66	0.66–0.68	0.68–0.70	0.70–0.72	0.72–0.74	0.74–0.76	0.76–0.78	0.78–0.80
TCP	RWG2a-3	4	1																								
TFB	USW G-1-3659																					5	3				

C. Clinopyroxene

Molecular Mg(Mg+Fe)

Unit Symbol	Sample	0.30–0.32	0.32–0.34	0.34–0.36	0.36–0.38	0.38–0.40	0.40–0.42	0.42–0.44	0.44–0.46	0.46–0.48	0.48–0.50	0.50–0.52	0.52–0.54	0.54–0.56	0.56–0.58	0.58–0.60	0.60–0.62	0.62–0.64	0.64–0.66	0.66–0.68	0.68–0.70	0.70–0.72	0.72–0.74	0.74–0.76	0.76–0.78	0.78–0.80
TFB	USW G-1-3598																					1	4			
	-3659																						3	2		
	Total																					1	7	2		

Cpx>Opx>Hbld for the TFB unit; compositions for each of these minerals are relatively Mg-rich in the mafic-rich, biotite-free TFB unit. Orthopyroxenes of the TCP unit are strikingly Mg-poor (Table XX); such compositions are very unusual and distinctive for this mineral.

D. Phenocrysts in Lithic Fragments

Frequency distributions for compositions of phenocrysts in lithic fragments match portions of the appropriate frequency distribution for the host unit. For example, compositions for plagioclase phenocrysts in lithic fragments within the TCT and TLR units are predominantly An-rich (Table XXI); both of these units contain a considerable proportion of plagioclase phenocrysts that have similar compositions (Table XV). Certainly, many such An-rich phenocrysts, particularly in the TCT1 unit which contains unzoned An-rich phenocrysts (Table XVIII), are actually xenocrysts derived from the lithic fragments. Compositions for phenocrysts of lithic fragments in the TPT1 unit are closely similar to those of the host unit, and they are petrograhically similar as well (see Table VII). There are three groups of compositions for plagicclase phenocrysts in lithic fragments of the TCT unit (Table XXI): an An-rich composition (58-60 mol% An) similar to phenocryst compositions for the TFB unit, compositions ranging between 36-50 mol% An, similar to those for the TRD unit, and compositions between 18-24 mol% An, similar to those for the TLR unit and those of the host unit itself (see Table XV). Sanidine phenocryst compositions in lithic fragments of the TCT unit, however, match only the most Or+Cn rich compositions found in the host unit (see Table XI). Plagioclase phenocryst compositions in lithic fragments of the TLR unit match those for the plagioclase-rich TT units, but compositions for sanidine phenocrysts in lithic fragments do not match those for units underlying the TLR unit in USW G-1, indicating the existence of a currently uncharacterized unit beneath the TLR unit.

VII. EVALUATION OF THE EFFECTS OF ALTERATION ON PHENOCRYST CHEMISTRY

It is critical that the effects of alteration on phenocryst chemistry are minimal or recognizable when severe. The consistency of phenocryst compositions throughout wide ranges in alteration that occur within many units is simply not possible unless such alteration has no effect. For example, alteration of individual samples of the TCB unit includes none (vitric),

TABLE XXI

FREQUENCY DISTRIBUTIONS FOR ANALYSES OF PHENOCRYSTS IN LITHIC FRAGMENTS

[Each value represents the number of analyses within the indicated class interval for all samples of the appropriate host unit given in Appendices A-II, B-II, C-II, D-II, and in Broxton et al. (1982).]

A. Sanidine

Or+Cn, mol%

Host Unit	Analyses	72–70	70–68	62–60	60–58	58–56	54–52	52–50	50–48	22–20
TPT1	4			3	1				1	
TCT	2	1	1							
TLR	5					1	1	1	1	1

BaO, wt%

Host Unit	Analyses	0.0–0.3	0.3–0.6	0.6–0.9	3.9–4.2
TPT1	4	4			1
TCT	2		1	1	
TLR	5	4	1		

B. Plagioclase

An, mol%

Host Unit	Analyses	16–18	18–20	20–22	22–24	28–30	30–32	32–34	34–36	36–38	38–40	40–42	42–44	44–46	46–48	48–50	52–54	58–60
TPT1	3	3																
TCB	1									1								
TCT	16		1	1	1					3	3	1		1	1	1		3
TLR	16	1		1		1	2	1	2	1	1	2	1	1		1	1	
TTB	1					1												

C. Biotite

Molecular Mg/(Mg+Fe)

Host Unit	Analyses	0.38–0.40	0.54–0.56	0.56–0.58	0.58–0.60	0.60–0.62	0.62–0.64	0.64–0.66	0.66–0.68	0.68–0.70	0.70–0.72	0.76–0.78	0.80–0.82	0.84–0.86
TCB	1	1												
TCT	12		1	1		2		1	2	2	1		1	1
TLR	2				1							1		
TTC	1						1							

D. Hornblende

Molecular Mg/(Mg+Fe)

Host Unit	Analyses	0.60–0.62	0.62–0.64	0.64–0.66	0.66–0.68
TCT	3	1		1	1
TLR	2		1		1

low-temperature secondary (zeolitic), and high-temperature deuteric (axiolitic, spherulitic, granophyric, and vapor phase) (Table V). Yet sanidine compositions are identical for all samples (Tables X, XI). Nonetheless, some samples contain phenocrysts that have markedly different compositions than those found in other samples of the same unit. In most cases such compositions are attributed to magmatic processes but in two cases these unusual compositions are considered the result of alteration.

A. Sanidine

Sanidine phenocrysts are highly resistant to destruction by the alteration conditions for all samples listed in Table V, and in no sample has the sanidine been even partially destroyed. Analyses of partially and completely destroyed sanidine phenocrysts in samples of Belted Range Tuff and related peralkaline rocks (Warren, in prep.) indicate that the result is identical to destruction of plagioclase (see discussion in a following section).

Sanidine phenocrysts generally have very uniform compositions within each sample and show no optical or analytical evidence of zoning. However, sodium enrichment often occurs within a narrow, optically distinct rim (see Fig. 10; Tables X, XI). Samples with such rims exhibit the complete range in alteration types listed in Table II; sodium enrichment must have preceded such alterations. Extraordinary sodium enrichment occurs for sanidine in samples of the TPTl unit from 1286- and 1292-ft depths in USW G-1 (Table X). The most sodium-rich composition ($Or_{5.3}Ab_{92.4}An_{2.2}$, Appendix A-I) approaches albite end-member composition and is markedly more sodium-rich than sanidine or anorthoclase phenocrysts of the TPC unit (Warren, in prep.), which are the most sodium-rich alkali feldspar compositions known for units of the NTS. The sample from 1286-ft depth spans the contact between the densely welded, devitrified zone and the vitrophyre below, and the sample from 1292-ft depth is therefore 6 ft below the contact, within the vitrophyre. Such marked sodium-enrichment, however, is lacking for sanidine phenocrysts in other samples from vitrophyres, including vitrophyres of the TCB unit (see TBF-1, Table XI) and TPC and TMRu units (Warren, in prep.). Extraordinary sodium-enrichment also occurs in sandine of a bedded tuff (USW G-2, 762-ft depth; see Broxton et al. 1982) and therefore is not limited to welded tuffs. The mechanism for Na-enrichment of sanidine in the examples cited is unknown, and may possibly result from fluid metasomatism associated with outgassing during eruption or compaction. However, the effect is readily recognizable because of the associated and readily observable features illustrated by Fig. 10.

B. Plagioclase

Plagioclase phenocrysts are more readily attacked during alteration than sanidine, and have been partially altered in some samples, particularly those of the TTC unit and the sample of the TCT unit from 2980-ft depth in J-13. In all such altered samples, each plagioclase phenocryst has been partially or completely replaced by albite, adularia, and calcite; often, the secondary minerals preserve the pattern of twinning in the plagioclase that they replace (Fig. 11). Relict plagioclase within a largely altered phenocryst as small as a few microns in width can be readily distinguished from the secondary feldspars by its higher optical relief. The plagioclase analyses reported for the sample of TCT unit from 2980 ft depth in J-13 were all obtained from such relicts and they match those for other samples of the TCT unit (Tables XV, XVI). Plagioclase alteration varies considerably among samples of the TTC unit, but there is no difference among the compositions determined for plagioclase in each sample of this unit (Tables XIII, XIV). The compositions of the plagioclase phenocrysts and the secondary feldspars (nearly pure albite end member and nearly pure orthoclase end member) are unmistakably distinct and, under the alteration conditions examined, compositions intermediate between the two are not produced.

C. Mafic Minerals

Mafic minerals are more readily altered than feldspar phenocrysts, and in many instances are altered even in vitric rocks. Certainly, the alteration state for each individual mafic phenocryst depends upon a complex set of factors. In general, however, excluding olivine and orthopyroxene, biotite is the most readily altered mafic mineral, clinopyroxene less readily altered, and hornblende the least. The relative ease of biotite alteration is certainly a result of ready access along its thin, easily separated plates.

All forms of high temperature, deuteric alteration, particularly vapor phase alteration, have a severe effect on the optical properties of biotite. As seen in transmitted light, many phenocrysts are blackened; in reflected light, streaks of Fe-Ti oxides are recognizable and the blackened portion has

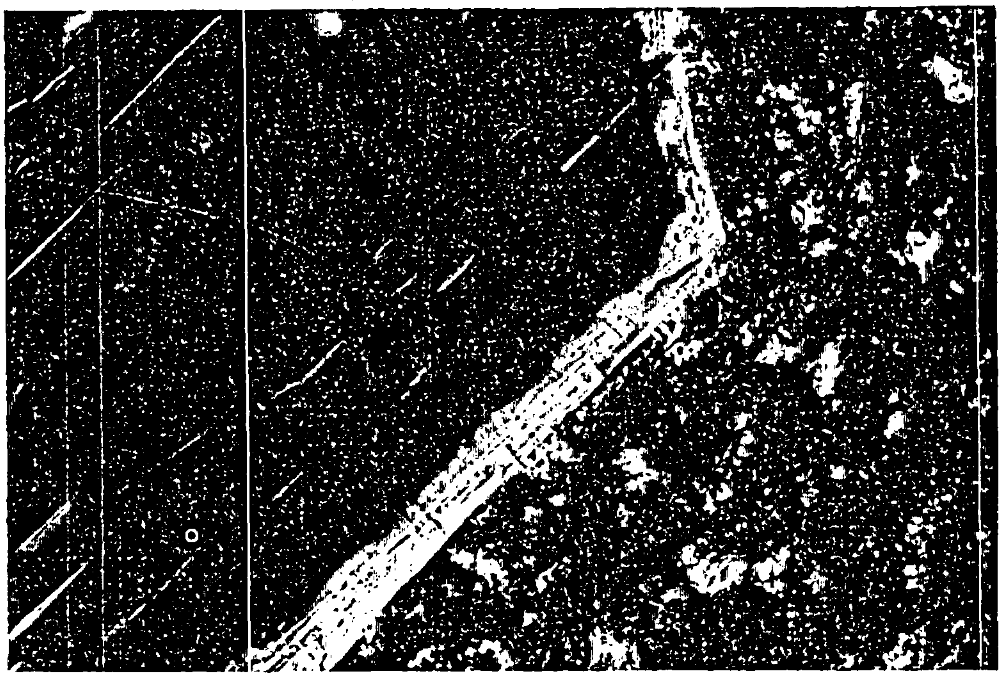

Fig. 10.
Transmitted light photomicrograph of sodium-enriched rim of sanidine phenocryst in sample CFLSM-5. Crossed nicols, field of view 0.35 x 0.25 mm.

Fig. 11.
Transmitted light photomicrograph (crossed nicols) of plagioclase phenocryst largely replaced by calcite, albite, and adularia. USW G-1, 5848-ft depth, field of view 1.0 x 1.4 mm.

a dull, brownish color and low reflectivity that resembles that of a clay mineral (Fig. 12). Amazingly, such altered areas produce electron microprobe analyses that are remarkably similar to those for unaltered areas and give nearly identical molecular Mg/(Mg+Fe) ratios; the most recognizable difference is the invariably higher Ca concentration in the altered area. Measured CaO contents for the freshest biotites are always $\leq$0.02%. Analyses of the freshest portions of biotite phenocrysts in samples affected by high temperature, deuteric alteration match those for biotite in samples of the same unit that have not been affected by alteration. However, biotite plates are often separated by matrix and abundant secondary sphene is observed in many biotite phenocrysts of the TTC unit (Fig. 13). No blackening is associated with such alteration of biotite in the lower portion of USW G-1 and it appears that biotite has simply dissolved away with increasing depth in USW G-1; presumably, Ti released during biotite dissolution combines with Ca (which always appears associated with biotite alteration) to form the secondary sphene. Although it becomes increasingly difficult to find biotite phenocrysts suitable for analysis, biotite compositions for the TLR, TTA, TTB, and TTC units do not change with depth in USW G-1 (see Table XIX), which indicates that the alteration conditions do not affect the biotite compositions (where they can be measured).

A very unusual type of alteration occurs for biotite in lithic fragments of the TCTl unit. In some samples, biotite with identical alteration is found in the groundmass of samples of the TCTl unit (Fig. 14); such biotites contrast remarkably with the fresh biotites that constitute the bulk of biotite phenocrysts in the groundmass and provide convincing evidence for the occurrence of xenocrysts. Analyses for fresh (f) and altered (a) portions of biotite with such alteration (Biotite E, USW G-1, 3501 ft depth) are found in Appendix C-II; these analyses are represented on a molecular basis in Table XXII. The distribution of cations for the fresh portion among the three available crystallographic sites is typical for biotites from NTS rocks (Appendix C; Warren, in prep.; Broxton et al. 1982): the most notable features are the very high proportion of total Fe as Fe(II) and the absence of Al in the octahedral (Y) site. By contrast, in the altered portions, there is a large portion of Al in the octahedral site and the maximum number of Si atoms (6) allowed in the tetrahedral (Z) site of the biotite structure. Assuming that the fresh portion represents the original phenocryst composition, the major

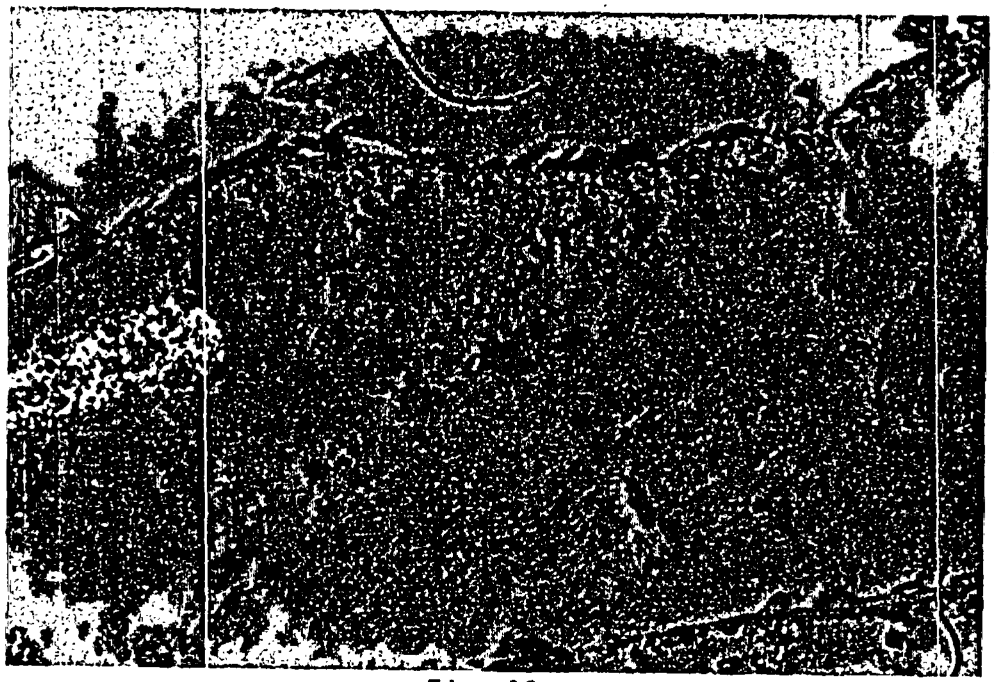

Fig. 12.
Reflected light photomicrograph of blackened biotite phenocryst in spherulitic lava. Note presence of hematite (reflective phase) along biotite plates that causes darkened appearance in transmitted light. Clinopyroxene at top of photo is unaltered. Sample U19ab-1380-1390, pyroxene-bearing rhyolite of Scrugham Peak Quadrangle. Field of view 0.7 x 0.5 mm.

Fig. 13.
Reflected light photomicrograph of secondary sphene in altered biotite phenocryst. Sphene occurs as numerous rounded, highly reflective grains in lower portion of altered biotite. USW G-1, 5848-ft depth. Field of view 1.0 x 1.4 mm.

Fig. 14.
Reflected light photomicrograph of biotite from USW G-1, 3258-ft depth, with unusual (herringbone) alteration in groundmass of TCT1 unit. (Field of view 1.8 x 1.2 mm.)

TABLE XXII

SITE OCCUPANCY FOR FRESH AND ALTERED PORTIONS OF BIOTITE E,
USW G-1, 3501-ft DEPTH

[Site occupancy based on 22 oxygens, using formula $X_2Y_{4-6}Z_8O_{22}\cdot 2H_2O$. X = dioctahedral (large) cations, Y = octahedral cations, Z = tetrahedral cations.]

	X					Y						Z			Total	Fe(II)/
	Na	K	Ca	Ba	Σ(+)	Mg	Fe(II)	Fe(III)	Al	Ti	Σ(+)	Al	Si	Σ(+)	Σ(+)	total Fe
fresh	0.194	1.658	0.000	0.048	1.904	2.957	2.270	0.160	0.000	0.550	12.814	2.394	5.525	29.282	44.000	0.93
altered	0.157	1.864	0.000	0.055	2.131	3.176	0.745	0.060	0.662	0.499	11.886	2.015	5.985	29.985	44.002	0.92
altered	0.146	1.840	0.000	0.029	2.044	3.498	0.634	0.050	0.392	0.609	11.926	1.970	6.030	30.030	44.000	0.92

chemical changes produced by alteration require removal of Fe, addition of Al, and addition of Si with concurrent shift of Al from the Z to Y site. It is remarkable that the biotite structure could be preserved during such a rearrangement of elements. It is highly unlikely, however, that such an altered chemistry for biotite could ever be mistaken as a primary composition because of the highly distinctive "herringbone" structure that accompanies this alteration (Fig. 14).

Clinopyroxene and hornblende are not appreciably affected by high-temperature deuteric alteration in any NTS unit (see Fig. 12), although they are thoroughly destroyed by such alteration in peralkaline units of the Silent Canyon Area (see Table II in Warren, in prep.). The relative resistance to alteration is Hbld>Cpx>Opx for mafic minerals of the TFB; fresh hornblende is found in all six samples, clinopyroxene in four, and orthopyroxene in two (see Tables IV, V). Fresh hornblende occurs as deep as 5948 ft depth in USW G-1 (Table V). Like biotite, hornblende within the lower portion of USW G-1 appears to be partially dissolved away.

Low-temperature zeolitic (chiefly clinoptilolite and mordenite) alteration has no effect on mafic minerals in many units (see Table II in Warren 1983a), yet thoroughly altered hornblende forms appear in most zeolitic samples of the TCB unit (see Tables IV, V). Fresh hornblende appears in single samples of the TCB unit (Table V) that are vitric (TBF-1), zeolitic (USW G-1-2555), and vapor-phase altered (TBF-4). A very small relict portion occurs in a typically altered hornblende within a single zeolitic sample (CFLSM-5); the relict has a composition identical to the dominant composition for hornblende of the TCB unit (see Table XX). The apparent independence of hornblende alteration and alteration conditions indicates that hornblende was already altered before eruption of the TCB unit.

VIII. SYNTHESIS OF PETROGRAPHIC AND ANALYTICAL RESULTS

The single most important finding of this study is the vertical and horizontal consistency of phenocryst compositions within ash-flow cooling units and within groups of ash-flow cooling units. Mafic mineral compositions are consistent among groups of units that closely correspond to petrographic suites of Byers et al. (1976). The molecular Mg/(Mg+Fe) contents of biotite are about 0.60 for the TT and TLR units, about 0.40-0.45 for the TC, TH, and TPTl units (Table XII), about 0.65 for members of the Paintbrush Tuff above the TPTl unit (Warren, in prep.; Broxton et al. 1982), and about 0.60 for the Timber Mountain Tuff (Warren, in prep.). Dominant compositions for sanidine and plagioclase phenocrysts, on the other hand, have characteristic values for each member of a petrographic suite and differ distinctly among each member (Table XII). Petrographic parameters, such as the amount of quartz as the percent of total felsic phenocrysts, also have generally characteristic values throughout a unit. However, these parameters may differ markedly within a unit, particularly within the uppermost portions.

When combined together, the petrographic and analytical results provide an extremely powerful correlative and interpretive tool. It must be assumed that the striking similarity for mafic mineral compositions within a group of units is not accidental, and that each member of such a group developed from closely similar magmas, probably derived from a common parent. Remarkably, however, each succeeding member of the Crater Flat Tuff developed a new and distinct set of feldspar compositions. For the Crater Flat Tuff, the geochemical transition between members is very sharp. The bedded unit above the TCB ash flow, near the top of the unit, contains sanidine that is compositionally identical to sanidine at the base of the ash flow (both have 61 mol% Or+Cn). The sanidine near the base of the overlying TCP unit, like sanidine near the top of the unit, contains 53 mol% Or+Cn. Nowhere is a unit known to occur between the TCB and TCP units that has sanidine with a composition intermediate between the two.

The upper, middle, and lower portions of the TCB unit contain significantly different concentrations of quartz and accessory minerals (Table VI). This requires that these phases are not homogeneously distributed throughout if a single magma chamber is the source of the TCB unit. Because of identical compositions for feldspars among upper, middle, and lower portions of the unit, it is highly unlikely that each portion developed from separate magma chambers. These considerations support the existence of a single magma chamber that has a zonal distribution of phenocryst phases, yet maintains chemical equilibrium throughout for feldspar. The nature of any petrographic variation observed within a unit will depend not only on the nature of zoning within each magma chamber, but also on the eruption mechanics which are unknown.

In most units, plagioclase phenocrysts are zoned from An-rich cores to the most Na-rich composition that dominates at rims (Table XVII). Plagioclase cores are often extremely An-rich, and for the TCP and TCB units there is a paucity of compositions intermediate between those of core and rim (see Tables XV, XVI). This indicates that such An-rich plagioclase cores did not crystallize continuously with the rims. The An-rich cores may have formed from the magma under different P, T conditions than the rims, or may have been introduced at an early stage, either by assimilation of wall rock or mixing of a magma containing plagioclase phenocrysts of such composition. The increase in An contents of plagioclase stratigraphically upward through the TLR, TLRa, TRD and TFB units (Table XV) suggests the latter process may indeed be the most important. Note also the similarity in hornblende and biotite compositions among these units (Tables XVIII-XX).

In the TCT1 unit, however, most plagioclase phenocrysts do not zone to the dominant composition, but rather have an An-rich composition at the rim that is similar to the core composition (see Table XVII). Most plagioclase phenocrysts of the TCT1 unit have compositions that match those for plagioclase phenocrysts within the abundant lithic fragments within the unit. At Pahute Mesa, the TRA(lr) unit of Warren (1983) is a lithic-rich unit that erupted through sanidine-rich peralkaline rocks, and incorporated numerous fragments of sanidine from these rocks as optically unrecognizable xenocrysts. Eruption of the TRA(lr) unit was contemporaneous with or just preceding major volcano-tectonic subsidence (VTS). Because of their similarities to the TRA(lr) unit, the TCT and TLR units are also considered to be units associated with VTS that erupted through plagioclase-rich rocks instead. Analyses for plagioclase xenocrysts (those that have An-rich rims, Table XVII) are not as numerous for the TLR1 unit compared to the TCT1 unit because the TLR unit contains a considerably higher content of plagioclase phenocrysts (Table VI). The TCT and TLR units both have a uniquely high proportion of very small plagioclase phenocrysts among units of USW G-1; this results in a markedly low value for plagioclase as the percent of felsic phenocrysts estimated from the largest grains only, compared to the percent estimated from all grains (see Fig. 6).

IX. SUMMARY AND CONCLUSIONS

A consistent and definitive set of petrographic characteristics and mineral compositions has been determined for each unit of USW G-1, and for widely separated outcrop samples of many of the units present in USW G-1. These characteristics provide an accurate and reliable means to correlate units in subsurface throughout the entire NTS, as demonstrated by Warren (1983). This provides the NNWSI and Containment Programs of Los Alamos with a tool to accurately define the subsurface geologic environment. Two processes, secondary alteration and magmatic processes, may affect the consistency of petrographic and mineral compositional characteristics within each unit. Alteration does not seriously affect these characteristics in USW G-1 and consequently does not interfere with their use in correlation. Magmatic processes, however, control variations in petrography and mineral chemistry that are substantial for many units. The general nature of these variations is summarized below.

Mafic mineral compositions are consistent for groups of units; units within each such group are certainly closely related, probably through a common or similar parent magma system such as that hypothesized by Hildreth (1981) and conversely, those in a different group are either unrelated or related through a highly significant process of geochemical evolution. Based on the mafic mineral compositions, units of USW G-1 define two petrographic suites: the TFB, TRD, TLR, TTA, TTB, and TTC units (relatively Mg-rich mafics) and the TC, TH, and TPTl units (relatively Mg-poor mafics). The TPTl unit is formally grouped with the Paintbrush Tuff (Byers et al. 1976), but the compositions of mafic minerals in the TPTu and all younger members of the Paintbrush Tuff are markedly more Mg-rich (Warren, in prep.; Broxton et al. 1982), indicating that the TPTl unit is chemically allied with underlying, rather than overlying units.

Although each succeeding unit of a petrographic suite was probably derived from a parent magma that closely resembled the parent of the preceding unit, most units formed feldspar phenocrysts with compositions that differ significantly from those of the preceding unit. This indicates that significant magmatic evolution has occurred during the time between eruption of such units. In other cases, however, two or more units show a continuous set of feldspar compositions and these units are probably components of a single, large magma system. Each system maintains limited chemical equilibrium (Warren 1983), but has a zonal distribution of phenocryst phases. Following eruption, the distribution of phenocrysts throughout the unit will depend on the extent of zoning in the magma and the (unknown) mechanics of eruption.

Within the older petrographic suite, the TLR and TTA units have identical feldspar compositions (Table XII) and differ only in the higher quartz and sanidine contents of the latter. These units certainly were derived from the same magma chamber and should be considered as members of the same unit. A high lithic content and certain other features indicate that the TLR unit is associated with volcano-tectonic subsidence in USW G-1. The TTC unit has feldspar that is considerably Na-poorer than those of the TLR/TTA units and clearly is a chemically distinct unit. The TTB unit has feldspar that has compositions intermediate between those of the TTC and TLR/TTA units and is considered a geochemically transitional unit between these units. The TRD and TFB units are mafic-rich units thought to be related to the mafic-poor TLR unit in much the same manner as the mafic-rich and mafic-poor members of the TMR unit are related to each other.

Within the younger petrographic suite, each member of the TC unit has a distinct set of feldspar compositions. Feldspar compositions for bedded units match those for the TC ash-flow cooling unit below, except that feldspar compositions for the bedded tuff beneath the TCT unit are similar to those of the TCT unit. These findings have resulted in a minor revision of the stratigraphic sequence in USW G-1 (Table III). Samples from the lower portion of the TCT unit contain unusually high contents of lithic fragments and plagioclase xenocrysts. These features indicate that the TCT unit at USW G-1 was deposited close to its source, probably within a volcano-tectonic subsidence structure. The TH1 and TH2 units have similar, distinctive feldspar chemistries that suggest that these units are components of a large, single magma system. The TPTl unit differs dramatically in mineral chemistry from the TPTu unit that caps it (Lipman et al. 1966); the TPTl unit is the youngest unit of a petrographic suite defined by Fe-rich mafics, and the TPTu unit is the oldest unit of a petrographic suite defined by Mg-rich mafics.

ACKNOWLEDGMENTS

The authors are indebted to Janet Repa and Anthony T. Garcia for preparation of the illustrations. To Marcia A. Jones, who typed the document, we owe a special gratitude for help in the design of very complex tables. We appreciate a very timely and helpful review by Ronald C. Gooley. Without the support and encouragement of Thomas A. Weaver and Wayne A. Morris, past and present Group Leaders of the Geochemistry Group, this work would not have been possible. Portions of this work were supported by the Nevada Nuclear Waste Storage Investigations Program of Los Alamos and the U.S. Geologic Survey, and by the Containment Program of Los Alamos.

REFERENCES

Bence, A. and A. Albee, "Empirical Correction Factors for Electron Microanalyses of Silicates and Oxides," J. Geol. 76, 382-403 (1968).

Bish, D. L., F. A. Caporuscio, J. F. Copp, B. M. Crowe, J. D. Purson, J. R. Smyth, and R. G. Warren, "Preliminary Stratigraphic and Petrologic Characterization of Core Samples from USW-G1, Yucca Mountain, Nevada," Los Alamos National Laboratory report LA-8840-MS, 66 pp. (November 1981).

Broxton, D. E., D. Vaniman, F. Caporuscio, B. Arney, and G. Heiken, "Detailed Petrographic Descriptions and Microprobe Data for Drill Holes USW G-2 and Ue-25b#1H, Yucca Mountain, Nevada," Los Alamos National Laboratory report LA-9324-MS (October 1982).

Byers, F. M., Jr., W. J. Carr, P. P. Orkild, W. D. Quinlivan and K. A. Sargent, "Volcanic Suites and Related Cauldrons of Timber Mountain - Oasis Valley Caldera Complex, Southern Nevada," U.S. Geol. Surv. Prof. Paper 919, 69 pp. (1976).

Byers, F. M., Jr., and R. G. Warren, "Revised Volcanic Stratigraphy of Drill Hole J-13, Fortymile Wash, Nevada, Based on Petrographic Modes and Chemistry of Phenocrysts," Los Alamos National Laboratory report LA-9652-MS (January 1983).

Caporuscio, F. A., R. G. Warren, D. E. Broxton, "Detailed Petrographic Descriptions and Microprobe Data for Tertiary Silicic Volcanic Rock in Drill Hole USW G-1, Yucca Mountain, Nevada," Los Alamos National Laboratory report LA-9323-MS (in preparation).

Carmichael, I. S. E., F. J. Turner, and J. Verhoogen, Igneous Petrology, (McGraw Hill, New York 1974) 739 pp.

Carr, W. J., "Structure and Clay Alteration," in Results of Exploration of Baneberry Site, Early 1971, (U.S. Geol. Surv. Denver, CO) USGS-474-145, pp. 7-18 (1974).

Carr, W. J., "Volcano-Tectonic History of Crater Flat, Southwestern Nevada, as Suggested by New Evidence From Drill Hole USW-VH-1 and Vicinity," U.S. Geol. Surv. Open-file report 82-457, 23 p. (1982).

Christiansen, R. L. and P. W. Lipman, "Geologic Map of the Topopah Spring NW Quadrangle, Nye County, Nevada," U.S. Geol. Surv., Denver, CO, Map GQ-444, scale 1:24 000 (1965).

Cornwall, H. R. and F. J. Kleinhampl, "Geology of the Bare Mountain Quadrangle, Nevada," U.S. Geol. Surv., Denver, CO, Map GQ-157, scale 1:62 500 (1961).

Glenn, H. D., J. T. Rambo and R. W. Terhune, "Calculational Examination of the Baneberry Event - Addendum," Lawrence Livermore National Laboratory report UCRL-53164, 71 pp. (1981).

Heiken, G. H. and M. L. Bevier, "Petrology of Tuff Units from the J-13 Drill Site, Jackass Flats, Nevada," Los Alamos Scientific Laboratory report LA-7563-MS, 55 pp. (February 1979).

Hildreth, W., "Gradients in Silicic Magma Chambers: Implications for Lithospheric Magmatism," J. Geophys. Res. 86(B11), 10153-10192, Nov. 10 (1981).

Ito, J., "A Study of Chevkinite and Perrierite," Am. Miner. 52, 1094-1104 (1967).

Izett, G. A. and R. E. Wilcox, "Perrierite, Chevkinite, and Allanite in Upper Cenozoic Ash Beds in the Western United States," Am. Miner. 53, 1558-1567 (1968).

Lipman, P. W., R. L. Christiansen, and J. T. O'Connor, "A Compositionally Zoned Ash-Flow Sheet in Southern Nevada," U.S. Geol. Surv. Prof. Paper 524-F, 47 pp. (1966).

Lipman, P. W. and E. J. McKay, "Geologic Map of the Topopah Spring SW Quadrangle, Nye County, Nevada," U.S. Geol. Surv., Denver, CO, Map GQ-368, scale 1:24 000 (1965).

Orkild, P. P., K. A. Sargent and R. P. Snyder, "Geologic Map of Pahute Mesa, Nevada Test Site and Vicinity, Nye County, Nevada," U.S. Geol. Surv., Denver, CO, Map I-567, scale 1:62 500 (1969).

Sargent, K. A., E. J. McKay, and B. C. Burchfiel, "Geologic Map of the Striped Hills Quadrangle, Nye County, Nevada," U.S. Geol. Surv., Denver, CO, Map GQ-882, scale 1:24 000 (1970).

Spengler, R. W., D. C. Muller, and R. B. Livermore, "Preliminary Report on the Geology and Geophysics of Drill Hole Ue25a-1, Yucca Mountain, Nevada Test Site," U.S. Geol. Surv. Open-file report 79-1244, 43 pp. (1979).

Spengler, R. W., F. M. Byers, Jr., and J. B. Warner, "Stratigraphy and Structure of Volcanic Rocks for Drill Hole USW-G1, Yucca Mountain, Nye County, Nevada," U.S. Geol. Surv. Open-file report 81-1349, 50 pp. (1981).

Sykes, M. L., G. H. Heiken and J. R. Smyth, "Mineralogy and Petrology of Tuff Units from the Ue25a-1 Drill Site, Yucca Mountain, Nevada," Los Alamos Scientific Laboratory report LA-8139-MS, 76 pp. (November 1979).

Warren, R. G., "Use of Petrology and Geochemistry to Define Petrographic Units in Drill Holes UE-19p, UE-19p#1, and UE-19ab, Southeastern Pahute Mesa, Nevada Test Site," Los Alamos National Laboratory report (in preparation).

Warren, R. G., "Geochemical Similarities between Volcanic Units at Yucca Mountain and Pahute Mesa: Evidence for a Common Magmatic Origin for Volcanic Sequences that Flank the Timber Mountain Caldera," in Proc. 2nd Containment Symposium (1983).

APPENDIX A-I

AVERAGED ELECTRON MICROPROBE ANALYSES FOR SANIDINE PHENOCRYSTS (All (n) analyses, in weight percent, within each interval defined in Table XI are separately averaged for all samples of each unit. See Table II for definition of unit symbols.)

Mol% Or+Cn	n	SiO_2	Al_2O_3	Fe_2O_3	MgO	CaO	BaO	Na_2O	K_2O	Total	Unit Symbol
70-72	1	66.5	17.4	0.00	0.00	0.20	0.00	3.12	12.0	99.2	TPT1
64-66	2	66.2	18.5	0.04	0.00	0.22	0.26	3.87	11.3	100.4	TPT1
62-64	5	65.4	18.4	0.04	0.00	0.20	0.15	4.06	10.9	99.6	TPT1
60-62	6	65.8	18.5	0.06	0.00	0.21	0.06	4.29	10.4	99.3	TPT1
58-60	10	65.9	18.6	0.06	0.00	0.24	0.07	4.49	10.1	99.5	TPT1
56-58	5	66.6	18.7	0.11	0.00	0.24	0.00	4.70	9.63	100.0	TPT1
54-56	6	65.7	18.7	0.16	0.00	0.32	0.00	4.89	9.41	99.2	TPT1
52-54	2	65.8	18.7	0.05	0.00	0.29	0.00	5.12	8.89	98.9	TPT1
48-50	1	66.1	18.9	0.09	0.00	0.31	0.00	5.45	8.14	98.9	TPT1
46-48	2	66.7	18.8	0.12	0.00	0.30	0.14	5.81	8.36	100.3	TPT1
44-46	1	65.1	18.9	0.04	0.00	0.34	0.00	6.01	7.79	98.2	TPT1
42-44	2	66.4	18.9	0.09	0.00	0.20	0.22	6.32	7.50	99.5	TPT1
40-42	1	67.3	18.8	0.09	0.01	0.36	0.00	6.43	6.81	99.8	TPT1
36-38	1	65.9	19.4	0.04	0.00	0.00	1.08	7.21	5.98	99.6	TPT1
28-30	1	67.4	19.2	0.13	0.00	0.39	0.15	7.83	5.10	100.3	TPT1
14-16	3	67.5	19.3	0.05	0.00	0.34	0.83	9.93	2.47	100.4	TPT1
6-8	2	67.0	19.4	0.00	0.00	0.38	0.00	10.9	1.22	98.9	TPT1
4-6	1	68.2	19.6	0.09	0.00	0.51	0.00	11.1	0.96	100.5	TPT1
68-70	21	66.0	18.6	0.02	0.00	0.20	0.22	3.48	11.8	100.3	TH1
66-68	17	66.3	18.5	0.00	0.00	0.15	0.13	3.57	11.5	100.2	TH1
50-52	2	66.3	18.8	0.05	0.00	0.26	0.00	5.35	8.73	99.5	TH1
46-48	2	66.6	18.8	0.03	0.00	0.31	0.10	5.80	8.27	99.9	TH1
74-76	1	66.2	18.2	0.11	0.00	0.18	1.11	2.57	12.2	100.6	TH2
72-74	12	65.0	18.7	0.01	0.00	0.17	1.03	2.92	12.1	99.9	TH2
70-72	1	66.2	18.5	0.01	0.02	0.17	0.45	3.28	12.4	101.0	TH2
56-60	2	66.7	19.0	0.10	0.00	0.26	0.10	4.72	10.0	100.9	TCP
54-56	21	66.5	18.9	0.10	0.00	0.26	0.12	5.02	9.28	100.2	TCP
52-54	74	66.5	18.8	0.10	0.00	0.28	0.13	5.22	9.14	100.3	TCP
50-52	23	66.6	18.9	0.10	0.00	0.29	0.08	5.35	8.87	100.2	TCP
48-50	3	67.4	19.0	0.11	0.00	0.31	0.18	5.45	8.41	100.9	TCP
46-48	3	65.2	18.8	0.10	0.00	0.46	0.07	5.87	8.09	98.6	TCP
42-46	2	67.2	18.9	0.11	0.00	0.34	0.24	6.31	7.57	100.7	TCP
26-28	1	69.0	18.9	0.08	0.00	0.25	0.66	8.50	4.54	101.9	TCP

Appendix A-I (cont)

Mol% Or+Cn	n	SiO_2	Al_2O_3	Fe_2O_3	MgO	CaO	BaO	Na_2O	K_2O	Total	Unit Symbol
62-64	4	65.9	18.8	0.11	0.00	0.23	0.36	4.10	10.6	100.1	TCBa
60-62	2	66.1	18.9	0.11	0.00	0.30	0.38	4.18	10.2	100.2	TCBa
58-60	4	65.6	19.3	0.12	0.00	0.34	0.52	4.32	9.88	100.3	TCBa
56-58	1	66.1	19.3	0.03	0.00	0.41	0.29	4.67	9.86	100.7	TCBa
54-56	1	66.7	19.1	0.07	0.00	0.59	0.59	5.04	9.42	101.5	TCBa
64-66	2	65.8	18.8	0.12	0.00	0.17	0.16	3.79	10.8	99.6	TCB
62-64	56	65.9	18.7	0.08	0.00	0.20	0.51	4.09	10.5	100.0	TCB
60-62	182	66.0	18.7	0.09	0.00	0.20	0.58	4.27	10.3	100.1	TCB
58-60	33	65.7	18.7	0.08	0.00	0.22	0.63	4.40	9.94	99.8	TCB
56-58	8	66.2	18.6	0.09	0.00	0.23	0.45	4.58	9.70	99.9	TCB
54-56	2	65.3	18.7	0.02	0.00	0.22	0.47	5.02	9.20	98.9	TCB
52-54	2	67.4	18.9	0.10	0.00	0.21	0.63	5.17	9.02	101.4	TCB
48-50	2	67.2	18.7	0.08	0.00	0.20	0.44	5.73	8.30	100.7	TCB
40-44	2	66.8	19.1	0.11	0.00	0.28	0.75	6.55	6.87	100.5	TCB
34-36	1	67.6	19.0	0.08	0.00	0.20	0.55	7.33	5.98	100.7	TCB
73-75	2	66.8	18.6	0.09	0.01	0.15	0.24	2.69	12.1	100.6	TCT
70-72	3	65.8	18.5	0.07		0.21	0.50	3.17	11.7	100.0	TCT
68-70	38	65.5	18.6	0.09	0.00	0.19	0.68	3.41	11.5	100.0	TCT
66-68	157	65.6	18.7	0.09	0.00	0.19	0.59	3.57	11.2	99.9	TCT
64-66	43	66.0	18.8	0.10	0.00	0.19	0.59	3.67	10.7	100.1	TCT
62-64	8	66.3	18.8	0.09	0.00	0.20	0.35	3.78	10.2	99.7	TCT
60-62	5	66.8	18.9	0.12	0.00	0.20	0.61	3.87	9.27	99.8	TCT
58-60	2	66.8	18.3	0.06	0.00	0.17	0.58	4.32	9.29	99.5	TCT
50-52	1	66.4	19.1	0.06	0.00	0.27	1.02	5.30	8.46	100.6	TCT
71-73	2	63.9	18.7	0.20	0.00	0.19	1.65	2.74	10.6	97.9	TLR
66-68	30	64.9	18.7	0.13	0.00	0.20	1.41	3.60	10.7	99.7	TLR
64-66	122	65.4	18.5	0.12	0.00	0.19	0.79	3.77	10.7	99.4	TLR
62-64	32	65.3	18.7	0.14	0.00	0.21	0.98	3.88	10.3	99.5	TLR
60-62	3	66.1	19.0	0.18	0.00	0.20	0.62	4.14	9.76	100.0	TLR
58-60	3	65.6	18.9	0.14	0.00	0.22	0.67	4.37	9.64	99.5	TLR
48-50	2	66.2	18.8	0.13	0.01	0.22	0.50	5.63	8.39	99.9	TLR
68-70	4	63.9	18.6	0.20		0.16	2.06	3.43	10.9	99.2	TTAB
66-68	22	65.4	18.5	0.15	0.00	0.18	1.08	3.58	11.0	99.9	TTAB
64-66	62	65.1	18.4	0.16	0.00	0.18	0.67	3.76	10.7	99.0	TTAB
62-64	45	65.9	18.4	0.16	0.00	0.20	0.55	3.88	10.3	99.4	TTAB
60-62	4	66.8	18.6	0.17	0.00	0.22	0.26	4.16	10.2	100.4	TTAB
58-60	1	66.3	18.6	0.12		0.26	1.27	4.45	9.68	100.7	TTAB
72-74	27	63.2	19.1	0.17	0.00	0.20	3.41	2.87	11.0	100.0	TTC
70-72	17	63.5	18.8	0.14	0.00	0.20	2.98	2.97	10.7	99.3	TTC

APPENDIX A-II

INDIVIDUAL ANALYSES FOR SANIDINE PHENOCRYSTS IN LITHIC FRAGMENTS

(All analyses in weight percent. See Table II for definition of host unit symbol. For grain identification numbers: C = core, M = mid, R = rim, as defined in text.)

Mol%													Grain		Host
Or	Cn	An	SiO_2	Al_2O_3	Fe_2O_3	MgO	CaO	BaO	Na_2O	K_2O	Total	I.D. No.	Sample	Unit Symbol
62.0	0.0	0.6	66.0	18.5	0.04	0.00	0.16	0.00	4.15	10.5	99.4	12C	USW G-1-1286	TPT1
61.1	0.0	1.2	66.6	18.6	0.03	0.00	0.25	0.00	4.29	10.6	100.4	12M	"	"
58.0	0.2	1.2	65.6	18.8	0.04	0.00	0.27	0.12	4.55	9.90	99.3	12R	"	"
48.6	0.2	1.2	66.9	18.6	0.09	0.00	0.27	0.15	5.52	8.20	99.7	28C	"	"
53.6	7.5	1.1	62.9	19.5	0.09	0.00	0.24	4.02	4.07	8.73	99.6	30C	USW G-1-1292	TPT1
67.1	1.2	0.8	65.6	18.9	0.09		0.19	0.70	3.51	11.6	100.6	A1C	J13-2980	TCT
56.6	0.1	1.1	65.4	18.4	0.10		0.24	0.07	4.76	9.69	98.7	39C	J13-3493	TLR
51.7	0.2	1.6	66.5	18.6	0.12		0.36	0.09	5.28	8.94	99.8	40C	"	"
48.5	0.0	2.0	67.7	18.9	0.08		0.42	0.00	5.72	8.51	101.3	43C	"	"
52.2	0.2	0.8	67.4	18.6	0.11		0.19	0.14	5.27	8.93	100.6	44C	"	"
20.7	0.5	5.3	66.2	19.7	0.22		1.14	0.36	8.53	3.77	99.9	12C	USW G-1-4504	TLR

APPENDIX B-I

AVERAGED ELECTRON MICROPROBE ANALYSES FOR PLAGIOCLASE PHENOCRYSTS (All (n) analyses, in weight percent, within each interval defined in Tables XV and XVI combined are separately averaged for all samples of each unit. See Table II for definition of unit symbols.)

Mol% An	n	SiO_2	Al_2O_3	Fe_2O_3	MgO	CaO	BaO	Na_2O	K_2O	Total	Unit Symbol
14-16	16	64.5	21.8	0.11	0.00	3.23	0.00	9.01	1.32	100.0	TPT1
16-18	18	64.2	22.1	0.12	0.00	3.63	0.00	8.92	1.18	100.2	TPT1
18-20	6	63.8	22.3	0.08	0.00	3.99	0.00	8.93	1.08	100.2	TPT1
20-22	1	63.7	22.8	0.10	0.00	4.45	0.00	8.54	1.16	100.8	TPT1
22-24	2	61.7	23.5	0.10	0.00	4.77	0.00	8.29	0.73	99.1	TPT1
24-26	2	62.0	23.5	0.14	0.01	5.09	0.06	8.26	0.81	99.9	TPT1
26-28	2	61.9	23.9	0.14	0.00	5.49	0.00	7.98	0.71	100.1	TPT1
28-30	1	60.1	24.4	0.13	0.00	6.04	0.00	8.04	0.35	99.1	TPT1
30-32	2	60.1	24.7	0.04	0.00	6.67	0.03	7.67	0.58	99.8	TPT1
32-34	5	59.5	25.0	0.07	0.00	6.83	0.08	7.39	0.52	99.4	TPT1
34-36	4	59.5	25.1	0.06	0.00	7.44	0.04	7.38	0.52	100.0	TPT1
36-38	1	58.8	25.3	0.22	0.04	8.05	0.03	6.92	0.63	100.0	TPT1
38-40	3	57.5	26.3	0.13	0.00	8.31	0.00	6.76	0.42	99.4	TPT1
40-45	1	57.1	26.8	0.20	0.01	8.54	0.06	5.88	0.25	98.8	TPT1
45-50	3	56.7	27.4	0.12	0.00	10.0	0.00	5.91	0.33	100.5	TPT1
50-54	3	54.9	28.0	0.21	0.02	10.2	0.02	5.16	0.31	98.8	TPT1
14-16	5	64.7	22.2	0.09	0.00	3.13	0.02	9.02	1.30	100.5	TH1
16-18	4	64.3	22.1	0.06	0.00	3.75	0.15	8.87	1.24	100.5	TH1
18-20	13	63.8	22.6	0.10	0.00	4.06	0.00	8.74	1.25	100.6	TH1
20-22	16	63.5	22.7	0.09	0.00	4.50	0.00	8.70	1.12	100.6	TH1
22-24	3	62.8	23.0	0.07	0.00	4.87	0.11	8.41	0.95	100.2	TH1
26-28	1	62.8	24.2	0.06	0.00	5.52	0.00	8.05	0.81	101.4	TH1
22-24	1	63.6	23.2	0.07	0.00	4.86	0.00	8.57	1.08	101.4	TH2
24-26	1	62.6	23.8	0.12	0.00	5.25	0.00	8.18	0.94	100.9	TH2
26-28	1	61.1	24.0	0.09	0.00	5.80	0.09	7.86	0.82	99.8	TH2
28-30	2	62.0	24.2	0.13	0.00	6.02	0.20	7.86	0.78	101.2	TH2
32-34	1	61.2	24.7	0.00	0.00	6.98	0.03	7.54	0.61	101.1	TH2
34-36	2	59.8	25.4	0.00	0.00	7.39	0.12	7.17	0.55	100.4	TH2
36-38	4	58.9	25.9	0.00	0.00	7.78	0.11	6.97	0.50	100.2	TH2
38-40	1	58.2	25.8	0.07	0.00	8.20	0.12	6.56	0.50	99.5	TH2
40-42	1	58.8	26.6	0.01	0.01	8.83	0.14	6.63	0.49	101.5	TH2

Appendix B-I (cont)

Mol% An	n	SiO_2	Al_2O_3	Fe_2O_3	MgO	CaO	BaO	Na_2O	K_2O	Total	Unit Symbol
8.0-9.0	2	66.6	20.9	0.17	0.00	1.86	0.09	9.47	1.93	101.0	TCP
9.0-10	17	66.5	20.8	0.13	0.00	2.07	0.00	9.34	1.85	100.7	TCP
10-12	59	65.9	21.1	0.12	0.00	2.31	0.01	9.21	1.71	100.4	TCP
12-14	17	65.2	21.1	0.17	0.00	2.72	0.00	9.28	1.43	99.9	TCP
14-16	1	66.3	21.3	0.20		3.05	0.02	9.39	1.38	101.6	TCP
18-20	1	63.5	22.5	0.11	0.00	4.27	0.00	8.93	1.08	100.4	TCP
20-30	10	61.7	23.9	0.14	0.00	5.67	0.08	8.12	0.70	100.3	TCP
30-40	14	59.2	25.3	0.16	0.00	7.30	0.06	7.21	0.50	99.7	TCP
40-50	7	56.6	26.9	0.22	0.01	9.54	0.03	6.11	0.31	99.7	TCP
50-62	4	55.0	28.7	0.18	0.00	11.2	0.00	5.02	0.21	100.3	TCP
14-16	2	65.2	21.7	0.22	0.00	3.29	0.09	8.46	1.83	100.8	TCBa
16-18	5	64.7	22.2	0.19	0.00	3.48	0.18	8.49	1.38	100.6	TCBa
18-20	2	64.2	22.0	0.20	0.00	3.89	0.12	8.54	1.28	100.3	TCBa
20-23	2	63.1	23.2	0.15	0.00	4.40	0.10	8.11	1.20	100.3	TCBa
26-30	2	61.1	24.0	0.07	0.01	5.70	0.15	7.17	1.41	99.6	TCBa
30-32	1	60.3	25.1	0.07	0.00	6.29	0.04	7.39	0.55	99.7	TCBa
34-36	1	59.0	26.2	0.04	0.00	7.41	0.18	7.07	0.49	100.4	TCBa
46-48	1	56.3	27.6	0.09	0.00	9.55	0.08	5.95	0.32	99.9	TCBa
54-56	1	55.2	29.2	0.23	0.01	11.1	0.16	5.02	0.22	101.1	TCBa
10-12	3	65.0	20.9	0.11	0.00	2.53	0.00	9.45	1.58	99.6	TCB
12-14	35	65.0	21.4	0.12	0.00	2.84	0.00	9.22	1.32	99.9	TCB
14-16	125	64.9	21.7	0.13	0.00	3.19	0.00	9.04	1.24	100.2	TCB
16-18	74	64.6	21.9	0.14	0.00	3.51	0.00	8.94	1.07	100.2	TCB
18-20	14	64.0	22.2	0.13	0.00	4.00	0.00	8.82	0.98	100.1	TCB
20-25	19	63.1	23.0	0.16	0.00	4.58	0.01	8.39	0.87	100.1	TCB
25-30	11	61.4	24.0	0.20	0.00	5.80	0.06	7.92	0.64	100.0	TCB
30-35	12	59.9	24.7	0.17	0.00	6.78	0.00	7.55	0.52	99.6	TCB
35-40	14	59.1	25.7	0.21	0.00	7.87	0.03	7.02	0.42	100.4	TCB
40-44	10	57.3	26.6	0.16	0.00	8.93	0.03	6.37	0.30	99.7	TCB
46-50	6	55.9	27.2	0.20	0.00	9.79	0.00	5.85	0.28	99.2	TCB
14-18	7	64.4	22.2	0.17	0.00	3.47	0.00	8.75	1.30	100.3	TCT
18-20	32	63.8	22.7	0.16	0.00	4.08	0.06	8.66	1.10	100.6	TCT
20-22	58	63.5	22.9	0.17	0.00	4.41	0.04	8.48	1.02	100.5	TCT
22-24	28	63.0	23.1	0.19	0.00	4.78	0.05	8.25	0.96	100.3	TCT
24-26	17	62.4	23.6	0.21	0.00	5.13	0.04	8.19	0.82	100.4	TCT
26-28	15	61.6	24.0	0.18	0.00	5.61	0.13	7.85	0.68	100.0	TCT
28-30	18	61.0	24.2	0.21	0.00	6.05	0.06	7.62	0.77	99.9	TCT
30-32	10	60.5	24.7	0.18	0.00	6.52	0.00	7.44	0.66	100.1	TCT
32-34	14	60.4	24.8	0.23	0.00	6.87	0.04	7.23	0.60	100.2	TCT
34-36	14	59.8	25.2	0.22	0.00	7.23	0.03	7.00	0.59	100.1	TCT
36-38	13	59.4	25.6	0.21	0.00	7.57	0.00	6.75	0.58	100.1	TCT

Appendix B-I (cont)

Mol% An	n	SiO_2	Al_2O_3	Fe_2O_3	MgO	CaO	BaO	Na_2O	K_2O	Total	Unit Symbol
38-40	13	58.4	26.0	0.28	0.00	7.91	0.01	6.43	0.58	99.6	TCT
40-45	14	58.1	26.5	0.24	0.00	8.61	0.05	6.29	0.52	100.3	TCT
45-50	9	56.4	27.4	0.32	0.00	9.75	0.00	5.68	0.40	100.0	TCT
50-55	8	55.5	27.9	0.40		10.3	0.01	5.15	0.38	99.6	TCT
55-60	4	54.8	28.7	0.40		11.7	0.00	4.78	0.27	100.7	TCT
60-67	8	52.7	29.3	0.60		12.8	0.00	4.02	0.27	99.7	TCT
44-46	1	56.2	26.0	0.62		9.11	0.00	5.67	0.78	98.4	TFB
46-48	9	56.0	26.5	0.72		9.72	0.09	5.63	0.58	99.2	TFB
48-50	4	56.4	27.0	0.59		10.1	0.24	5.49	0.53	100.4	TFB
50-52	4	55.3	27.7	0.66		10.6	0.00	5.37	0.47	100.1	TFB
54-56	4	54.0	28.0	0.50		11.3	0.00	4.82	0.40	99.0	TFB
56-58	8	53.0	28.6	0.57		11.9	0.04	4.64	0.33	99.1	TFB
58-60	5	53.5	29.2	0.47	0.09	12.2	0.02	4.50	0.35	100.2	TFB
60-62	14	53.0	29.0	0.57	0.05	12.6	0.02	4.28	0.26	99.8	TFB
62-64	7	52.0	29.6	0.50		13.0	0.02	4.07	0.25	99.4	TFB
64-66	7	51.5	29.7	0.54		13.3	0.00	3.78	0.24	99.1	TFB
66-68	5	50.9	30.1	0.38	0.05	13.6	0.00	3.53	0.21	98.7	TFB
70-72	1	50.9	30.7	0.63		14.7	0.00	3.17	0.35	100.5	TFB
72-74	3	49.3	31.0	0.58		14.9	0.04	3.01	0.12	99.1	TFB
74-76	2	50.0	32.0	0.59	0.06	15.5	0.00	2.69	0.13	101.0	TFB
76-78	2	49.1	31.9	0.56		16.0	0.05	2.53	0.12	100.3	TFB
78-80	3	48.4	32.5	0.70	0.04	15.9	0.05	2.30	0.13	99.9	TFB
26-28	1	61.8	24.4	0.10		5.86	0.09	7.99	0.82	101.1	TLRa
38-40	2	53.3	26.2	0.18		8.14	0.12	6.71	0.62	100.3	TLRa
40-42	2	57.9	26.7	0.32		8.76	0.07	6.28	0.65	100.7	TLRa
42-44	3	57.3	26.7	0.36		8.92	0.22	6.23	0.53	100.3	TLRa
46-48	1	56.8	26.9	0.30		9.45	0.13	5.79	0.50	99.9	TLRa
48-50	2	56.2	27.8	0.13		10.0	0.03	5.59	0.42	100.2	TLRa
52-54	1	54.9	28.6	0.33		11.0	0.00	4.99	0.31	100.1	TLRa
14-16	6	65.0	21.5	0.20	0.00	3.13	0.06	8.74	1.58	100.2	TLR
16-18	27	64.1	21.9	0.22	0.00	3.61	0.04	8.76	1.26	99.9	TLR
18-20	40	63.2	22.3	0.22	0.00	3.99	0.04	8.72	1.07	99.5	TLR
20-22	20	62.9	22.8	0.23	0.00	4.36	0.06	8.42	0.97	99.7	TLR
22-24	18	62.3	23.0	0.22	0.00	4.86	0.09	8.35	0.85	99.7	TLR
24-26	15	62.2	23.2	0.22	0.00	5.23	0.12	8.14	0.82	99.9	TLR
26-28	10	61.5	23.3	0.26	0.00	5.59	0.08	7.95	0.74	99.4	TLR
28-30	12	60.9	24.0	0.21	0.00	6.03	0.10	7.59	0.72	99.6	TLR
30-32	5	59.7	24.4	0.22	0.02	6.39	0.20	7.54	0.66	99.0	TLR
32-34	9	59.8	24.7	0.24	0.00	6.72	0.16	7.20	0.59	99.4	TLR

Appendix B-I (cont)

Mol% An	n	SiO_2	Al_2O_3	Fe_2O_3	MgO	CaO	BaO	Na_2O	K_2O	Total	Unit Symbol
34-36	5	59.1	25.5	0.27	0.00	7.07	0.08	6.90	0.51	99.4	TLR
36-38	4	58.5	25.5	0.17	0.00	7.62	0.17	6.78	0.49	99.2	TLR
38-40	7	58.1	26.1	0.23	0.00	7.99	0.13	6.62	0.40	99.6	TLR
40-45	7	57.9	26.4	0.26	0.00	8.66	0.17	6.46	0.36	100.2	TLR
45-50	5	56.9	27.3	0.26	0.00	9.49	0.11	5.78	0.30	100.1	TLR
58-60	2	52.9	29.1	0.26	0.02	11.9	0.07	4.62	0.19	99.1	TLR
14-16	5	64.3	21.9	0.28	0.00	3.26	0.04	8.97	1.31	99.8	TTAB
16-18	17	63.7	22.1	0.24	0.00	3.54	0.03	8.83	1.07	99.5	TTAB
18-20	23	63.5	22.1	0.24	0.00	3.95	0.00	8.61	1.13	99.5	TTAB
20-22	12	62.6	22.6	0.24	0.00	4.41	0.02	8.59	0.93	99.4	TTAB
22-24	11	62.0	22.8	0.24	0.00	4.81	0.00	8.37	0.87	99.1	TTAB
24-26	7	61.7	23.3	0.27	0.00	5.31	0.08	8.15	0.79	99.6	TTAB
26-28	14	61.0	24.0	0.23	0.00	5.56	0.06	7.91	0.67	99.5	TTAB
28-30	16	60.9	24.0	0.28	0.00	6.02	0.02	7.85	0.65	99.7	TTAB
30-32	12	60.2	24.5	0.28	0.00	6.44	0.01	7.51	0.60	99.5	TTAB
32-34	5	60.4	24.8	0.26	0.00	6.86	0.00	7.52	0.56	100.4	TTAB
34-36	6	58.8	24.8	0.31	0.00	7.46	0.00	7.28	0.50	99.2	TTAB
36-38	2	58.1	25.6	0.37	0.00	7.88	0.20	7.14	0.37	99.7	TTAB
40-45	7	56.9	26.6	0.26	0.00	8.67	0.06	6.15	0.35	99.0	TTAB
45-50	2	56.1	27.5	0.33	0.00	9.72	0.00	5.73	0.26	99.6	TTAB
50-52	1	54.8	28.3	0.37	0.00	10.2	0.00	5.20	0.25	99.1	TTAB
56-58	1	54.6	29.3	0.37	0.00	11.5	0.08	4.76	0.21	100.8	TTAB
26-28	5	61.5	23.3	0.27	0.00	5.70	0.17	7.97	0.83	99.7	TTC
28-30	20	60.8	24.0	0.26	0.00	6.26	0.05	7.63	0.79	99.8	TTC
30-32	17	60.3	24.4	0.27	0.00	6.48	0.05	7.41	0.74	99.7	TTC
32-34	16	59.9	24.7	0.27	0.00	6.84	0.08	7.21	0.69	99.7	TTC
34-36	14	59.5	25.2	0.26	0.00	7.13	0.05	6.94	0.65	99.7	TTC
36-38	2	58.8	25.5	0.29	0.00	7.61	0.09	6.51	0.56	99.4	TTC
38-40	5	58.4	25.9	0.32	0.00	7.87	0.01	6.37	0.58	99.5	TTC
40-42	2	57.1	26.6	0.30	0.00	8.28	0.04	6.04	0.49	98.9	TTC
42-44	3	57.5	26.8	0.33	0.00	8.84	0.00	6.10	0.46	100.0	TTC
44-46	3	57.1	26.6	0.32	0.00	8.81	0.08	5.75	0.46	99.1	TTC

APPENDIX B-II

INDIVIDUAL ANALYSES FOR PLAGIOCLASE PHENOCRYSTS IN LITHIC FRAGMENTS. (All analyses in weight percent. See Table II for definition of host unit symbol. For grain identification numbers: C = core, M = mid, R = rim, as defined in text.)

Mol% Or	Mol% Cn	Mol% An	SiO_2	Al_2O_3	Fe_2O_3	MgO	CaO	BaO	Na_2O	K_2O	Total	Grain I.D. No.	Sample	Host Unit Symbol
6.9	0.0	17.4	63.6	21.4	0.16	0.00	3.63	0.00	8.68	1.22	98.7	17C	USW G-1-1286	TPT1
4.0	0.0	17.6	64.6	22.1	0.12	0.00	3.73	0.00	9.17	0.73	100.6	17R	"	"
6.6	0.0	17.9	63.8	22.1	0.22	0.00	3.71	0.00	8.61	1.17	99.6	17R	"	"
3.2	0.0	36.2	58.3	25.6	0.09	0.00	7.55	0.00	6.97	0.57	99.1	78C	USW G-1-2436	TCB
4.3	0.0	39.0	59.2	25.4	0.29		8.20	0.04	6.57	0.78	100.5	L1C	USW G-1-3372	TCT
5.0	0.0	38.4	59.2	25.6	0.31		7.87	0.04	6.38	0.88	100.3	L2C	"	"
4.2	0.4	39.9	56.7	25.6	0.30		8.14	0.23	6.26	0.73	98.0	LXC	"	"
4.9	0.0	37.0	60.2	25.1	0.32		7.61	0.00	6.61	0.85	100.7	L3C	"	"
4.2	0.0	45.1	57.0	26.4	0.31		9.14	0.04	5.67	0.72	99.3	L4C	"	"
4.3	0.2	41.2	58.2	25.9	0.20		8.31	0.15	6.05	0.75	99.6	L5C	"	"
5.7	0.0	20.7	62.0	22.8	0.12		4.46	0.00	8.79	1.05	99.2	B5C	J13-2382	"
5.4	0.0	23.7	62.3	23.2	0.20		5.07	0.00	8.41	0.98	100.2	C5C	"	"
6.7	0.0	18.2	62.7	22.3	0.08		3.95	0.00	9.02	1.22	99.3	A4C	"	"
3.8	0.3	36.5	60.1	25.2	0.48		7.93	0.18	7.14	0.69	101.8	38C	RWRyb-1	"
6.2	0.1	14.7	65.8	21.3	0.09		3.15	0.03	9.34	1.11	100.8	46C	J13-3493	TLR
5.2	0.1	30.8	60.8	24.3	0.20		6.55	0.05	7.53	0.93	100.4	50C	"	"
3.7	0.0	39.0	59.3	25.5	0.28		8.09	0.00	6.58	0.65	100.4	49C	"	"
3.1	0.0	40.4	58.2	26.1	0.24		8.55	0.05	6.63	0.57	100.3	3C	USW G-1-4095	"
1.9	0.2	53.4	54.3	27.7	0.37		11.2	0.16	5.17	0.36	99.3	29C	-4208	"
4.1	0.0	34.4	59.5	24.9	0.27	0.00	7.00	0.00	6.90	0.70	99.3	5C	-4296	"
4.7	0.2	31.3	61.4	24.9	0.34	0.00	6.31	0.13	7.13	0.82	101.0	5M	"	"
5.4	0.0	22.0	63.2	22.7	0.22	0.00	4.56	0.00	8.30	0.96	99.9	5R	"	"
4.0	0.4	33.7	59.8	25.1	0.36	0.00	6.80	0.24	6.90	0.70	99.9	6C	"	"
3.6	0.2	34.1	58.4	24.8	0.19		7.14	0.10	7.18	0.64	98.5	30C	-4342	"
2.7	0.3	45.5	56.7	27.3	0.23	0.00	9.30	0.18	5.83	0.50	100.0	18C	-4401	"
3.7	0.6	37.6	58.0	24.8	0.37	0.02	7.72	0.37	6.59	0.66	98.5	18R	"	"
3.1	0.4	40.1	58.4	26.3	0.30	0.00	8.27	0.26	6.43	0.53	100.5	18R	"	"
2.1	0.0	48.5	54.8	27.2	0.26		9.97	0.00	5.61	0.38	98.2	3C	-4504	"
3.1	0.0	43.5	56.5	26.2	0.31		8.84	0.05	5.98	0.54	98.4	1C	"	"
5.2	0.3	28.2	61.9	23.8	0.31		5.95	0.21	7.75	0.92	100.8	19C	-4612	"
4.0	0.1	28.9	61.7	23.7	0.22		6.18	0.10	7.88	0.72	100.5	24C	-5349	TTB

APPENDIX C-I

AVERAGED ELECTRON MICROPROBE ANALYSES FOR BIOTITE PHENOCRYSTS
(All (n) analyses, in weight percent, within each interval defined in Table XIX are separately averaged for all samples of each unit. See Table II for definition of unit symbols.)

Mol% Mg/(Mg+Fe)	n	SiO_2	TiO_2	Al_2O_3	FeO	MgO	CaO	BaO	Na_2O	K_2O	Total	Unit Symbol
0.38-0.40	3	33.9	4.03	12.3	26.1	9.53	0.06	0.01	0.60	8.29	94.8	TPT1
0.40-0.42	2	37.4	4.53	12.4	22.0	8.47	0.11	0.71	0.49	8.17	94.3	TPT1
0.42-0.44	2	39.2	4.21	12.0	20.4	8.87	0.10	0.00	0.52	8.76	94.1	TPT1
0.44-0.46	1	35.5	4.32	13.7	23.0	10.3	0.06	0.07	0.61	8.73	96.3	TPT1
0.46-0.48	2	36.4	4.49	12.3	21.8	10.6	0.15	0.00	0.53	8.43	94.7	TPT1
0.50-0.52	1	37.5	4.33	12.9	19.5	11.7	0.13	0.00	0.64	8.56	95.3	TPT1
0.64-0.66	1	37.8	4.39	13.9	13.3	13.3	0.09	0.00	0.63	8.84	92.3	TPT1
0.34-0.36	1	36.2	4.13	12.2	23.8	7.39	0.16	0.00	0.41	8.36	92.8	TH1
0.36-0.38	6	36.0	4.46	12.6	24.4	8.13	0.06	0.00	0.46	8.50	94.6	TH1
0.38-0.40	2	35.6	4.59	12.9	24.6	8.63	0.08	0.04	0.42	8.70	95.6	TH1
0.42-0.44	2	35.6	4.23	13.1	23.2	10.1	0.05	0.20	0.53	8.49	95.5	TH1
0.42-0.44	1	36.5	3.90	13.8	22.2	9.27	0.13	0.13	0.41	8.66	95.0	TH2
0.44-0.46	2	35.9	4.27	13.8	22.2	9.89	0.09	0.62	0.34	8.60	95.7	TH2
0.46-0.48	2	38.6	4.15	13.1	19.2	9.47	0.18	0.00	0.14	8.01	92.9	TH2
0.34-0.36	1	34.8	4.29	11.7	26.8	7.95	0.11	0.00	0.58	8.42	94.7	TCP
0.38-0.40	2	34.5	4.67	12.8	23.6	8.68	0.09	1.61	0.56	8.12	94.6	TCP
0.40-0.42	6	35.0	4.62	13.4	23.2	9.17	0.04	1.83	0.67	8.15	96.1	TCP
0.42-0.44	3	35.9	4.91	13.8	21.7	9.37	0.06	1.69	0.71	8.19	96.3	TCP
0.44-0.46	5	36.5	4.75	13.9	20.5	9.31	0.04	1.89	0.74	8.25	95.9	TCP
0.50-0.52	2	36.6	4.94	14.0	18.0	10.9	0.08	1.63	0.73	7.82	94.7	TCP
0.52-0.54	2	38.4	5.00	14.0	16.8	10.2	0.05	1.40	0.71	8.16	94.7	TCP
0.60-0.62	1	39.3	4.82	15.0	13.9	12.1	0.05	1.06	0.61	8.70	95.6	TCP
0.40-0.42	2	36.2	5.14	12.6	23.3	9.42	0.09	0.51	0.57	8.98	96.8	TCBa
0.44-0.46	1	35.7	5.49	13.1	21.5	10.2	0.03	1.65	0.59	8.83	97.1	TCBa
0.52-0.54	1	35.7	5.72	13.6	19.3	12.4	0.07	1.52	0.64	8.61	97.6	TCBa
0.30-0.32	1	33.0	4.14	11.9	28.9	7.45	0.23	1.04	0.50	7.34	94.5	TCB
0.34-0.36	3	34.3	4.51	12.4	27.0	8.20	0.08	0.93	0.39	8.38	96.2	TCB
0.36-0.38	5	35.3	4.58	13.1	25.0	8.38	0.03	1.04	0.51	8.47	96.4	TCB
0.38-0.40	24	35.7	4.61	12.9	24.3	8.69	0.01	0.82	0.52	8.64	96.1	TCB
0.40-0.42	32	36.5	4.45	12.6	23.5	9.14	0.02	0.22	0.52	8.75	95.7	TCB
0.42-0.44	4	36.0	4.60	12.7	23.3	9.83	0.02	0.48	0.54	8.72	96.2	TCB

Appendix C-I (cont)

Mol% Mg/(Mg+Fe)	n	SiO_2	TiO_2	Al_2O_3	FeO	MgO	CaO	BaO	Na_2O	K_2O	Total	Unit Symbol
0.56-0.58	1	34.7	4.16	14.4	17.4	13.5	0.00	2.37	0.55	8.73	95.8	TCB
0.58-0.60	5	36.5	4.28	13.8	17.0	13.8	0.00	1.92	0.57	8.74	96.6	TCB
0.60-0.62	2	37.2	4.32	13.5	16.1	13.8	0.00	1.03	0.62	8.86	95.4	TCB
0.62-0.64	1	36.8	4.44	14.1	15.1	14.7	0.00	1.67	0.81	8.23	95.8	TCB
0.64-0.66	1	37.2	5.12	14.1	15.3	15.4	0.00	1.17	0.98	8.49	97.6	TCB
0.32-0.34	1	34.2	4.38	12.0	29.4	8.35	0.00	0.09	0.57	8.52	97.5	TCT
0.34-0.36	4	34.7	4.47	12.3	27.2	8.30	0.02	0.15	0.52	8.58	96.2	TCT
0.36-0.38	5	34.1	4.78	12.6	26.1	8.82	0.03	0.55	0.57	8.46	96.0	TCT
0.38-0.40	8	34.8	4.65	12.8	25.0	8.99	0.07	0.79	0.56	8.36	96.0	TCT
0.40-0.42	22	35.3	4.73	12.9	23.9	9.35	0.07	0.93	0.54	8.53	96.3	TCT
0.42-0.44	27	35.9	4.78	13.0	23.0	9.77	0.03	0.87	0.51	8.65	96.5	TCT
0.44-0.46	13	36.2	4.60	12.8	22.2	10.1	0.02	0.24	0.47	8.68	95.3	TCT
0.46-0.48	4	35.7	4.70	13.8	20.5	10.3	0.03	1.07	0.41	8.82	95.3	TCT
0.48-0.50	6	35.5	4.80	13.6	20.9	11.3	0.04	1.19	0.50	8.88	96.7	TCT
0.50-0.52	1	37.1	4.75	12.7	20.6	12.2	0.06	0.00	0.62	9.19	97.2	TCT
0.56-0.58	2	36.6	4.89	13.8	17.7	13.1	0.03	1.59	0.52	9.02	97.3	TCT
0.58-0.60	3	36.8	5.02	13.7	17.3	13.9	0.05	1.31	0.50	8.90	97.5	TCT
0.62-0.64	2	37.4	4.90	13.1	15.9	14.9	0.02	1.18	0.48	8.53	96.4	TCT
0.64-0.66	1	36.8	5.45	13.6	15.3	15.3	0.00	1.39	0.58	8.86	97.2	TCT
0.68-0.70	1	37.0	4.92	14.4	12.0	15.7	0.00	1.61	0.22	9.68	95.4	TCT
0.78-0.80	1	40.1	7.21	13.2	7.90	17.3	0.08	0.00	0.98	8.25	94.9	TFB
0.64-0.66	1	37.5	5.43	14.8	13.2	14.2	0.12	1.91	0.73	7.43	95.3	TLRa
0.66-0.68	1	37.0	5.60	14.2	13.4	14.8	0.02	1.87	0.71	7.77	95.4	TLRa
0.54-0.56	6	36.2	4.78	13.4	17.7	12.4	0.01	1.35	0.51	8.50	94.9	TLR
0.56-0.58	10	36.6	4.75	13.4	17.1	12.8	0.03	1.54	0.54	8.56	95.3	TLR
0.58-0.60	12	36.3	4.55	13.3	16.6	13.4	0.01	1.06	0.52	8.75	94.5	TLR
0.60-0.62	9	37.4	4.46	12.9	16.0	14.0	0.01	0.68	0.53	8.78	94.8	TLR
0.62-0.64	4	36.2	4.96	13.5	15.1	14.3	0.01	1.30	0.65	8.66	94.7	TLR
0.52-0.54	2	35.7	4.77	13.1	18.3	11.7	0.00	1.50	0.50	8.49	94.1	TTAB
0.54-0.56	8	36.4	4.24	13.0	18.4	12.6	0.04	0.73	0.49	8.40	94.5	TTAB
0.56-0.58	2	36.6	4.23	13.0	18.1	13.3	0.05	0.54	0.49	8.13	94.4	TTAB
0.58-0.60	3	36.5	4.83	13.2	16.4	13.0	0.03	1.31	0.47	8.50	94.2	TTAB
0.60-0.62	1	36.5	4.68	12.8	15.7	13.8	0.06	1.38	0.51	8.49	93.9	TTAB
0.60-0.62	2	36.4	4.96	13.5	16.0	14.0	0.14	1.00	0.30	7.92	94.2	TTC
0.62-0.64	3	36.7	4.73	13.4	15.4	14.3	0.15	1.18	0.36	8.16	94.4	TTC
0.66-0.68	1	37.2	5.08	13.1	13.7	15.9	0.07	1.46	0.66	8.66	95.8	TTC

APPENDIX C-II

INDIVIDUAL ANALYSES FOR BIOTITE PHENOCRYSTS IN LITHIC FRAGMENTS

[All analyses in weight percent. See Table II for definition of host unit symbol. For biotite E, USW G-1-3501, f = fresh (unaltered portion), a = altered portion.]

Molecular Mg/(Mg+Fe)	SiO_2	TiO_2	Al_2O_3	FeO	MgO	CaO	BaO	Na_2O	K_2O	Total	Grain I.D. No.	Sample	Host Unit Symbol
0.390	36.5	4.72	13.0	24.5	8.80	0.00	0.12	0.39	8.96	97.0	J	J13-2175	TCB
0.691	37.0	4.77	14.2	13.4	16.8	0.05	1.36	0.80	8.06	96.4	K	USW G-1-2790	TCT
0.615	36.1	5.11	14.5	15.4	13.8	0.08	1.64	0.36	9.29	96.3	E	-2854	"
0.681	36.7	5.55	14.0	13.8	16.5	0.00	2.26	0.52	8.56	98.0	E	-3197	"
0.551	36.6	5.20	14.0	18.7	12.9	0.04	1.80	0.22	9.06	98.5	G	"	"
0.663	37.5	5.36	13.4	14.1	16.4	0.00	2.13	0.60	8.84	98.3	D	-3258	"
0.616	36.7	4.51	13.6	16.3	14.7	0.01	1.43	0.48	8.89	96.6	H	"	"
0.718	37.6	5.22	14.3	11.9	16.9	0.04	2.06	0.37	8.91	97.3	J	"	"
0.671	37.2	4.67	14.4	13.5	15.5	0.05	2.23	0.79	8.25	96.6	B	-3321	"
0.644	36.7	5.18	14.0	14.6	14.9	0.00	0.66	0.47	8.91	95.4	A	-3372	"
0.566	36.8	4.87	13.6	18.2	13.3	0.00	0.90	0.67	8.71	97.0	E(f)	-3501	"
0.810	41.9	4.60	15.9	6.27	15.0	0.00	1.03	0.58	10.3	95.6	E(a)	"	"
0.845	42.3	5.68	14.1	5.34	16.5	0.00	0.59	0.54	10.2	95.3	E(a)	"	"
0.686	38.4	5.32	13.4	12.7	15.5	0.02	0.80	0.69	8.60	95.4	M	-4612	TLR
0.595	37.3	4.73	13.6	16.6	13.7	0.00	0.80	0.67	8.87	96.3	H	RWBWa-4	"
0.771	39.4	2.95	11.0	9.95	19.8	0.05	0.00	0.50	8.93	92.6	/L5	"	"
0.631	35.7	5.27	13.3	15.7	15.1	0.09	0.73	0.55	9.04	95.5	A	USW G-1-5848	TTC

APPENDIX D-I

AVERAGED ELECTRON MICROPROBE ANALYSES FOR HORNBLENDE PHENOCRYSTS

(All (n) analyses, in weight percent, within each interval defined in Table XX are separately averaged for all samples of each unit. See Table II for definition of unit symbols.)

Mol% Mg/(Mg+Fe)	n	SiO_2	TiO_2	Al_2O_3	FeO	MgO	CaO	BaO	Na_2O	K_2O	Total	Unit Symbol
0.32-0.34	1	44.5	1.51	6.32	24.8	6.60	9.57	0.27	2.07	0.68	96.3	TCP
0.36-0.38	1	46.6	1.23	5.66	23.4	7.64	9.65	0.22	2.09	0.63	97.1	TCP
0.50-0.52	1	44.0	2.39	9.14	18.1	10.5	11.8	0.05	2.36	0.76	99.1	TCP
0.60-0.62	1	43.2	3.34	10.8	13.9	12.2	11.1	0.05	2.67	0.80	98.1	TCP
0.36-0.38	1	41.4	2.21	10.5	22.5	7.63	10.7	0.28	2.51	0.87	98.6	TCB
0.42-0.44	7	45.3	1.43	6.60	21.8	9.21	10.1	0.12	1.92	0.72	97.2	TCB
0.44-0.46	5	45.3	1.48	6.81	20.9	9.49	10.4	0.19	1.93	0.76	99.0[a]	TCB
0.62-0.64	2	42.6	2.13	10.0	14.1	12.9	11.5	0.03	2.17	0.94	96.4	TCB
0.62-0.64	1	42.0	2.92	11.2	13.3	12.8	11.1	0.00	2.16	0.81	96.3	TFB
0.64-0.66	9	42.8	3.04	10.8	12.7	13.5	11.5	0.01	2.21	0.91	97.5	TFB
0.66-0.68	12	43.5	2.85	10.1	12.3	13.9	11.4	0.07	2.14	0.89	97.3	TFB
0.68-0.70	2	42.7	3.38	11.1	11.3	13.6	11.5	0.17	2.50	0.76	97.0	TLRa

[a] Includes 1.70% MnO (from single analysis of CFLSM-5).

APPENDIX D-II

INDIVIDUAL ANALYSES FOR HORNBLENDE PHENOCRYSTS IN LITHIC FRAGMENTS (All analyses in weight percent. See Table II for definition of host unit symbol.)

Molecular Mg/(Mg+Fe)	SiO_2	TiO_2	Al_2O_3	FeO	MgO	CaO	BaO	Na_2O	K_2O	Total	Grain I.D. No.	Sample	Host Unit Symbol
0.616	44.1	2.30	8.82	15.2	13.6	11.5	0.00	2.21	0.88	98.6	NE/C	USW G-1-3001	TCT
0.667	45.8	1.90	8.16	13.1	14.6	11.5	0.00	1.55	0.81	97.4	E	-3258	"
0.657	45.0	1.94	8.51	13.3	14.2	11.4	0.10	1.50	0.75	96.7	K	"	"
0.667	44.0	2.73	9.75	12.3	13.8	11.7	0.00	2.20	0.92	97.4	Ld	-3941	TLR
0.635	45.6	2.05	7.97	13.0	13.3	11.2	0.00	1.78	0.84	95.7	E/3	-4095	"

APPENDIX E-I

AVERAGED ELECTRON MICROPROBE ANALYSES FOR ORTHOPYROXENE PHENOCRYSTS (All (n) analyses, in weight percent, within each interval defined in Table XX are separately averaged for all samples of each unit. See Table II for definition of unit symbols.)

Mol% Mg/(Mg+Fe)	n	SiO_2	TiO_2	Al_2O_3	FeO	MgO	CaO	BaO	Na_2O	K_2O	Total	Unit Symbol
0.28-0.30	4	49.7	0.09	0.20	35.8	8.28	1.43	0.03	0.04	0.00	95.6	TCP
0.30-0.32	1	49.6	0.06	0.18	35.2	8.66	1.42	0.00	0.07	0.01	95.2	TCP
0.68-0.70	5	51.8		1.39	18.8	23.7	1.30	0.14	0.06	0.00	97.3	TFB
0.70-0.72	3	53.5	0.37	1.74	17.9	24.6	1.34	0.03	0.02	0.00	99.5	TFB

APPENDIX F-I

AVERAGED ELECTRON MICROPROBE ANALYSES FOR CLINOPYROXENE PHENOCRYSTS (All (n) analyses, in weight percent, within each interval defined in Table XX are separately averaged for all samples of each unit. See Table II for definition of unit symbols.)

Mol% Mg/(Mg+Fe)	n	SiO_2	TiO_2	Al_2O_3	FeO	MgO	CaO	BaO	Na_2O	K_2O	Total	Unit Symbol
0.70-0.72	1	50.8	0.75	3.17	9.71	13.8	21.1	0.00	0.38	0.00	99.6	TFB
0.72-0.74	7	51.3	0.48	2.19	9.24	14.4	20.7	0.02	0.32	0.00	99.7	TFB
0.74-0.76	2	51.0	0.46	2.13	9.00	14.6	20.7	0.04	0.35	0.01	98.2	TFB

APPENDIX F-II

INDIVIDUAL ANALYSES FOR CLINOPYROXENE IN LITHIC FRAGMENTS

(All analyses in weight percent. See Table II for definition of host unit symbol.)

Molecular Mg/(Mg+Fe)	SiO_2	TiO_2	Al_2O_3	FeO	MnO	Mgo	CaO	Na_2O	Total	Grain[a] I.D. No.	Sample	Host Unit Symbol
0.441	52.3	0.04	0.53	16.0	2.32	7.08	22.9	0.77	101.9	A_2	TBF-1	TCB
0.669	52.7	0.00	0.59	9.78	1.46	11.1	24.2	0.30	100.1	B_2	"	"
0.581	53.0	0.01	0.45	12.5	1.80	9.69	23.6	0.36	101.4	C_2	"	"
0.574	52.6	0.04	0.44	12.7	1.84	9.60	23.7	0.36	101.3	D_2	"	"
0.706	53.7	0.05	0.22	9.07	1.24	12.2	22.7	0.91	100.1	A_3	"	"
0.722	54.1	0.00	0.26	8.70	0.39	12.7	24.8	0.33	101.3	B_3	"	"
0.773	54.6	0.00	0.40	7.14	0.69	13.6	24.4	0.43	101.3	C_3 Core	"	"
0.716	54.0	0.02	0.32	8.89	0.96	12.6	22.8	0.92	100.5	C_3 rim	"	"
0.853	55.2	0.00	0.17	4.71	0.27	15.4	25.4	0.03	101.2	D_3	"	"
0.796	55.0	0.03	0.57	6.46	0.59	14.2	24.5	0.37	101.7	E_3	"	"
0.807	54.6	0.00	0.49	5.92	0.41	13.9	24.6	0.31	100.2	F_3 core	"	"
0.706	53.7	0.01	0.33	9.04	1.03	12.2	22.8	0.88	100.0	F_3 rim	"	"
0.161	49.4	0.11	0.70	21.9	4.15	2.35	20.4	1.51	100.5	A_1	"	"
0.598	54.5	0.07	0.29	11.6	1.49	9.66	21.1	0.91	99.6	B_1	"	"

[a] Grains with subscript 1 are from fragment of peralkaline rock; those with subscripts 2 and 3 are from pyroxenite.

☆U.S. GOVERNMENT PRINTING OFFICE:1984—776-026/4103

Printed in the United States of America
Available from
National Technical Information Service
US Department of Commerce
5285 Port Royal Road
Springfield, VA 22161

Microfiche (A01)

Page Range	NTIS Price Code	Page Range	NTIS Price Code	Page Range	NTIS Price Code	Page Range	NTIS Price Code
001-025	A02	151-175	A08	301-325	A14	451-475	A20
026-050	A03	176-200	A09	326-350	A15	476-500	A21
051-075	A04	201-225	A10	351-375	A16	501-525	A22
076-100	A05	226-250	A11	376-400	A17	526-550	A23
101-125	A06	251-275	A12	401-425	A18	551-575	A24
126-150	A07	276-300	A13	426-450	A19	576-600	A25
						601-up*	A99

*Contact NTIS for a price quote.

Los Alamos